





This is to certify that the

dissertation entitled

SYNTHESIS, ELECTROCHEMICAL, AND
SPECTROCHEMICAL CHARACTERIZATION OF MIXED
HETEROCYCLIC CONDUCTING POLYMERS

presented by

Evaldo de Armas

has been accepted towards fulfillment
of the requirements for

Ph.D. degree in Chemistry

Major professor

Date 10-11-91

LIBRARY
Michigan State
University

PLACE IN RETURN BOX to remove this checkout from your record.
TO AVOID FINES return on or before date due.

DATE DUE	DATE DUE	DATE DUE
<div> <div></div> <div> <div></div> <div>14</div> <div>1998</div> </div> </div>	<div></div>	<div></div>
<div> <div></div> <div> <div></div> <div></div> <div></div> </div> </div>	<div></div>	<div></div>
<div></div>	<div></div>	<div></div>
<div></div>	<div></div>	<div></div>
<div></div>	<div></div>	<div></div>
<div></div>	<div></div>	<div></div>
<div></div>	<div></div>	<div></div>

MSU is An Affirmative Action/Equal Opportunity Institution

c:\circ\datedue.pm3-p.1

**SYNTHESIS, ELECTROCHEMICAL AND SPECTROCHEMICAL
CHARACTERIZATION OF MIXED HETEROCYCLIC
CONDUCTING POLYMERS**

By

Evaldo de Armas

A DISSERTATION

**Submitted to
Michigan State University
in partial fulfillment of the requirements
for the degree of**

DOCTOR OF PHILOSOPHY

Department of Chemistry

1991

ABSTRACT

SYNTHESIS, ELECTROCHEMICAL, AND SPECTROCHEMICAL CHARACTERIZATION OF MIXED HETEROCYCLIC CONDUCTING POLYMERS

By

Evaldo de Armas

The electropolymerization of 2,5-bis(2-pyrrolyl)thiophene, **1a**, or 2,5-bis(4-methyl-2-pyrrolyl)thiophene, **1b**, yielded copolymers that have a known stoichiometry and sequence distribution of heterocyclic units. These copolymers exhibit excellent stability both in the neutral and oxidized form, and show relatively high conductivity values. The addition of small substituents (methyls) at the 4-position of the pyrroles, blocks the formation of α,β' and β,β' coupling reactions, hence a more ordered α,α' -linked copolymer is obtained. Spectroelectrochemical results are consistent with a polaron/bipolaron model.

A new method, using trimethylaluminum to activate the amine functionality, is being developed, that allows the condensation with 1,4-diketones to be carried out at room temperature. Using this new method, 1,4-bis[2,5-bis(2-thienyl)-1-pyrrolyl]benzene (**6**) was synthesized. Monomer **6** is capable of forming a multidimensional conductive polymer. Electropolymerization of **6** resulted in a polymer that is not very conductive, but shows good spectroelectrochemical response. Cyclic voltammograms of **6** resemble those of a polymer possessing non-interactive sites.

Four other monomers: 1-amino-4-[2,5-bis(2-thienyl)-1-pyrryl]benzene (16), N-[4-[2,5-bis(2-thienyl)-1-pyrryl]phenyl]acetamide (17), N-[2,5-bis(2-thienyl)-1-pyrryl]benzene (22), and 1-(dimethylamino)-4-[2,5-bis(2-thienyl)-1-pyrryl]benzene (23) were also synthesized. Electrochemical polymerization of 16, and 17 resulted in polymers with low conductivity values, but with dramatic electrochromic characteristics. Electropolymerization of 22 and 23, resulted in the formation of soluble conductive polymers.

To my wife, Raquel Pilar, and son Evaldo Jr.

To my father, Leandro R. de Armas, and
my mother Maria Zoraida de Armas.

ACKNOWLEDGEMENTS

I would like to thank Dr. Eugene LeGoff for his guidance, openness, and helpful discussions during this learning experience. I have learned a lot of organic chemistry under his direction. I am also grateful to Dr. John Gaudiello for his teaching and guidance during my first year at MSU.

I am indebted to Dr. Bryon Merrill and Michael Benz for the synthesis of various compounds in this thesis, and their willingness to teach me laboratory techniques. Special thanks to Michael Waldo and David Gale for their help, friendship, helpful discussions, and making my stay here more enjoyable.

I would like to thank the chemistry department at Michigan State for their financial support in the form of teaching assistantships, and to the Center for Fundamental Material Research in financing part of this research project.

TABLE OF CONTENTS

	<u>Page</u>
LIST OF TABLES	vii
LIST OF FIGURES	viii
LIST OF SCHEMES	xii
INTRODUCTION	1
A. Instrumentation	23
B. Glassware	24
C. Electrochemical Solvents and Reagents	25
D. Electrochemical Techniques	26
E. Spectroelectrochemistry	28
F. Conductivity	29
G. Synthesis	33
RESULTS AND DISCUSSION	38
A. Synthesis of 1,4-bis[2,5-bis(2-thienyl)- 1-pyrryl]benzene	38
B. Electrochemistry and Conductivity	53
C. Spectroelectrochemistry	97
CONCLUSION	114
APPENDIX	116
LIST OF REFERENCES	130

LIST OF TABLES

	<u>Page</u>
Table 1 Oxidation potential and conductivity of substituted systems	15
Table 2 Electrochemical data for N-aryl-substituted pyrrole films	17
Table 3 Electrochemical and optical data for Ferraris' copolymers	20
Table 4 Electrochemical data for synthesized monomers and polymers	96
Table 5 Summary of spectroscopic data of synthesized polymers	113

LIST OF FIGURES

		<u>Page</u>
Figure 1	Room temperature conductivities of common materials. Conductivities are in Siemens/cm.	3
Figure 2	Electronic structure of materials.	6
Figure 3	Structure and conductivities of common organic conductive polymers. Conductivities are in S/cm at room temperature.	9
Figure 4	Conjugated π -electron structure of organic conducting polymers.	10
Figure 5	Four-point-probe electrode.	31
Figure 6	Gap electrode for <i>in situ</i> conductivity measurement.	32
Figure 7	Electrochemical polymerization of 1,4-bis(1-pyrrolyl)benzene (5) 0.01 M monomer and 0.10 M TBABF ₄ in acetonitrile. Potential vs. Ag/Ag ⁺ .	56
Figure 8	Cyclic voltammogram of polymerized 5 in acetonitrile with 0.10 M TBABF ₄ . Scan rate 50 mV/sec. Potential vs. Ag/Ag ⁺ .	58
Figure 9	Electrochemical polymerization of 2,5-bis(2-pyrrolyl)thiophene (1a). 0.01 M monomer and 0.10 M TBABF ₄ in acetonitrile. Potential vs. SSCE.	60
Figure 10	Electrochemical polymerization of 2,5-bis(4-methyl-2-pyrrolyl)thiophene (1b). 0.01 M monomer and 0.10 M TBABF ₄ in acetonitrile. Potential vs. SSCE.	62
Figure 11	Electrochemical polymerization of 1,4-bis[2,5-bis(2-thienyl)-1-pyrrolyl]benzene (6). 1 X 10 ⁻³ M monomer and 0.10 M TBABF ₄ in dichloromethane. Potential vs. Ag/Ag ⁺ .	64

	<u>Page</u>
Figure 12 Electrochemical polymerization of 1-amino-4-[2,5-bis(2-thienyl)-1-pyrrolyl]benzene (16). 1×10^{-3} M monomer and 0.10 M TBABF ₄ in dichloromethane. Potential vs. Ag/Ag ⁺ .	66
Figure 13 Electrochemical polymerization of N-[4-[2,5-bis(2-thienyl)-1-pyrrolyl]phenyl]acetamide (17). 1×10^{-3} M monomer and 0.10 M TBABF ₄ in dichloromethane. Potential vs. Ag/Ag ⁺ .	68
Figure 14 Electrochemical polymerization of 2,5-bis(2-thienyl)pyrrole (18). 1×10^{-3} M monomer and 0.10 M TBABF ₄ in dichloromethane. Potential vs. Ag/Ag ⁺ .	70
Figure 15 Electrochemical polymerization of 1-(dimethylamino)-4-[2,5-bis(2-thienyl)-1-pyrrolyl]benzene (23). 1×10^{-3} M monomer and 0.10 M TBABF ₄ in tetrahydrofuran. Potential vs. Ag/Ag ⁺ .	72
Figure 16 Electrochemical polymerization of N-[2,5-bis(2-thienyl)-1-pyrrolyl]benzene (22). 1×10^{-3} M monomer and 0.10 M TBABF ₄ in dichloromethane. Potential vs. Ag/Ag ⁺ .	74
Figure 17 Electrochemical polymerization of 3,4-dibutyl-2,5-bis(2-thienyl)pyrrole (28). 1×10^{-3} M monomer and 0.10 M TBABF ₄ in dichloromethane. Potential vs. Ag/Ag ⁺ .	76
Figure 18 Cyclic voltammograms of polymerized 2,5-bis(2-pyrrolyl)thiophene (1a) in acetonitrile with 0.10 M TBABF ₄ , at 20, 10 and 5 mV/sec. Potential vs. SSCE.	79
Figure 19 Cyclic voltammograms of polymerized 2,5-bis(4-methyl-2-pyrrolyl)thiophene (1b) in acetonitrile with 0.10 M TBABF ₄ , at 50, 20, and 10 mV/sec. Potential vs. SSCE.	81
Figure 20 Cyclic voltammograms of polymerized 1,4-bis[2,5-bis(2-thienyl)-1-pyrrolyl]benzene (6) in dichloromethane with 0.10 M TBABF ₄ , at 50, 20, 10, and 5 mV/sec. Potential vs. Ag/Ag ⁺ .	83
Figure 21 Cyclic voltammograms of polymerized 1-amino-4-[2,5-bis(2-thienyl)-1-pyrrolyl]benzene (16) in dichloromethane with 0.10 M TBABF ₄ , at 25, 10, and 5 mV/sec. Potential vs. Ag/Ag ⁺ .	85
Figure 22 Cyclic voltammograms of polymerized 1-amino-4-[2,5-bis(2-thienyl)-1-pyrrolyl]benzene (16) in dichloromethane with 0.10 M TBABF ₄ , at 25, 10, and 5 mV/sec. Potential vs. Ag/Ag ⁺ .	87

	<u>Page</u>	
Figure 23	Cyclic voltammograms of polymerized 2,5-bis(2-thienyl) pyrrole (18) in dichloromethane, with 0.10 M TBABF ₄ , at 50, 25, and 10 mV/sec. Potential vs. Ag/Ag ⁺ . The polymer film slowly dissolves and hence is not well anchored to the electrode.	89
Figure 24	Cyclic voltammograms of polymerized 2,5-bis(2-thienyl) pyrrole (18) in dichloromethane, with 0.10 M TBABF ₄ , at 50, 25, and 10 mV/sec. Potential vs. Ag/Ag ⁺ . The film is well anchored and shows a linear relationship of peak current versus scan rate.	91
Figure 25	Cyclic voltammograms of polymerized 1-(dimethylamino)-4-[2,5-bis(2-thienyl)-1-pyrro]benzene in tetrahydrofuran, with 0.10 M TBABF ₄ , at 50, 25, 10 , and 5 mV/sec. Potential vs. Ag/Ag ⁺ .	93
Figure 26	<i>In situ</i> spectroelectrochemistry of polymerized 1a film on an ITO electrode, with 0.10 M TBABF ₄ in acetonitrile. Trace a at 0.00 V, trace b at 0.20 V, and trace c at 0.80 V. Potentials versus SSCE.	100
Figure 27	<i>In situ</i> spectroelectrochemistry of polymerized 1b film on an ITO electrode, with 0.10 M TBABF ₄ in acetonitrile. Trace a at -0.10 V, and trace b at 0.20 V. Potentials versus SSCE.	102
Figure 28	<i>In situ</i> spectroelectrochemistry of polymerized 6 film on an ITO electrode, with 0.10 M TBABF ₄ in dichloromethane. Trace a at 0.00 V, trace b at 0.70 V, and trace c at 1.40 V. Potentials versus Ag/ Ag ⁺ .	105
Figure 29	<i>In situ</i> spectroelectrochemistry of polymerized 16 film on an ITO electrode, with 0.10 M TBABF ₄ in dichloromethane. Trace a at 0.00 V, trace b at 0.60 V, and trace c at 0.80 V. Potentials versus Ag/ Ag ⁺ .	107
Figure 30	<i>In situ</i> spectroelectrochemistry of polymerized 17 film on an ITO electrode, with 0.10 M TBABF ₄ in dichloromethane. Trace a at 0.00 V, trace b at 0.50 V, and trace c at 0.75 V. Potentials versus Ag/Ag ⁺ .	109
Figure 31	<i>In situ</i> spectroelectrochemistry of polymerized 23 film on an ITO electrode with 0.10 M TBABF ₄ in tetrahydrofuran. Trace a at 0.00 V, and trace b at 1.00 V. Potentials versus Ag/Ag ⁺ .	111

	<u>Page</u>
Figure A1 300 MHz ¹ H-NMR spectrum of 1,4-bis[2,5-bis(2-thienyl)-1-pyrryl]benzene (6).	116
Figure A2 300 MHz ¹ H-NMR spectrum of 1-amino-4-[2,5-bis(2-thienyl)-1-pyrryl]benzene (16).	117
Figure A3 75.4 MHz ¹³ C-NMR spectrum of 1-amino-4-[2,5-bis(2-thienyl)-1-pyrryl]benzene (16).	118
Figure A4 300 MHz ¹ H-NMR spectrum of N[4-[2,5-bis(2-thienyl)-1-pyrryl]phenyl]acetamide (17).	119
Figure A5 75.4 MHz ¹³ C-NMR spectrum of N[4-[2,5-bis(2-thienyl)-1-pyrryl]phenyl]acetamide (17).	120
Figure A6 300 MHz ¹ H-NMR spectrum of N-[2,5-bis(2-thienyl)-1-pyrryl]benzene (22).	121
Figure A7 75.4 MHz ¹³ C-NMR spectrum of N-[2,5-bis(2-thienyl)-1-pyrryl]benzene (22).	122
Figure A8 300 MHz ¹ H-NMR spectrum of 1-(dimethylamino)-4-[2,5-bis(2-thienyl)-1-pyrryl]benzene (23).	123
Figure A9 75.4 MHz ¹³ C-NMR spectrum of 1-(dimethylamino)-4-[2,5-bis(2-thienyl)-1-pyrryl]benzene (23).	124
Figure A10 Fourier-transform IR spectrum of 1,4-bis[2,5-bis(2-thienyl)-1-pyrryl]benzene (6) in KBr.	125
Figure A11 Fourier-transform IR spectrum of 1-amino-4-[2,5-bis(2-thienyl)-1-pyrryl]benzene (16) in KBr.	126
Figure A12 Fourier-transform IR spectrum of N[4-[2,5-bis(2-thienyl)-1-pyrryl]phenyl]acetamide (17) in KBr.	127
Figure A13 Fourier-transform IR spectrum of N-[2,5-bis(2-thienyl)-1-pyrryl]benzene (22) in KBr.	128
Figure A14 Fourier-transform IR spectrum of 1-(dimethylamino)-4-[2,5-bis(2-thienyl)-1-pyrryl]benzene (23) in KBr.	129

LIST OF SCHEMES

	<u>Page</u>
Scheme 1 Proposed mechanism of the electrochemical polymerization reaction.	12
Scheme 2 Benzenoid and quinonoid conformation of conductive polymers.	19
Scheme 3 Merrill's tercycles.	21
Scheme 4 Synthesis of 1,4-bis(1-pyrryl)benzene.	38
Scheme 5 Two-dimensional conductive polymer from 1,4-bis(1-pyrryl)benzene.	39
Scheme 6 Synthesis of phenylene-bridged tercycle 6.	40
Scheme 7 Condensation of bicyclophenyl-2,2'-dione with p-phenylenediamine.	41
Scheme 8 Merrill's phenylene-bridged tercycles.	42
Scheme 9 Two-step synthesis of 11.	43
Scheme 10 The Stetter reaction.	44
Scheme 11 Initial attempts at the Paal-Knorr reaction.	45
Scheme 12 Two-step synthesis attempt of 6.	45
Scheme 13 Attempted condensation with propionic acid.	46
Scheme 14 Lewis acid catalized formation of pyrroles	47
Scheme 15 Various attempts to make 6.	48
Scheme 16 Possible mechanism of alkylchloroaluminum amine reactions	49

	<u>Page</u>
Scheme 17 Condensation of 14 with various substituted phenylamines.	51
Scheme 18 Condensation of 16 with squaric acid (26).	52

INTRODUCTION

Traditional materials can be categorized into three distinct groups based on their electrical conductivity: metals, semiconductors, and insulators. Common metals such as copper or silver have conductivities in the 10^6 S/cm ($S=1/\Omega$) range, at room temperature. The semiconductors such as silicon or germanium, have conductivities in the range of 10^{-4} to 10^2 S/cm. The insulators which comprises the largest category, have conductivities in the range of 10^{-18} to about 10^{-5} S/cm. This includes such materials as teflon, polyethylene, PVC, *cis* and *trans*-polyacetylenes. (Fig. 11).

In the late 1970s it was found that certain organic polymer insulators could become relatively good conductors if they were partially oxidized or reduced ("doped").² It was also discovered that this "doping" process could be accomplished both chemically or electrochemically. Therefore a tremendous effort to understand and make useful applications of these materials began.

To better understand how these polymer materials become conductive, it is better to look at them in terms of their electronic structure. The theory that most reasonably explains the electronic structure of materials is band theory. In the solid state, the atomic orbitals of each atom overlap with the same orbital of their neighboring atoms in all directions to produce molecular orbitals. In a solid, the number of molecular orbitals is quite high (Avogadro's number). When this many molecular orbitals are spaced together in a given range of energies, they form a virtually continuous energy band.³ The highest occupied band is called the valence band (VB). The lowest unoccupied band is called the

Figure 1. Room temperature conductivities of common materials.
Conductivities are in Siemens/cm.

Room temperature conductivities of common materials.
Conductivities are in Siemens/cm

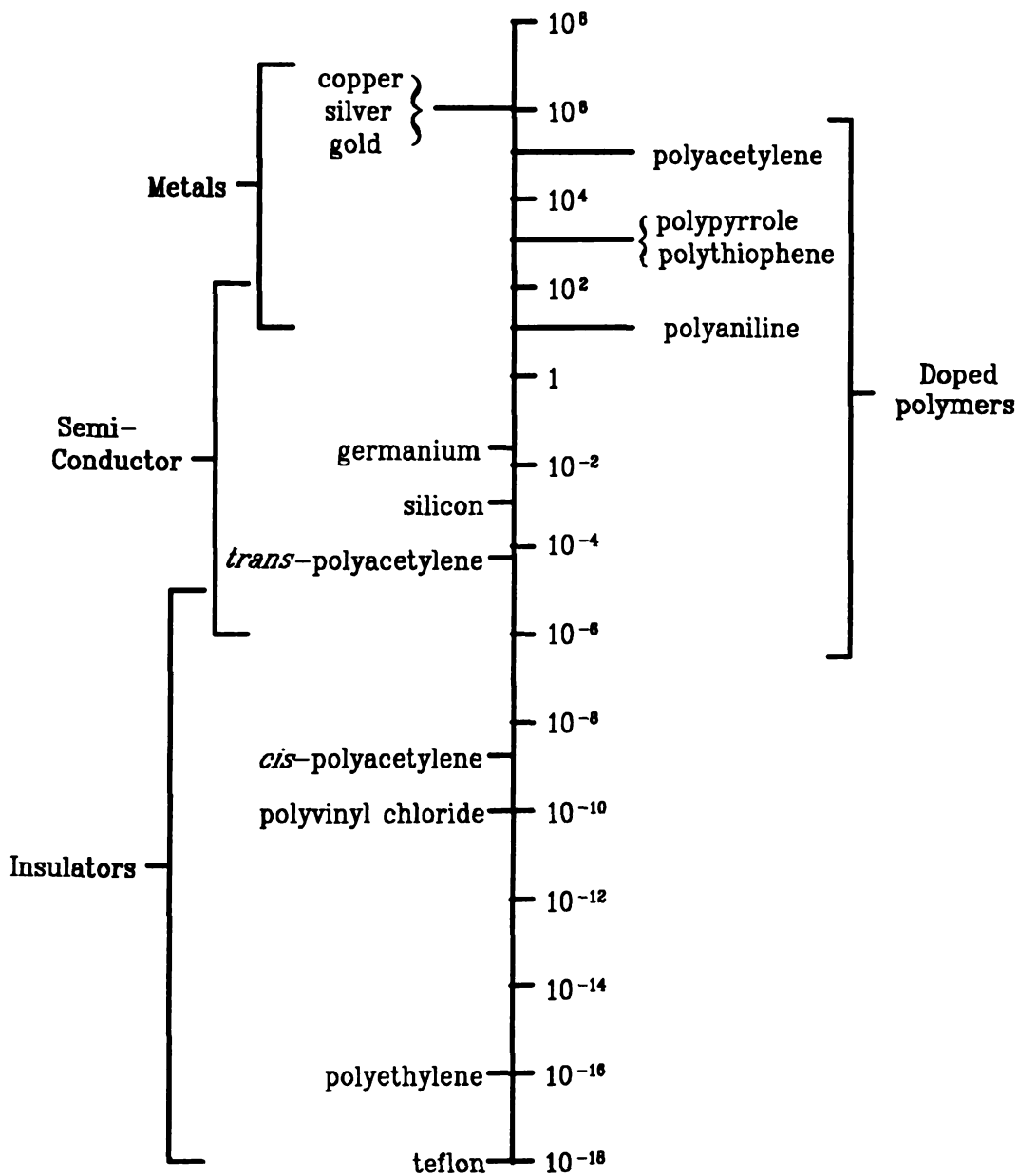


Figure 1

conduction band (CB). Depending on the way these bands are filled with electrons, and the energy gap between them (E_g), will determine the intrinsic electronic characteristics of the material.

Insulators are defined as materials which have a filled VB, and an empty CB, separated by a relatively large band gap (E_g). Thus it is very difficult to promote electrons from the VB to the CB. There are no charge carriers.

Semiconductors are materials which also have a filled VB and an empty CB, but the band gap is relatively small. In this case it is possible to promote electrons from the VB to the CB by thermal excitation. At higher temperatures more electrons can be promoted into the CB, therefore the conductivity increases with increasing temperature.

Metals are materials which either have a partially filled VB, a partially empty CB or a zero band gap. The magnitude of the conductivity of such a material will depend on the number of available charge carriers as well as the mobility of the charge carriers. (Fig. 2).

Neutral or undoped polymers are classified as insulators due to their low conductivity. However when they are partially oxidized or reduced, their conductivity increases to the order of the metal range. This is why they are called "synthetic metals". Recently a group of researchers at BASF, West Germany, reported the synthesis of oxidized polyacetylene with a conductivity of 1.5×10^5 S/cm, very close to the conductivity of metals.⁴

Simple band theory cannot fully explain the conductivity of these organic polymer materials, because they conduct without having a partially filled conduction band or a partially empty valence band. In a conjugated neutral or undoped polymer, the VB is filled, separated by a band gap from the CB, which is empty. Therefore the polymer is an insulator. When an electron is removed from the VB (partially oxidized), it leads to the formation of a charge that is

Figure 2. Electronic structure of materials.³

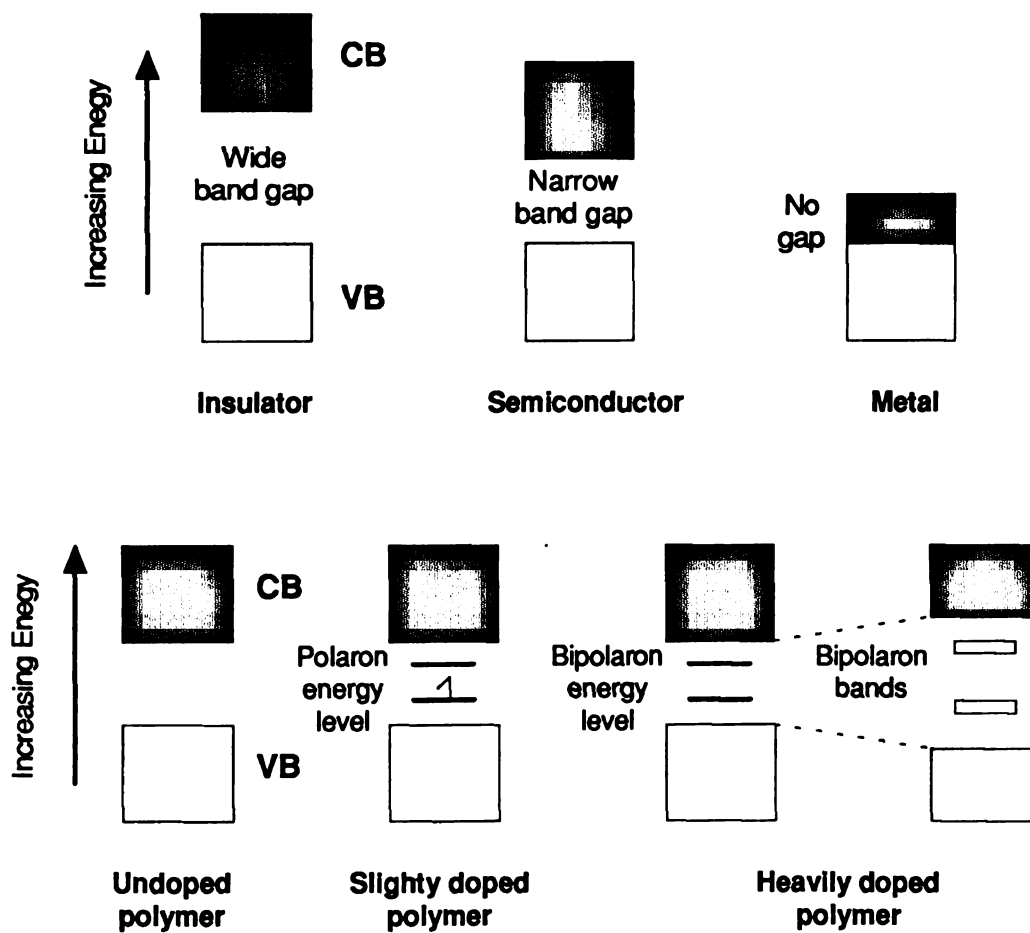


Figure 2

localized along the polymer chain accompanied by a local distortion of the lattice. This is termed a "polaron". In chemical terminology, the polaron represents a radical cation (spin $1/2$). This localized radical cation forms a localized electronic state within the band gap. If the polymer is oxidized further by removing another electron, two possibilities arise. In one, the electron can be removed from the VB, leading to the formation of another polaron state, or the electron can be removed from the first polaron level, to form a bipolaron, which is a dication that is localized along the polymer chain. If further oxidation takes place, and more bipolarons are formed, their energies can overlap which leads to the formation of bipolaron bands within the band gap. It should be noted that the VB remains filled and the CB remains empty, but the band gap has increased (Fig.2).

Not every organic polymer can become a conductor. There are some requirements which have to be met. First, there has to be the presence of a conjugated π -electron system. Second, the polymer material has to be in a partially oxidized or reduced form. Highly conjugated materials are able to either gain or lose electrons with relative ease via the π -system, while still maintaining the structural integrity of the polymer through the sigma bonds.⁵ Figure 3 lists some of the more common conductive polymers with their associated conductivities.

Polyacetylene, which is the most conductive polymer discovered so far, has had limited use because of its low stability in air and its poor mechanical characteristics.⁷ In contrast, electrochemical polymerization of heteroaromatic monomers such as pyrrole, thiophene, and furan, yields polymers which exhibit good electrical conductivities and are stable in air.⁸ There are four basic reasons why it is better to make and study conductive polymers by electrochemical means. First, the polymers are made as clean, doped films, which can be cycled repeatedly between the oxidized conducting state and the neutral insulating

Figure 3. Structure and conductivities of common organic conductive polymers. Conductivities are in S/cm at room temperature.⁶


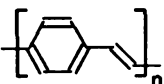

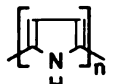
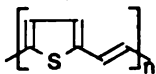
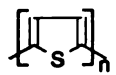

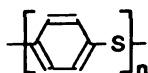
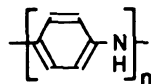

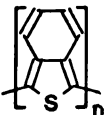
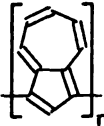
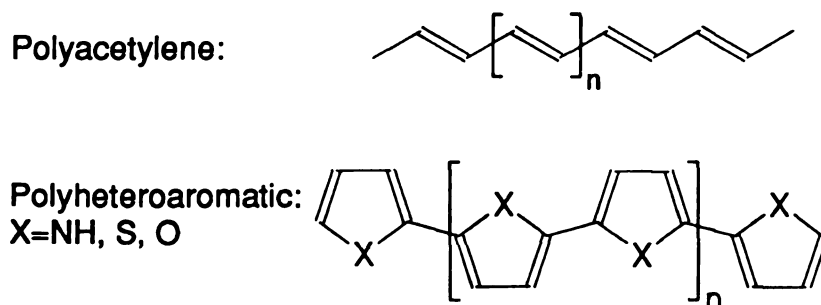
Polymer	Structure	Conductivity (S/cm)
Polyacetylene		10,000
Polyphenylenevinylene		10,000
Poly(3-alkyl)thiophene		1000-10,000
Polypyrrole		500-7500
Polythienylenevinylene		2700
Polythiophene		1000
Polyphenylene		1000
Polyphenylene Sulfide		500
Polyaniline		200
Polyfuran		100
Polyisothianaphthene		50
Polyazulene		1

Figure 3

state without apparent degradation of the material.⁹ Second, the oxidation potentials of both monomers and polymers can be determined. Third, the rate as well as the extent of polymerization can be controlled, and fourth, one can easily determine the stability of the polymer in different solvents.

Figure 4 shows that the conjugated π -electron structure is maintained in the polyheteroaromatics. The heteroatoms ($X=N, S, O$) can be viewed as acting as bridges holding the *trans*-polyacetylene portion of the structure in a rigid *trans*-cisoid conformation.

Figure 4. Conjugated π -electron structure of organic conducting polymers



The study of conducting polymers based on polyheteroaromatic molecules has received much attention recently due to the interesting electrical and optical changes generated when they are doped, which makes them candidates for use as materials for electronic and optical devices such as batteries¹⁰, transistors^{11,12}, antistatic fabrics¹³, heat reflecting windows³, and as chemical vapors sensors^{6,14}.

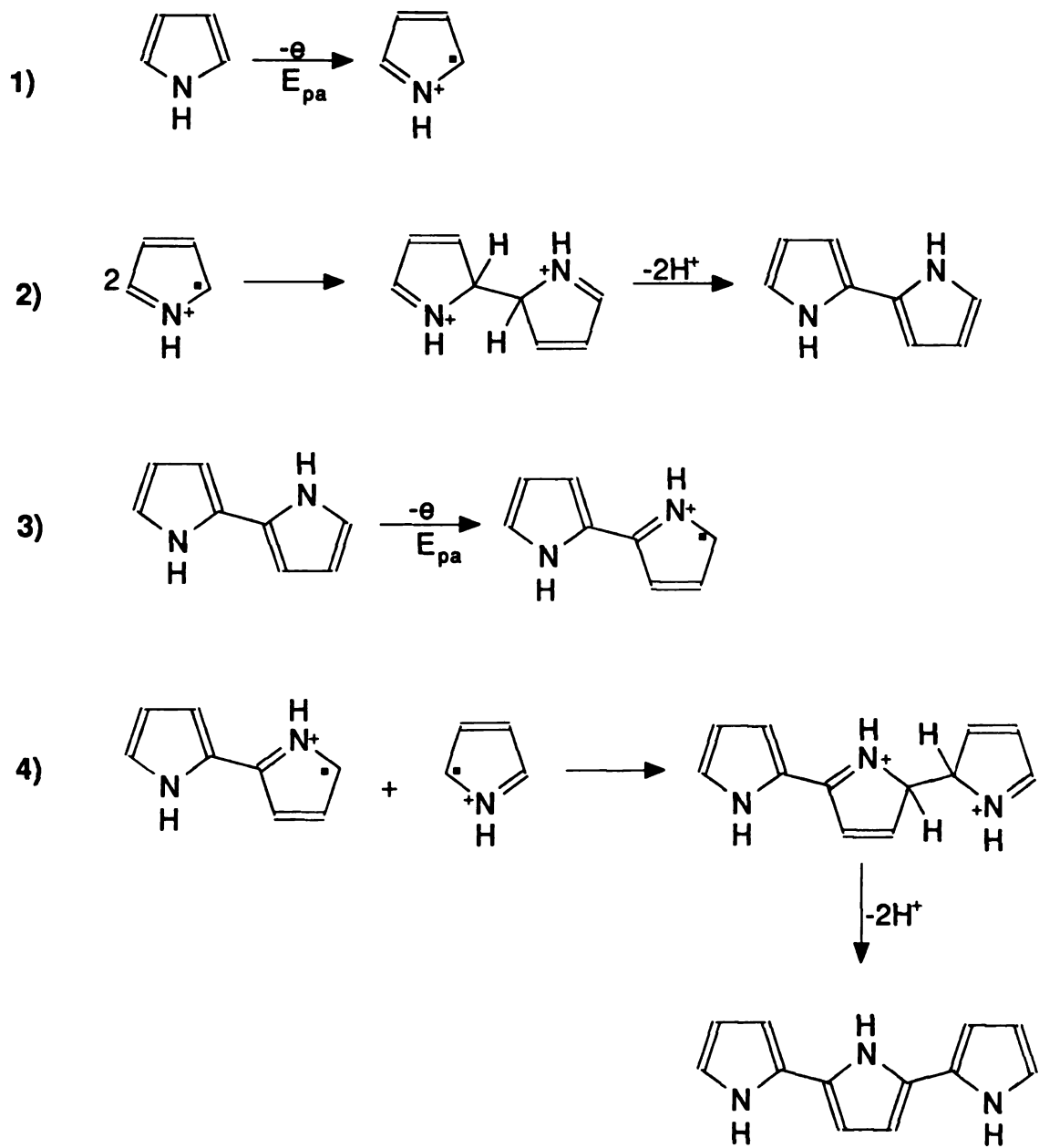
The conductivity values observed for the heteroaromatic polymers can vary over several orders of magnitude depending upon the method of polymerization and doping, as well as the counter anion used.^{15,16,17} These are

experimental factors which are independent of the monomer composition. Under a set of standard reaction conditions, it should be possible to investigate the effect of changes in the structure of the monomer on the electrical and optical response of the polymer. By adjusting structural features, physical parameters such as oxidation potential, band gap energy, and bandwidth may be able to be 'tuned' to meet specific needs.^{18,19}

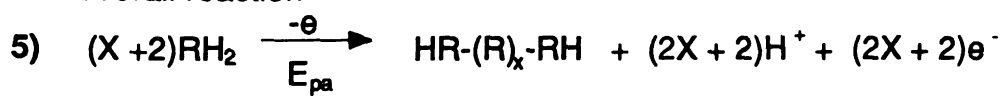
In order to determine the synthetic design factors which will result in the desired modifications, the mechanistic aspects of the electropolymerization and oxidative doping reactions need to be understood.

When a molecule (R) is electrooxidized at an electrode surface, a radical cation ($R^{\bullet+}$) is formed. The electron transfer reaction is much faster than the rate of diffusion of R from the bulk solution to the electrode surface. Accordingly, at the applied voltage, molecules close to the electrode surface region will occur only in oxidized state $R^{\bullet+}$. This insures a high concentration of $R^{\bullet+}$ at the electrode surface, which is continuously maintained by the steady state diffusion of R from the bulk. These monomeric radical cations can undergo a variety of subsequent reactions depending upon their intrinsic stability (chemical reactivity).²⁰ When $R^{\bullet+}$ is relatively stable, it can diffuse away from the electrode surface and undergo reaction to form low molecular weight soluble products. If $R^{\bullet+}$ is very unstable, it can rapidly undergo indiscriminate reaction with either the solvent or anions to form low molecular weight, soluble products. Between these two extremes, $R^{\bullet+}$ can undergo dimerization reaction or electropolymerization. As an illustrative example Scheme 1 shows the electropolymerization of pyrrole.

Evidence for such a reaction path, in which chain propagation is dependent on the presence of $R^{\bullet+}$, is reflected in the following: (a) the cyclic voltammograms reveal an $E(CE)_n$ process,^{21,22} i.e., a sequence of steps whereby an electron transfer event (E) is followed by a chemical reaction (C) and a

Scheme 1. Proposed mechanism of the electrochemical polymerization reaction

Overall reaction



subsequent electron transfer reaction (E). Since the film forming reaction can be described as a cascade of ECE reactions, the term $E(CE)_n$ is used;²³ (b) in order to sustain film growth at the electrode surface the electrode potential has to be maintained at the electrochemical oxidation potential of R; (c) The film-forming reaction is surfaced localized, and no evidence of polymerization in the bulk of the solution has been observed. It has been observed that during the electropolymerization reaction, the pH of the solution becomes increasingly acidic, consistent with the elimination of protons.²⁴

One of the important features found with the electropolymerization reaction is that it proceeds with electrochemical stoichiometry.²⁵ The film forming reactions typically proceed with n values (n is the number of faradays of electricity per mole of electroactive substance) in slight excess of 2.0.²⁰ The n value can be measured in several ways. One of the most convenient is from cyclic voltammograms, utilizing the Nicholson and Shain treatment for a totally irreversible reaction.²⁶ However, the n values derived from voltammograms really represent the total reaction at the surface and can include secondary chemical reactions that accompany the electropolymerization, such as dimerization reactions to form soluble products. A more quantitative estimate of the degree of oxidation in the polymer film comes from elemental analysis data. It has been found that the extent of oxidation is between 0.07 and 0.45.^{8a,8b,25}

The actual number of monomer units in the polymer is unknown, although recent tritium labelling studies²⁷ of poly(3,4-dimethylpyrrole)ClO₄ indicate that there can be as many as 750 units, which corresponds to a molecular weight of about 100,000.

The idealized structure of the heteroaromatic conductive polymer as shown in Figure 4, consists of a series of α,α' -linked monomer units.²⁵ This hypothesis has been supported primarily by the failure of 2-substituted pyrrole to

electropolymerize. Also oxidative degradation studies of chemically synthesized polypyrrole yielded mainly 2,5-disubstituted products.²⁸

Waltman and Bargon have done studies using INDO (intermediate neglect of differential overlap) molecular orbital calculations for pyrrole, and thiophene, which show that the α position does contain the highest unpaired electron density.¹⁶ However, as the oligomers grow in size, delocalization of the radical cation through the extended π -system causes the distribution of unpaired electron density to become more diffuse, so that after the chain has incorporated three or four monomer units, neither the α nor the β positions of the oligomer are strongly favored in the coupling process. The result is that a number of α,β' -cross-links can be expected. X-ray photoemission studies show that as many as one out of three pyrrole rings is affected by structural disorder.²⁹ As a consequence, the bandwidth, which is related to the conjugation of the polymer, decreases together with the conductivity.³⁰

By altering the heteroatom composition, the sequence distribution and the peripheral substituents of monomers, it is possible to change the electrical, optical and mechanical properties of conducting polymers. The most effective method to accomplish this has been the addition of substituents to the polymer skeleton.¹⁶ The substituents can influence the electropolymerization by either a steric effect or an electronic effect. Table 1 summarizes the cyclic voltammetry data for thiophene, 3-substituted thiophene, pyrrole, 1 and 3 substituted pyrroles. By appropriately substituting the 3-position of thiophene, the monomers and polymers are electroactive in different regions of the electrochemical voltage scale. Electron-donating substituents stabilize the radical cation intermediate so that the oxidation potentials for the monomer and polymer are lowered. By lowering the oxidation potential of the monomer, less side reactions between monomeric cation radicals and other species occur. Electron-withdrawing

substituents, such as cyano or nitro groups, destabilize the radical cation intermediates. These leads to a higher E_{pa} and no film forming reactions. In general, small alkyl groups provide the most positive influence on the electrochemistry of the monomers.

The positioning of a stabilizing substituent on the 3 or 4 positions of thiophene increases the availability of the α, α' bonds (2,5-position) by blocking the β positions therefore yielding a more ordered and hence more conductive polymer. This is illustrated by the fact that poly-3-methylthiophene displays a $10^2 - 10^3$ fold enhancement in conductivity over polythiophene, when the films are prepared under the same conditions. The same thing is true with pyrroles.

Table 1. Oxidation potential and conductivity of substituted systems ^{18,33}

Monomer	Monomer E_{pa} (V)	Polymer E_{pa} (V)	Conductivity (S/cm)
3-Methylpyrrole	0.86	-0.25	5000
N-methylpyrrole	1.12	0.50	0.001
Pyrrole	1.20	-0.15	1000
3-Methylthiophene	1.86	0.72	1000
3-Iodothiophene	2.03	-----	--
Thiophene	2.06	0.96	1-100
3-Bromothiophene	2.10	1.06	--
3-Cyanothiophene	2.46	-----	--
3-Nitrothiophene	2.69	-----	--

Another advantage of adding alkyl groups to the monomers, is that it improves the solubility of the polymers. Ezquerro and coworkers synthesized a series of n-alkyl substituted pyrroles ranging from n=1 to 17, and found that the neutral as well as the oxidized polymers were soluble in most organic common organic solvents.³¹ Since the polymers were soluble they were able to determine

a molecular weight which was in the range of 5000 to 10,000 ($X=25-50$) by gel permeation chromatography. Also Elsembaumer and coworkers studied thiophenes and found that alkyl substituents equal to or greater in size than butyl, greatly improved the solubility of both doped and undoped polymers. It was interesting to find that neither the substituents nor the nature of the dopant had much effect on the conductivity of the doped polymers.³² The molecular weights were generally about 2500 as determined by end group analysis.

Another example in which substituents give rise to modifications in the properties of polymer films comes from N-alkyl-substituted pyrroles.³⁴ From Table 1, the conductivity of polypyrrole and poly-N-methylpyrrole is 1000 and 10^{-3} respectively. The reason for such a tremendous change in conductivity is explained by the fact that polypyrrole is able to achieve a coplanar conformation in the oxidized state,¹⁶ while poly-N-methylpyrrole is thought to be in a twisted conformation.³⁴ This is the result of steric interference to a planar conformation of the rings. If steric interference results in a deviation from coplanarity of greater than 40% then a significant lowering in conductivity is observed.³⁵ This steric interference argument is supported by the fact that a copolymer of pyrrole and N-methylpyrrole has a conductivity that is half way (1 S/cm) between the conductivity of the parent polymers.³⁶ In this case the pyrrole serves as an spacer to decrease the undesired steric interaction of the N-methyl group.

Pyrrole is unique by the fact that it can be functionalized at the nitrogen position by a wide variety of substituents. The N-phenyl substituent assumes a particular important role because it provides a means of introducing a wide selection of functional groups into a polymer. Salmon and coworker, prepared a series of N-arylpyrrole polymers by the electropolymerization of the monomers listed on Table 2.^{37,38}

Of particular interest is the p-nitrophenyl derivative polymer. It shifts the anodic peak by 200mV, because of the inductive effect of the nitro group (electron withdrawing), through the phenyl substituent. For this effect to take place the phenyl and pyrrole rings must lie in the same plane (or nearly so) and be conjugated. When the p-nitrophenyl polypyrrole polymer is scanned cathodically (reduced) another peak is observed at -1.00 V. In this case the negative charge is localized on the nitro group and is not extensively delocalized through the polymer π -electron structure. This result suggests that the p-nitrophenyl and the pyrrole rings must be orthogonal to each other and thus poorly conjugated.

Table 2. Electrochemical data for N-aryl-substituted pyrrole films

<u>N-Substituent</u>	<u>Monomer E_{pa} (V/SSCE)</u>	<u>Polymer E_{pa} (V/SSCE)</u>
p-Dimethyl aminophenyl	1.29	-----
p-Anisyl	1.36	0.70
p-Tolyl	1.50	0.70
p-Nitrophenyl	1.60	0.90
Phenyl	1.80	0.74

Another method to "tune" the properties of conductive polymers is the manipulation of the heteroatom composition. The preparation of copolymers containing a mixture of pyrrole, thiophene, furan, and selenophene, have been investigated to only a very limited extent. By making copolymers, it is hoped that the unique physical, chemical and electronic properties of the individual heterocycles can be transferred throughout the polymer via the π -system.¹⁸

Theoretical studies indicate that the electronic properties of a copolymer should be intermediate between those of the corresponding homopolymers.³⁹

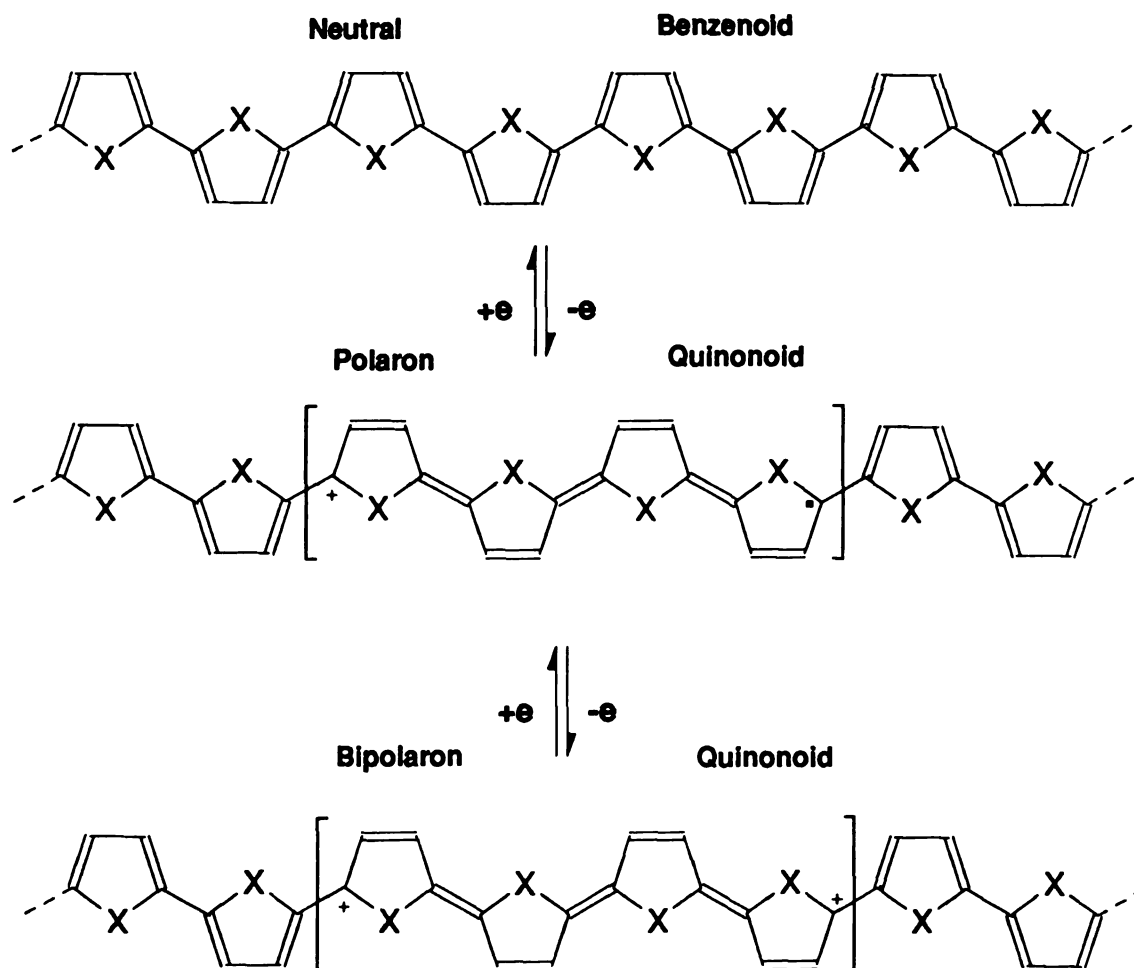
Since pyrrole, thiophene, and furan, each possess unique oxidation potentials, then copolymers containing a range of heterocycle stoichiometries should provide a continuum of intermediate oxidation potential values. The conductivity of a heteroaromatic polymer depends upon its ability to form a quinonoid (bipolaron) conformation, and since the ability to form the quinonoid structure depends upon the aromatic character of each heteroaromatic unit, then it may be possible to change the conductivity as well as the band gap.⁴⁰ It has been calculated that the energy required to form the quinonoid conformation from the aromatic conformation is 16 Kcal/mole per ring for thiophene, but only 14.4 Kcal/mole per ring for pyrrole.⁴¹ This means that increasing the pyrrole concentration in the copolymer should lead to increased conductivity (Scheme 2). This in fact has been shown to be the case.

The synthesis of copolymers has been very difficult mainly because of the large difference in oxidation potential of the heteroaromatic units, e.g. pyrrole $E_{pa}=1.20$ V, thiophene $E_{pa}=2.06$ V. When one tries to polymerize thiophene and pyrrole together, there is no control over either the stoichiometry or the sequence distribution of the monomeric unit. In contrast, α -terthiophene ($E_{pa}=1.05$ V) has an oxidation potential relatively close to pyrrole, so that a copolymer between these two monomers has been made with a conductivity of 1.0 S/cm.⁴² However, the composition of the copolymer is unknown. Very few copolymers have been synthesized in which both the stoichiometry and sequence distribution is known. Naitoh reported the synthesis of a polymer consisting of an equal mixture of pyrrole and thiophene units, by the electropolymerization of 2-(2-thienyl)pyrrole.⁴³ Due to the lack of symmetry in the monomer, the sequence distribution of the copolymer is unknown. The

oxidation potential of the copolymer is 0.50 V which is midway between that of polypyrrole (-0.15V) and polythiophene (0.96 V).

Wynberg and coworkers⁴⁴ were the first ones to synthesize mixed monomers of pyrrole and thiophene which were used by Ferraris as monomers for the preparation of mixed polymer systems.⁴⁵ Because the monomers are

Scheme 2. Benzenoid and Quinonoid conformations of conductive polymers



symmetrical, the resulting copolymers do have a known stoichiometry and sequence distribution of heteroaromatic units. The electrical properties obtained are dependent upon the nature of the heteroatom X (Table 3). The peak oxidation potential for both the monomer and polymeric materials span a range of 0.6 to 1.0 V. The conductivity values vary over four orders of magnitude.

Table 3. Electrochemical and optical data for Ferraris' copolymers⁴⁵

Monomers	Monomer E_{pa} (V/SCE)	Polymer E_{pa} (V/SCE)	E(eV)	Conductivity (S/cm)
SNS	0.66	0.60	2.77	280
SMS	0.73	0.96	2.96	1
SOS	0.94	0.82	2.61	0.3
SSS	1.01	0.89	2.70	20

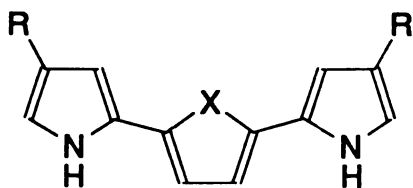
S=Thiophene N=Pyrrrole M= N-Methylpyrrole O=Furan

The main question that arises from using these tercylic, mixed monomers is whether the two α,α' -linkages incorporated into the monomer increases the linearity of the polymer. The literature presents conflicting experimental findings as to whether an increase in the number of rings in the monomer increases the degree of conjugation in the resulting polymer.^{46,47} From a statistical point of view, two-thirds of the linkages are guaranteed to be α,α' , but from INDO calculations it is known that as the number of rings get larger, the preference for α coupling over β diminishes. Henzie⁴⁸ conducted an experiment in which he electropolymerized thiophene, α -bithiophene, and α -quaterthiophene. He found that in the case of the tetramer polymerization, a sharp and intense anodic and cathodic wave was obtained, this is the typical

behavior for a polymer with regular structure but a narrow molecular weight distribution. A similar experiment, by Garnier and coworkers indicated that increasing the chain length of the starting monomer leads to a lower degree of polymerization and to a less conjugated polymer.⁴⁷

Merrill and coworkers made an alternate series of symmetrical tricycles of pyrrole and thiophene in which the sequence of the heteroatom is reversed to those of Ferraris' (Scheme 3).⁴⁹ Experimental results for copolymers made from **1a** and **1b** will be presented in this thesis.

Scheme 3. Merrill's tercycles



1a.	R=H	X=S
1b.	R=CH ₃	X=S
2a.	R=H	X=NH
2b.	R=CH ₃	X=NH
3.	R=H	X=O

Most conductive polymers have a linear chain structure, and conduct along the chains. Any cross-linkages in the chain are considered as defects which interrupts conjugation and decrease the conductivity. However, cross-linkages can make the polymer film flexible and stable to oxidation or mechanical destruction and strengthens adhesion to metal surfaces,⁵⁰ as well as the possibility of a two-dimensional conducting network. Aviram, of the IBM

Corporation has suggested that two-dimensional conducting networks should exhibit properties that would make it suitable for interconnection into future molecular electronic devices.⁵¹ It is interesting to study the possibility of synthesis of composite monomers which would make cross-linked conductive polymers and be able to produce two-dimensional conducting networks.

In this study we present our attempts to synthesize a series of monomers with defined stoichiometry that have the possibility of becoming conducting polymers upon electrochemical or chemical oxidation. The polymers will be characterized by electrochemical and spectroscopic methods and thus relate polymer structure to electrical and spectroscopic properties.

EXPERIMENTAL

1. Instrumentation

Electrochemical

A Princeton Applied Research (PAR) 273 potentiostat/galvanostat was interfaced to a Zenith 248AT 8Mhz computer with a National Instrument PC 2A IEEE-48 card for instrument control and data acquisition. The experimental results were recorded on a Hewlett-Packard 7475A plotter. This setup was used to make the polymers and study their charging/discharging characteristics. A Bioanalytical System (BAS) 100A potentiostat was interfaced to a Zenith 158XT 8Mhz computer and a Hewlett-Packard Colorpro plotter. This setup was used for cyclic voltammetry and to control the potential during the *in situ* spectroelectrochemical experiments. A Pine Instruments AFRDE4 bipotentiostat was used in conjunction with the PAR 273 to do the *in situ* conductivity measurements.

Spectroscopic

Proton nuclear magnetic resonance spectra were obtained on either a Varian Gemini 300MHz, or a Bruker WM-250 (250MHz) spectrometer. Chemical shifts are reported in parts per million (δ) using the proton resonance of the residual solvent as the internal reference.

Infrared spectra were obtained in a Nicolet 740 Fourier transform spectrophotometer using KBr pressed pellets. The UV-Vis-NIR absorption spectra were recorded on a Beckman DU-64 single beam spectrophotometer.

Electron impact mass spectra (EI-MS) were recorded on a Finnigan 4000 with a INCOS 4021 data system. High mass spectra were obtained on a JOEL HX110 by fast atom bombardment (FAB), at the Michigan State University Regional Mass Spectrometry Facility, Department of Biochemistry, East Lansing, MI.

Miscellaneous

Flash column chromatography was performed according to the procedure of Still, et.al.⁵⁶ Chromatography parameters are reported as follows: g of solid phase, column outer diameter (od), eluent, R_f (distance that a spot of interest has moved from origin divided by the distance the solvent front has moved from origin.).

Melting points were determined on a Thomas-Hoover capillary melting point apparatus and are uncorrected.

2. Glassware

Two different types of glass electrochemical cells, that can be connected directly to a high vacuum line were constructed and used in this study. Cyclic voltammetry was carried out mostly in a one-compartment cell, with a three electrode arrangement. The counter electrode was made from a platinum wire flattened at one end so that it was parallel to the working electrode. This ensures that there are no potential gradients on the working electrode. The reference electrode was a silver wire which was saturated with silver nitrate. This was accomplished by immersing a silver wire in concentrated nitric acid, rinsing with water and drying. The working electrode was a 0.018 cm² platinum disk (Bioanalytical Systems Inc.) encapsulated in an epoxy material.

The other glass electrochemical cell was a two-compartment cell in which the compartments were separated by a fine porosity glass frit. In this

arrangement the counter electrode (Pt) and working electrode (Pt disk, 0.018cm²) were placed in one compartment and the reference electrode was placed in the other. The reference electrode was a sodium saturated calomel electrode (SSCE) that differs by 7 mV from a regular saturated calomel electrode (SCE). The reason for not using a SCE reference is that it clogs up in a non-aqueous media, while the SSCE does not.

An indium-tin-oxide (ITO) conducting glass working electrode, a platinum flag counter electrode and a silver wire reference electrode were used in the optical characterization experiments.

Prior to beginning of the electrochemical experiments, the solvents were transferred into the electrochemical cells via a high vacuum line (10⁻⁶ torr). The cells were then backfilled with argon (Matheson 99.95%) to maintain an air, and moisture-free atmosphere throughout the experiments. The argon was previously passed through a drying column to remove residual oxygen and moisture.

3. Electrochemical Solvents and Reagents

Acetonitrile (HPLC grade, Burdick and Jackson) was dried over calcium hydride and then decanted. The decanted solvent was degassed in the high vacuum line by employing several freeze-pump-thaw cycles and then vacuum-transferred to a greaseless round bottomed flask containing activated 3A molecular sieves and stored under vacuum. Tetrahydrofuran (HPLC grade, Burdick and Jackson) was dried over sodium-potassium alloy and the same procedure used for acetonitrile was used to degas, transfer and store the solvents. Dichloromethane (Spectra grade, Mallinckrodt) and polycarbonate (Aldrich) were used without further purification.

Tetrabutylammonium fluoroborate (electrometric grade, Southwestern Analytical Chemicals) was recrystallized from ethyl acetate/diethyl ether (5:1 volume ratio, at 60° C) and vacuum dried for three days.

4. Electrochemical Techniques

Controlled potential coulometry (CPC), or bulk electrolysis as it is also called, is an experiment in which an electrochemical reaction is allowed to proceed at an electrode held at a constant potential. The total charge passed during the electrolysis is obtained by integrating the current passed over time. CPC is commonly used to determine the number of moles of material electrolyzed (N) or the number of electrons involved in the electrolysis process (n). This is accomplished by knowing the amount of charge (Q) passed through the cell during electrolysis. These quantities are related by Faraday's law:

$$Q = nFN$$

where :

Q = charge transferred

n = number of electrons involved in the reaction

F = Faraday's constant (96485 C/mol)

N = moles of material electrolyzed

Normally CPC is used to determine the degree of partial oxidation or reduction as a function of potential. This is an extremely useful quantity to know so that one can calculate the degree of partial oxidation or reduction that will yield the most conducting state of a conductive polymer. Regrettably, this only applies to a system that is in solution. Conductive polymer materials are anchored on the surface of the electrode and act like a variable capacitor, so that the current that is measured is a combination of capacitive and faradaic currents. In addition to that, the medium used is non-aqueous, which is somewhat resistive, even with the addition of supporting electrolyte. For these

reasons CPC is only used to control the potential of the working electrode during spectroelectrochemical experiments, and cannot be used to find out the degree of partial oxidation or reduction of the conductive materials.

Probably the most widely used electrochemical technique is cyclic voltammetry (CV). Cyclic voltammetry is carried out by sweeping the potential from an initial potential E_1 , where no electron transfer reaction occurs to a final potential E_2 where all the electroactive material at the electrode surface is oxidized or reduced. When E_2 is reached, the direction of voltage scan is reversed back to, but not always, the initial potential E_1 . Either 1 cycle (from E_1 to E_2 and back to E_1) or more than one cycle can be carried out. Scan rates can be varied over a wide range; this is an extremely useful feature of CV. This experiment, though relatively simple, is capable of providing a great deal of useful information about electrochemical behavior with relative little experimental effort.

Cyclic voltammetry was used in this study to make the conductive polymers from their respective monomers at a concentration of 0.01 to 1×10^{-3} M. Polymerization was carried out at 0° C in an electrolytic solution of either acetonitrile, dichloromethane, tetrahydrofuran, or polycarbonate, containing 0.1 M supporting electrolyte (TBABF₄). The polymers were made as films anchored on the electrode surface by scanning the respective solutions at 50 mV/sec. Neutral or oxidized forms of the polymer films were prepared by placing the polymer in a clean (no monomer) solution and applying adequate potentials to obtain the desired oxidation level. One interesting factor about the cyclic voltammograms of conductive materials is that the magnitude of the anodic or cathodic peaks varies proportionally to the scan rate and not the square root of the scan rate. This is because the electroactive material is already at the electrode; it does not have to migrate from the solution.

Apart from the usual electrochemical quantities derived from CV, there is another effect that takes place when conductive polymer films are attached to the electrode surface. During the course of a CV a large current jump is observed when the sweep is reversed. This is commonly called the "capacitive effect". A number of studies have been done to determine the source of the capacitive effect.^{53,54,55} It has been found that there are two different doping mechanisms. One is a relatively rapid ionic doping associated to a double layer formation around the conductive polymer chains. The second doping process which is very slow can be attributed to a diffuse faradaic doping mechanism. It is the ions associated with the double layer that are responsible for the capacitive effect. Therefore, when a capacitive effect is observed, it may be interpreted to mean that there is a possibility that the polymer material will be a conductor.

5. Spectroelectrochemistry

Conductive polymers are also being investigated because of their non-linear optical behavior. They change their optical characteristics as a function of doping level. Experimental and theoretical studies have shown that the doping process induces localized charges along the polymer chain.^{57,58} These modifications markedly affect the electronic structure of the polymer. For conductive polymers without a degenerate ground state such as pyrrole or thiophene, polarons and bipolarons are the dominant charge storage configuration. A common way to study the existence of polarons and bipolarons is by investigating the optical absorption spectra of the conductive polymer. When a neutral conductive polymer is lightly oxidized, it forms radical cations that are localized along the chains as shown in scheme 2. This means that there is the possibility of at least four optical transitions. They are from the VB to the CB, from the VB to the lower polaron level from the VB to the higher polaron

level and from the lower polaron level to the higher polaron level. It is very hard to see the transitions between the polaron levels because the radical cations (polarons) tend to couple up, forming a bond.

In the case of a strongly oxidized polymer, the most likely configuration is that involving bipolarons (scheme 2). There should only be three distinct optical transitions. They are from the VB to the CB, from the VB to lower bipolaron band, and from the VB to higher bipolaron band (Figure 2).

As a rule of thumb⁵⁷, if the band gap (E_g) is greater than 3 eV, the undoped insulating polymer is transparent (or lightly colored), whereas after doping, the conductive polymer is typically highly absorbing in the visible. If, however, E_g is small (1-1.5 eV), the neutral polymer will be highly absorbing in the visible, and after doping, the conductive polymer is transparent in this same region. Polymers derived from thiophene or pyrrole usually have a band gap in the range of 3-4 eV, with transitions between the VB and higher bipolaron band in the range of 1.5 -2.5 eV, and VB to lower bipolaron band below 1 eV.

Spectroelectrochemistry is extremely useful in observing these transitions as a function of the oxidation potential applied to the conductive polymer film. The experimental setup consists of a 1x1x4 cm quartz cuvette fitted with an indium-tin oxide transparent electrode which functioned as the working electrode, a platinum flag as counter electrode, and a silver wire as reference electrode. The electrodes were held in place by fitting them in a teflon top.

One problem associated with this setup is that the transparent ITO electrode, cuts off at about 300 nm, and the upper wavelength of the spectrophotometer is 900 nm. This means that one cannot see the transitions below 1.4 eV. The other problem is that not all monomers make films that adhere to the ITO electrode surface.

6. Conductivity

Among the impressive properties of conductive polymers, conductivity is the most interesting and promising detail. Besides the obvious implications of absolute conductivities and relative conductivity changes for various applications, a detailed understanding of this characteristic material property provides helpful knowledge for the development of mechanistic conductivity models for these materials. Together with results from a broad variety of spectroscopic and spectroelectrochemical methods a deeper understanding of structure and properties of conductive polymers should be achievable.⁵⁹

Most conductivity measurements reported so far were made *ex situ* by doping the samples chemically and pressing them into pellets. The conductivities measured this way do not reflect the true conductivities of the materials. It would be much better to be able to measure the conductivity of a conductive polymer as a film, *in situ*. For this reason two different types of electrodes were constructed for the *in situ* conductivity measurement as a function of oxidation potential applied to the polymer. This way it is possible to find out what oxidation level gives the highest conductivity.

The best method to measure conductivity is by a four-point-probe method.⁶⁰ Only two designs based on microlithographically prepared electrodes have been described,^{61,62, 63, 64,65} but such electrodes are not available and are difficult to prepare without access to specialized equipment.

A four-point-probe electrode was constructed by burying four thin platinum wires between five platinum strips that were separated by thin teflon sheets, as illustrated by Figure 5. By passing a current through the polymer film using the outer leads and measuring the potential drop across the inner leads, one can know the resistance of the polymer film. The resistivity (ρ) is given by:

$$\rho = (V/I) \times (w) \times (\pi/\ln 2) \times F(w/s)$$

were:

V = Potential across inner leads

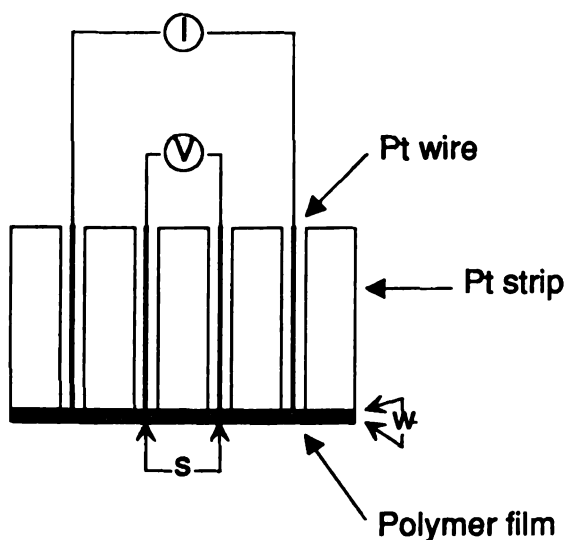
I = current passed through outer leads

w = Thickness of film

s = Distance between leads

$F(w/s)$ is a function of the thickness of the film (w) and the distance between the probe points (s). As long as (w/s) is less than 0.4, then $F(w/s)$ will be very close to unity and can be neglected.⁶⁰ The conductivity is the reciprocal of resistivity. This electrode works well if the polymerized film covers the entire electrode surface.

Figure 5. Four-point-probe electrode



To be able to measure the conductivity of polymers that do not grow very easily, a two-band electrode was constructed following the design of Schiavon⁶⁶ and Holze.⁶⁷ In this method an electrode comprised of two platinum strips

separated by a very thin gap is used. By using the configuration shown in Figure 6 one can measure the conductivity of the polymer as function of the applied oxidation potential. Two potentiostats are needed. The only problem with this design is that all dimensions of the polymer film must be known. It is very difficult to know the thickness of the films. It is estimated that the thickness of the film must be at least half of the gap distance between the strips. In this design the conductivity σ is given by:

$$\sigma = (I/V) \times (w/sL)$$

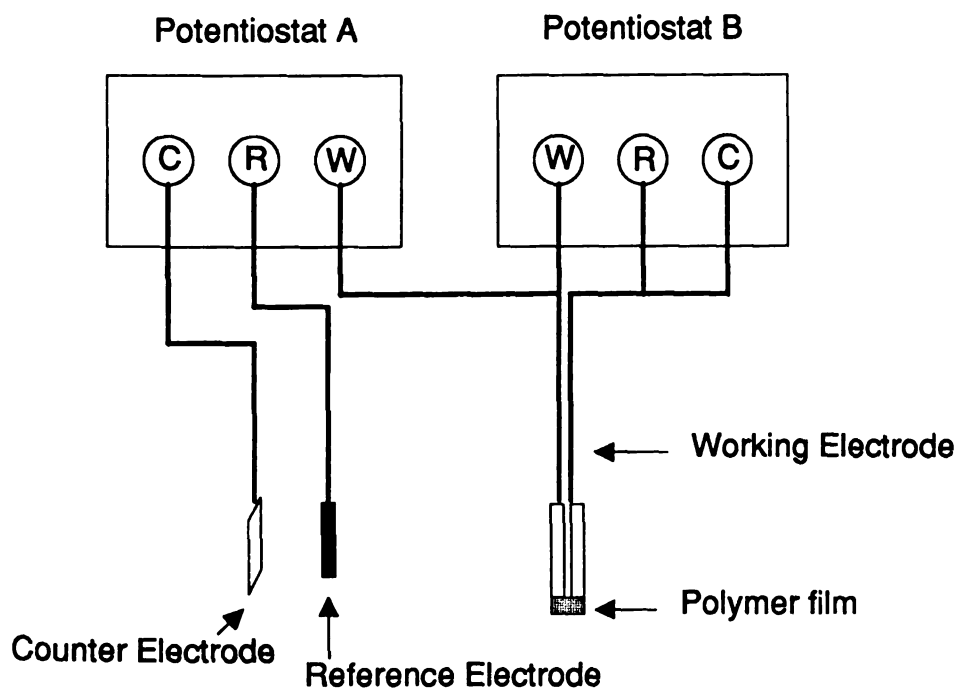
where:

I = Current passed through the film L = Strip length

V = Voltage across film s = Distance across gap

w = Thickness

Figure 6. Gap electrode for *in situ* conductivity measurement



7. Synthesis

1,4-bis(1-pyrryl)benzene (5). 0.660 g of dimethoxytetrahydrofuran (5×10^{-3} M) and 0.270 g of p-phenylenediamine (2.5×10^{-3}) were dissolved in 20 ml of acetic acid and then the solution was heated in a steam bath. A light brown precipitate formed immediately. After the solution had refluxed for 10 minutes, 20 ml of acetic acid were added and again heated for 5 more minutes. The hot solution was filtered through a medium-porosity funnel and a small amount of brown precipitate was collected. After the filtrate had cooled it was filtered again yielding light-brown crystals that were washed with ether and dried. The yield was 0.205 g of the desired material (42 %), 228-229° C, lit. 229-231° C. **5** is partially soluble in acetonitrile, and very soluble in CH_2Cl_2 .

1-Amino-4-[2,5-bis(2-thienyl)-1-pyrryl]benzene (16). A saturated solution was made by adding enough p-toluenesulfonic acid to 25 ml of degassed toluene. In a separate 100 ml round bottom flask, 0.69 g of 1,4-diketone **14** (2.78×10^{-3} mols) and 0.90 g of p-phenylenediamine (**4**) (8.55×10^{-3} mols), were added to 30 ml of degassed toluene. To this solution was added the 25 ml of saturated solution of p-TSA under argon, and left refluxing for 3 days. The toluene was removed by evaporation and the solid material was dissolved in ethyl acetate. TLC in 50:50 ethyl acetate/hexane revealed three fractions at $R_f=0.5$, $R_f=0.3$, and $R_f=0.1$. Flash column chromatography of the product (50g of 230-400 mesh silica gel, 30 mm o.d. column, 50:50 ethyl acetate/hexane) provided 0.793 g of **16** (89 % yield). Elemental analysis resulted in 67.30 % C, 4.60 % H, 8.53 % N, 19.52 % S. The calculated values are 67.05 % C, 4.38 % H, 8.69 % N, 19.88 % S. $^1\text{H-NMR}$ (DMSO) δ 7.25 (dd, $J=5.0$, 1.1 Hz 2H), 6.94 (d, $J=8.7$ Hz 2H), 6.87 (m, 2H), 6.74 (dd, $J=3.7$, 1.3 Hz, 2H), 6.63 (d, $J=8.6$ Hz, 2H), 6.50 (s, 2H), 5.50

(s, 2H). EI-MS (70 eV), m/z (relative intensity) 324 ((M+2)⁺, 5.0), 323 ((M+1)⁺, 10.1), 322 ((M)⁺, 60.0), 212 (31.1), 203 (10.0), 180 (15.0), 161 (15.0), 144 (23.0), 121 (13.1), 92 (20.0), 77 (21.0), 65 (100.0), 57 (21.1). $\epsilon=1.83 \times 10^4$ l/cm mol at 340 nm.

1,4-Bis[2,5-bis(2-thienyl)-1-pyrrolyl]benzene (6). A solution was made by mixing 0.595 g of **16** (1.85×10^{-3} mols) with 0.462 g of **14** (1.847×10^{-3} mols) in 50 ml of degassed toluene. To this solution was added 10 ml of acetic acid, then the solution was refluxed for 3 days. The toluene and acetic acid were removed by evaporation over nitrogen. The solid residue was cast in ethyl acetate and filtered. A brown precipitate was collected and washed with ethyl acetate and ether, then dried. 0.30 g (3 %) of **6** m.p. 305-307° C, was collected. ¹H-NMR (CD₃Cl) δ 7.36 (s, 4H), 7.13 (dd, J=5.2, 1.1 Hz, 4H), 6.86 (m, 4H), 6.61 (dd, J=3.6, 1.1 Hz, 4H), 6.55 (s, 4H). EI-MS (70 eV), m/z (relative intensity) 538 (M⁺, 7.75), 537 (M⁺, 23.36), 536 (M⁺, 100), 306 (1.13), 126 (1.75), 46 (3.16), 45 (58.92), 44 (47.62), 41 (2.60). $\epsilon=1.5 \times 10^4$ l/cm mol at 325 nm.

Alternate route to 6. To a two-neck 50 ml round bottom flask were added 0.535 g of p-phenylenediamine hydrochloride (2.95×10^{-3} mols) and 7.38 ml of 2.0 M solution of trimethylaluminum in toluene, under nitrogen. After 1 hour the solution became clear and all the hydrochloride salt had dissolved and the evolution of methane had stopped. In a separate two-neck 50 ml round bottom, 1.464 g **14** (5.90×10^{-3} mols) were dissolved in 30 ml of degassed, dried toluene. To this solution was added very slowly, under nitrogen, the previously prepared aluminum reagent. A brown precipitate formed immediately. The solution was left stirring at room temperature for 12 hours, then 25 ml of 5 % HCl solution was added to quench any unused aluminum reagent. A brown precipitate was collected by filtration and washed with ethyl acetate, and ether to

remove any starting material, then dried. 0.36 g of product were collected, which had a m.p. $> 300^{\circ}\text{C}$. EI-MS revealed a parent peak at m/z 536 which is the desired material 6.

N-[4-[2,5-bis(2-thienyl)-1-pyrryl]phenyl]acetamide (17). A solution was made by dissolving 2.47 g of **14** (9.88×10^{-3} mols) and 0.485 g of **4** (4.49×10^{-2} mols) in 25 ml of acetic acid. The solution was refluxed for 24 hours, then the acetic acid was removed by evaporation over a nitrogen stream. The solid residue was dissolved in 50 ml of saturated NaHCO_3 solution and extracted with 100 ml of CH_2Cl_2 . TLC of the product with 50:50 hexane/ethyl acetate revealed two fractions with $R_f=0.5$ and $R_f=0.2$. The first fraction was identified as starting material **14**. Flash column chromatography of the crude product (160 g of 230-400 mesh silica gel, 30 mm od column, 50:50 hexane/ethyl acetate) yielded 3.1 g of **17** (90 % yield) as white needles, m.p. $243\text{--}244^{\circ}\text{C}$. Elemental analysis resulted in 64.64 % C, 4.46 % H. The calculated values are 64.32 % C, and 4.59 % H assuming 0.5 equivalents of H_2O . $^1\text{H-NMR}$ (DMSO) δ 10.2 (s, 1H) 7.71 (d, $J=8.7$ Hz, 2H), 7.28 (m, 4H), 6.90 (m, $J=3.6$, 2H), 6.70 (dd, $J=3.6$, 1.1 Hz, 2H), 6.56 (s, 2H), 2.10 (s, 3H). $^{13}\text{C-NMR}$ (DMSO) δ 168.1, 139.9, 133.6, 131.4, 129.9, 129.3, 126.5, 124.1, 123.4, 118.6, 108.6, 23.5. EI-MS (70 eV), m/z (relative intensity) 365 ($(M+1)^+$, 7.5), 364 ($(M)^+$, 26.0), 321 (7.0), 212 (38.0), 203 (16.9), 180 (14.1), 171 (33.8), 152 (11.3), 121 (27.5), 108 (15.2), 91 (35.2), 77 (43.0), 65 (100.0). $\epsilon=1.44 \times 10^4$ l/cm mol at 341 nm.

N-[2,5-bis(2-thienyl)-1-pyrryl]benzene (22). A solution was made by dissolving 1.629 g of **14** (6.50×10^{-3} mols) and 1.28 g of aniline with a few grains of p-toluenesulfonic acid, in 25 ml of degassed, dried toluene under nitrogen atmosphere. This solution was refluxed for 4 days. The toluene was removed

by evaporation. TLC of the crude product with 25:75 ethyl acetate/hexane showed one fraction with $R_f=0.7$. Flash column chromatography (50g of 230-400 mesh silica gel, 30 mm od column, 25:75 ethyl acetate/hexane) provided a white-gray powder with a m.p. of 177-178°. Elemental analysis resulted in 69.83 % C, 4.47 % H. The calculated elemental composition is 70.32 % C and 4.26 % H. $^1\text{H-NMR}$ (DMSO) δ 7.51 (m, 3H), 7.35 (dd, $J=8.0$, 2H), 7.28 (dd, $J=5.0$, 2H), 6.86 (t, $J=3.7$, 2H), 6.62 (d, $J=3.5$, 2H), 6.55 (s, 2H). $^{13}\text{C-NMR}$ (DMSO) δ 133.5, 129.5, 129.1, 129.06, 128.9, 126.5, 124.2, 123.6, 108.9. EI-MS (70 eV), m/z (relative intensity) 309 ($(M+2)^+$, 5), 308 ($(M+1)^+$, 12), 307 ($(M)^+$, 70), 230 (6), 197 (20), 172 (22), 153 (9), 137 (20), 121 (20), 77 (100), 69 (23), 63 (20), 57, (13). $\epsilon=1.47 \times 10^4$ l/cm mol at 336 nm.

Alternate route to 22. To a two-neck 50 ml round bottom flask were added 2.340 g of aniline hydrochloride (**21**) (1.80×10^{-2} mols) and 27 ml of 2.0 M solution of trimethylaluminum in toluene (5.41×10^{-2} mols), under nitrogen. After 1 hour the solution became clear and all the hydrochloride salt had dissolved and the evolution of methane had stopped. In a separate two-neck 50 ml round bottom, 4.464 g **14** (1.80×10^{-2} mols) were dissolved in 30 ml of degassed, dried chlorobenzene at 70° C. To this solution was added very slowly, under nitrogen, the previously prepared aluminum reagent. A dark-brown precipitate formed immediately. The solution was left stirring at 70° C for 12 hours, then 100 ml of 5 % HCl solution was added to quench any unused aluminum reagent. TLC of the organic layer in 70:30 hexane/ethyl acetate revealed three fractions. The first fraction was identified as the desired material **22**. Flash column chromatography (150 g of 230-400 mesh silica gel, 50 mm od column, 70:30 hexane/ethyl acetate) yielded 0.55 g (10%) of **22**, m.p. 177-179° C.

1-(Dimethylamino)-4-[2,5-bis(2-thienyl)-1-pyrryl]benzene (23). In a 100 ml round-bottom flask were placed 23.2 mmols of N,N-dimethyl-1,4-phenylenediamine (25), 11.6 mmols of 1,4-diketone (14), a few grains of p-toluenesulfonic acid, and 25 ml of dried, degassed toluene as solvent. The mixture was refluxed for 2 days. The toluene was removed by evaporation. TLC (50:50 hexane/ethyl acetate) of the crude revealed 2 fractions with $R_f=0.8$ and $R_f=0.2$. Flash column chromatography (150 g of 230-400 mesh silica gel, 50 mm o.d. column, 50:50 hexane/ethyl acetate) yielded 3.9 g (95 %) of **23**, as white needles, m.p. 188 - 189° C. $^1\text{H-NMR}$ (DMSO) δ 7.60 (d, $J=5.0$ Hz, 2H), 7.10 (d, $J=8.5$ Hz, 2H), 6.88 (t, $J=4.1$ Hz, 2H), 6.75 (m, 4H), 6.54 (s, 2H), 3.00 (s, 6H). $^{13}\text{C-NMR}$ (DMSO) δ 150.0, 133.9, 129.9, 129.5, 126.3, 124.7, 123.8, 122.9, 111.2, 108.1. EI-MS (70 eV), m/z (relative intensity) 350 (M^+ , 9.2), 240 (7.0), 197 (10.6), 175 (26.8), 149 (10.6), 121 (17.6), 97 (19.0), 77 (43.7), 57 (100.0). $\epsilon=1.66 \times 10^4$ l/cm mol at 342 nm.

(28) Condensation of squaric acid (26) with 16. To 10 ml of DMF in a 25 ml round-bottom were added 0.93 mmols of **16** and 0.47 mmols of squaric acid (26). After 1 hour of refluxing with stirring, a yellow precipitate began to form and the solution turned dark brown from its original yellow-green color. The hot solution was filtered and the precipitate, washed with acetone. 0.07 g of yellow-green solid was collected. FAB-MS gave a fragmentation pattern consistent with the condensation of squaric acid and the phenylamine **16**, with the exception that the parent peak was at m/z 767.

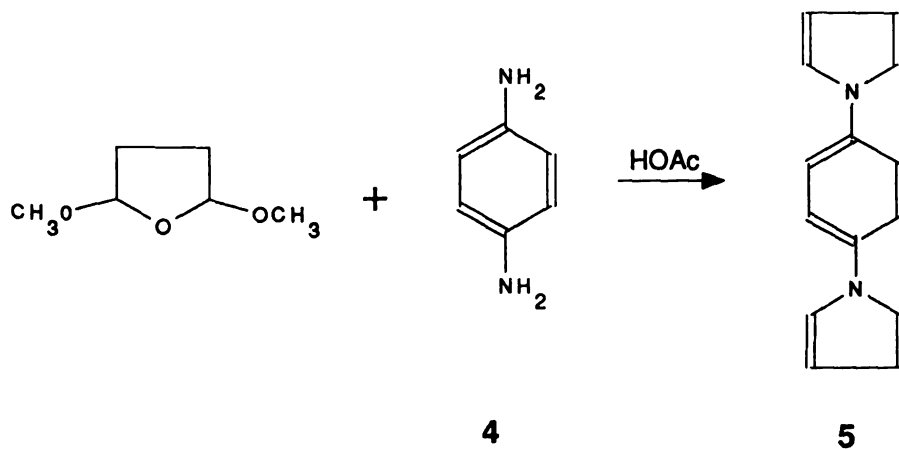
RESULTS AND DISCUSSION

A. Synthesis of 1,4-bis[2,5-bis(2-thienyl)-1-pyrrolyl]benzene

Heteroaromatic polymers such as polypyrrole and polythiophene form linear one-dimensional chains. Monomers such as 1,4-bis(1-pyrrolyl)benzene (5) in which two heteroaromatic molecules are held together by a phenylene bridge, could form a two or three-dimensional heteroaromatic polymer. Very few articles have been published on the preparation and electrical properties of a multi-dimensional conducting polymer.

As a precursor for a multi-dimensional conducting polymer, 1,4-bis(1-pyrrolyl)benzene (DPB) (5) was chosen. DPB is easily made by the method of Elming and Clauson-Kaas,⁵² by reacting p-phenylenediamine (4) with 2,5-dimethoxytetrahydrofuran with acetic acid as solvent and catalyst (Scheme 4).

Scheme 4. Synthesis of 1,4-bis(1-pyrrolyl)benzene



1,4-bis(1-pyrrolyl)benzene has the possibility of polymerizing through the 2 and 5 positions of the pyrrole rings (Scheme 5). One would expect the oxidation potential of DPB to be lower than for pyrrole, since the phenyl group helps to stabilize the radical cation. However, when DPB was subjected to electrochemical oxidation, it displayed a large oxidation potential which shifted anodically as the polymer film grew. These facts suggest that the 2 and 5 positions of DPB are hindered, and that polymerization might be taking place through the 3 and 4 positions of the pyrrole, leading to a polymer that is not well conjugated and thus less conductive, so that as the film grows the electrode becomes more resistive and higher overpotentials are needed for radical cation formation.

Scheme 5. Two-dimensional conductive polymer from 1,4-bis(1-pyrrolyl)benzene.

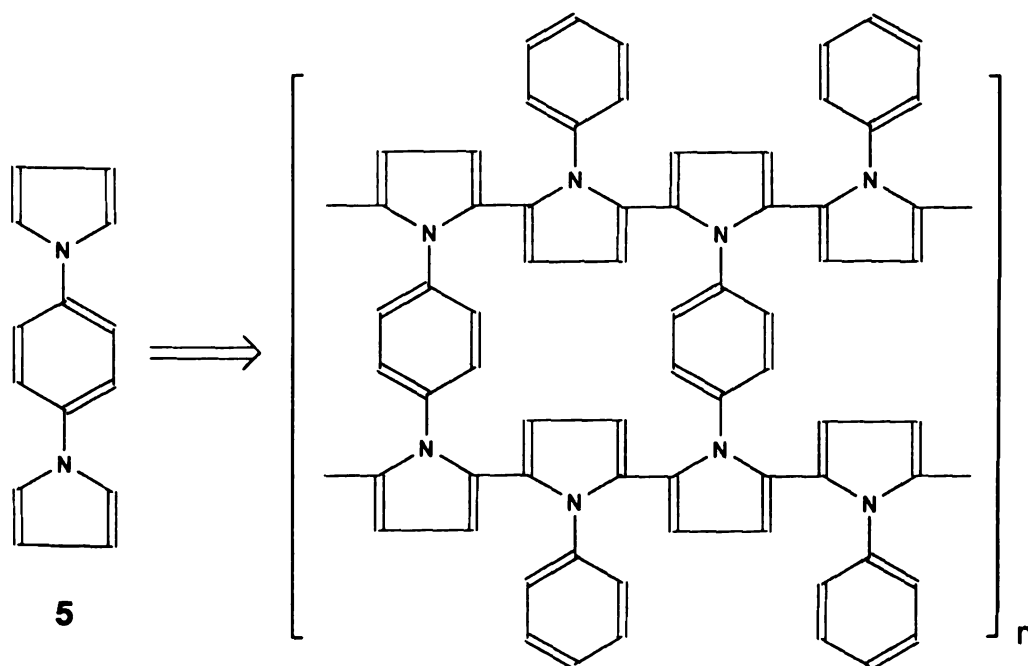
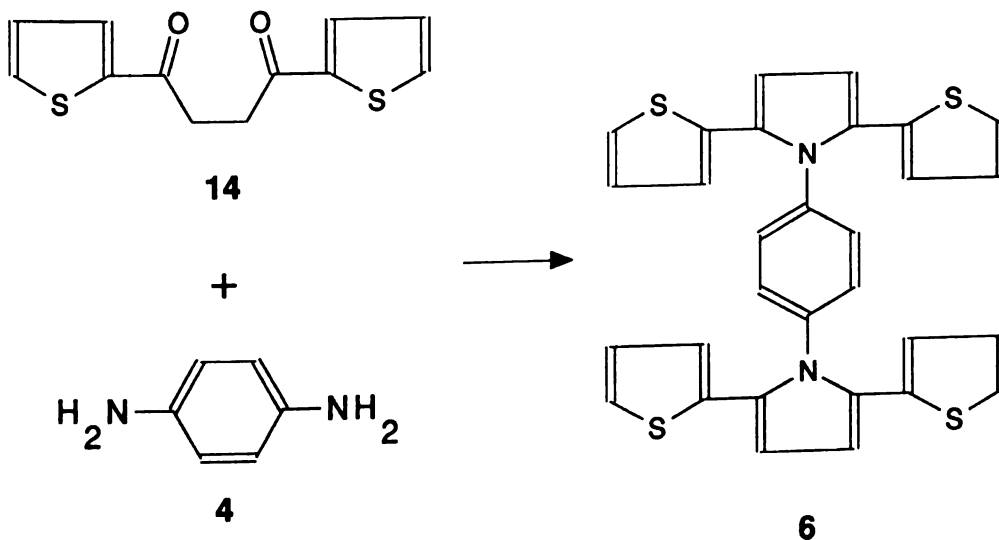


Figure 7 shows the electropolymerization of DPB by cyclic voltammetry. Polymerized DPB anchors itself very strongly to the electrode surface, and exhibits a capacitive effect, as demonstrated in Figure 8. It is a light copper color in the neutral form and dark green in the oxidized form, which suggests that the thin film is somewhat conductive.

To synthesize a two-dimensional polymer with improved characteristics, it was suggested that adding other heteroaromatic groups (thiophenes) to the pyrrole to make 1,4-bis[2,5-bis(2-thienyl)-1-pyrrolyl]benzene (BBTPB) (**6**), would lead to a less sterically hindered monomer. This would also lead to a lower oxidation potential, making it easier to polymerize as well as increasing conjugation in the polymer chains.

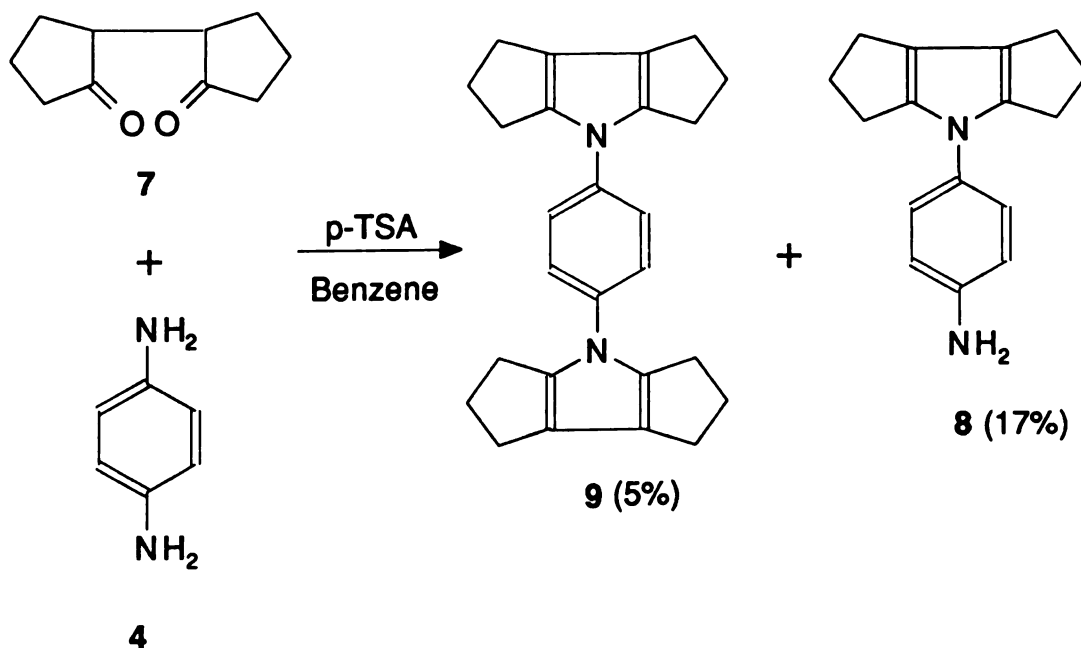
1,4-bis[2,5-bis(2-thienyl)-1-pyrrolyl]benzene may be synthesized from *p*-phenylenediamine and the heteroaromatic 1,4-diketone prepared by the Stetter reaction (Scheme 6).

Scheme 6. Synthesis of phenylene-bridged tercycle **6**



A literature search for reactions involving 1,4-diketones with p-phenylenediamine revealed that it is possible to make such systems, but with low yields.^{18, 68, 69} Nagarajan and coworkers reacted bicyclopentyl-2,2'-dione (7) with p-phenylenediamine with p-phenylenediamine, (Scheme 7) to obtain a 17% yield of the monocondensed product (8) along with 5% of the bis-condensation product (9).⁶⁸

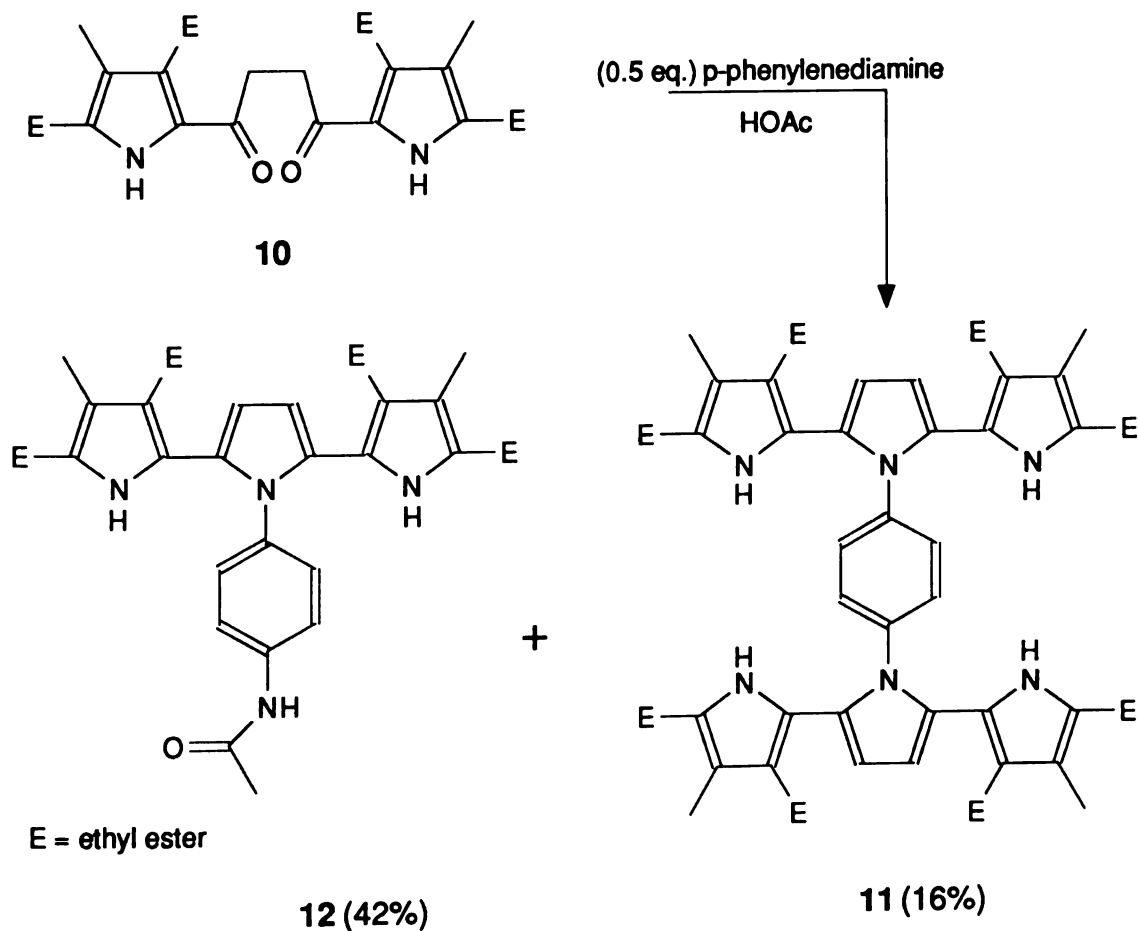
Scheme 7. Condensation of bicyclopentyl-2,2'-dione with p-phenylenediamine



In our laboratory, Merrill also attempted to condense the 1,4-diketone, 10, with p-phenylenediamine, using acetic acid as catalyst, and obtained the bis-condensation product 11 in 16% yield. The major product was the acetylated product 12 (42%). This indicates that the condensation to form the second

pyrrole moiety is very slow. Direct reaction of an amine with an acid is generally a slow reaction, yet in this case formation of the pyrrole is even slower (Scheme 8).¹⁸

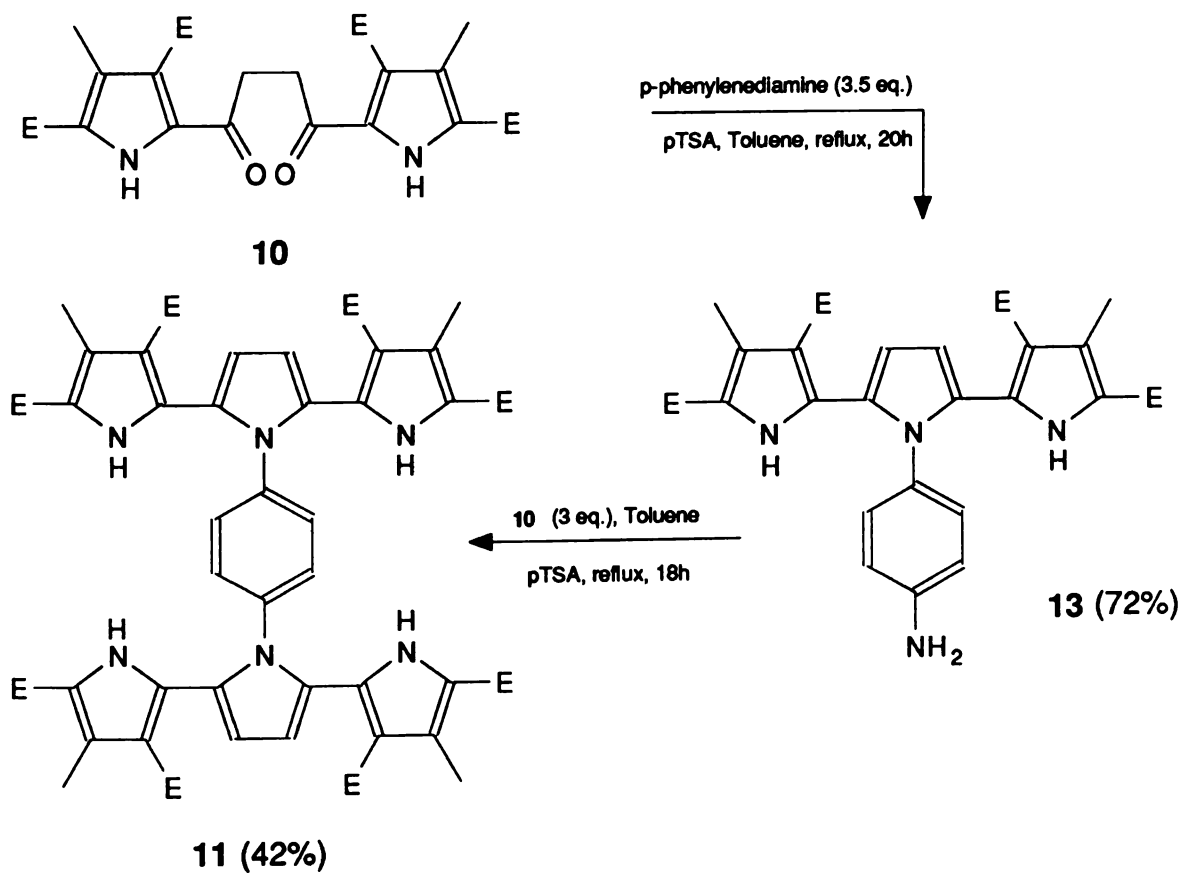
Scheme 8. Merrill's phenylene-bridged tercycles.



In order to improve the yields obtained for **11** a two-step procedure was implemented which utilized excess quantities of each reactant. Reaction of 1,4-diketone **10** with 3.5 equivalents of p -phenylenediamine resulted in 72% yield of the mono-condensed product **13**. Reaction of the mono-condensed product with

a three-fold excess of 1,4-diketone **10** gave the desired product **11** in a 42% yield (Scheme 9).

Scheme 9. Two-step synthesis of **11**

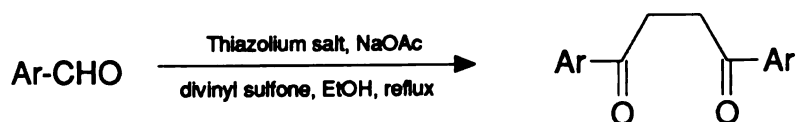


These two examples suggest that condensing 1,4-diketones with p-phenylenediamine under modified Paal-Knorr conditions yields a phenylene-bridged monomer capable of two-dimensional polymerization.

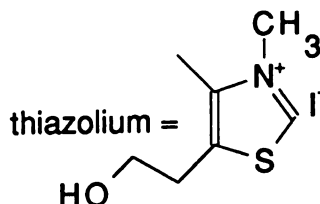
Symmetrical 1,4-diketones can be made via the thiazolium salt-catalyzed addition of aliphatic, aromatic, or heterocyclic aldehydes to activated double

bonds (the Stetter reaction) as shown in Scheme 10.⁷⁰ 1,4-Bis(2-thienyl)-1,4-butanedione (**14**) is made by reacting thiophene carboxaldehyde (**15**) with divinyl sulfone under the Stetter conditions as shown above.

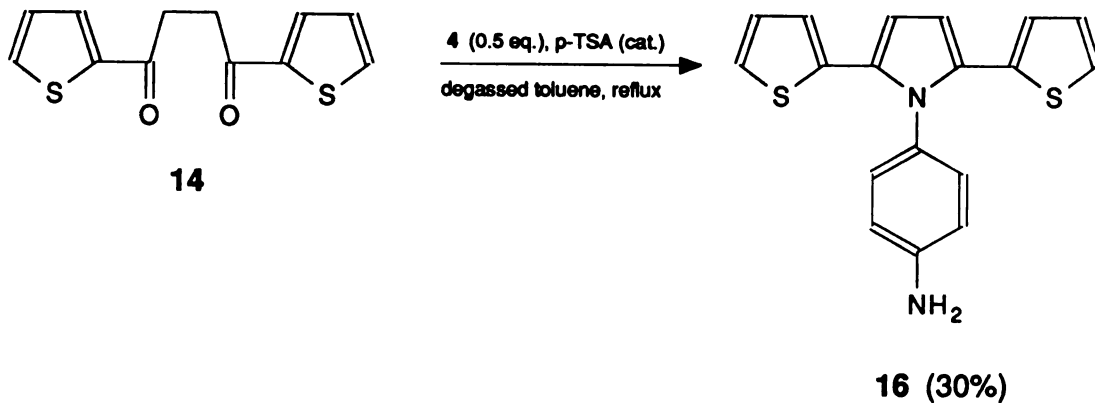
Scheme 10. The Stetter reaction



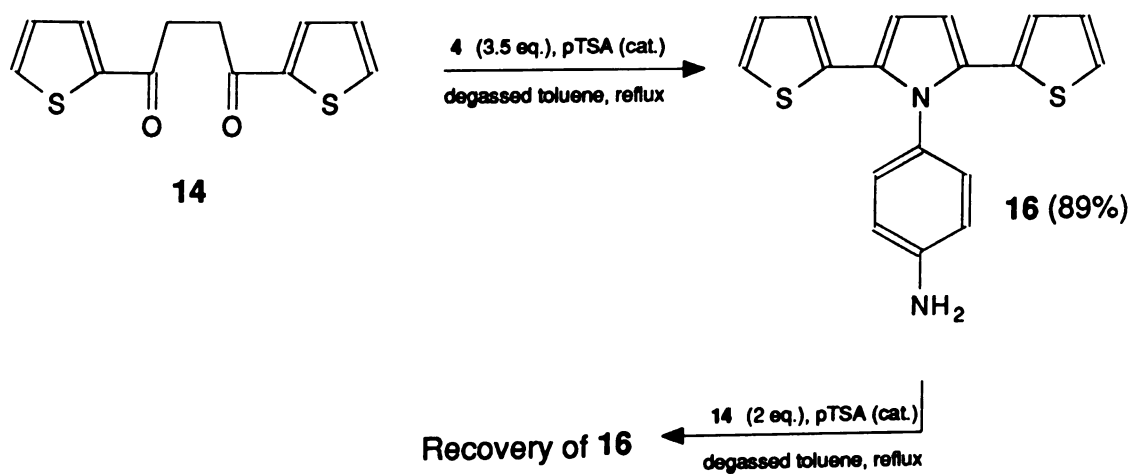
Ar	Yield %
phenyl	46
4-toluy	35
2-thienyl	48
2-furyl	75



An attempt to make 1,4-bis[2,5-bis(2-thienyl)-1-pyrrolyl]benzene (**6**), by reacting p-phenylenediamine with 1,4-diketone **14** under similar conditions to Nagarajan resulted in the formation of a black insoluble (polymer) solid, which means that condensation is so slow that oxidation takes place instead. To solve the oxidation problem, degassed toluene was used as solvent and the reaction was carried out under nitrogen. Only the monosubstituted pyrrole **16** was obtained as outlined in Scheme 11.

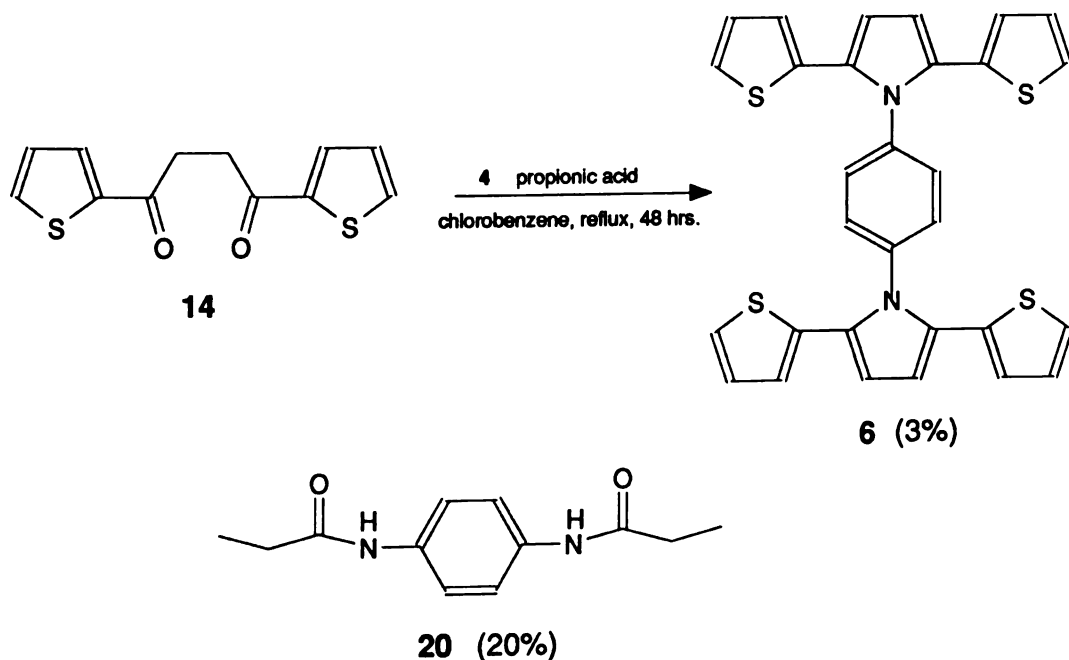
Scheme 11. Initial attempts at the Paal-Knorr reaction

Using the same two-step method as Merrill¹⁸ yielded 89% of the monosubstituted pyrrole **16**. Reaction of **16** with excess **14** resulted in the recovery of the starting materials. Condensation to form the second pyrrole is too slow under these conditions.

Scheme 12. Two-step synthesis attempt of **6**

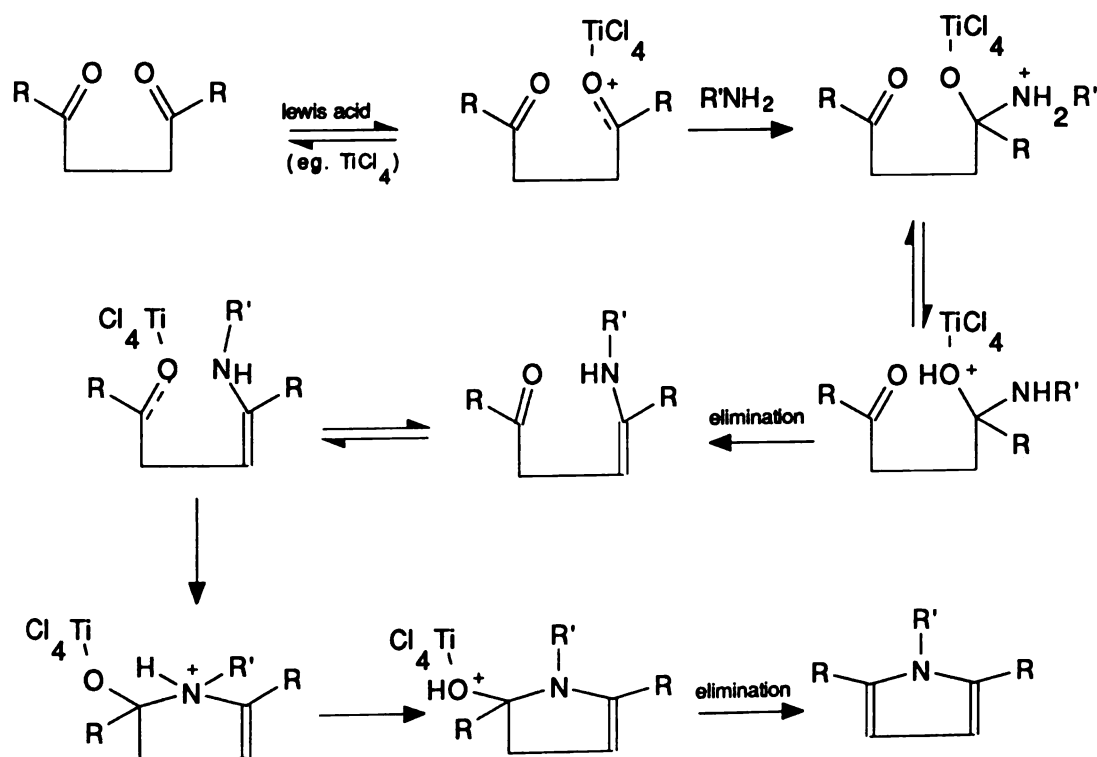
Reaction of **14** with **4**, with acetic acid as catalyst resulted in 70% of the acetylated aniline **17** plus 5% of the desired compound **6**. This is very similar to Merrill's results in which the reaction of amine with acetic acid (slow) competes with the condensation reaction to form the pyrrole. Since the acetylated aniline **17**, was the major product obtained when acetic acid was used as the catalyst, it was suggested that propionic acid which is slightly more hindered and has a higher boiling point, could give less of the acetylated product and more of the desired product **6**. When this reaction was attempted, it resulted in 20% of the di-propanoylated product **20** along with 3% of the desired product **6** as summarized in Scheme 13.

Scheme 13. Attempted condensation with propionic acid



Olsen and coworkers synthesized a number of sterically hindered pyrroles using a Lewis acid such as titanium(IV)tetrachloride to enhance the electrophilicity of the carbonyl carbon atom and as a scavenger of product water.⁷⁰ Scheme 14 demonstrates how a Lewis acid catalyzes the condensation of a 1,4-diketone and an amine to make pyrrole. Reaction of **14** with **4** with titanium(IV)isopropoxide as catalyst did not give any product.

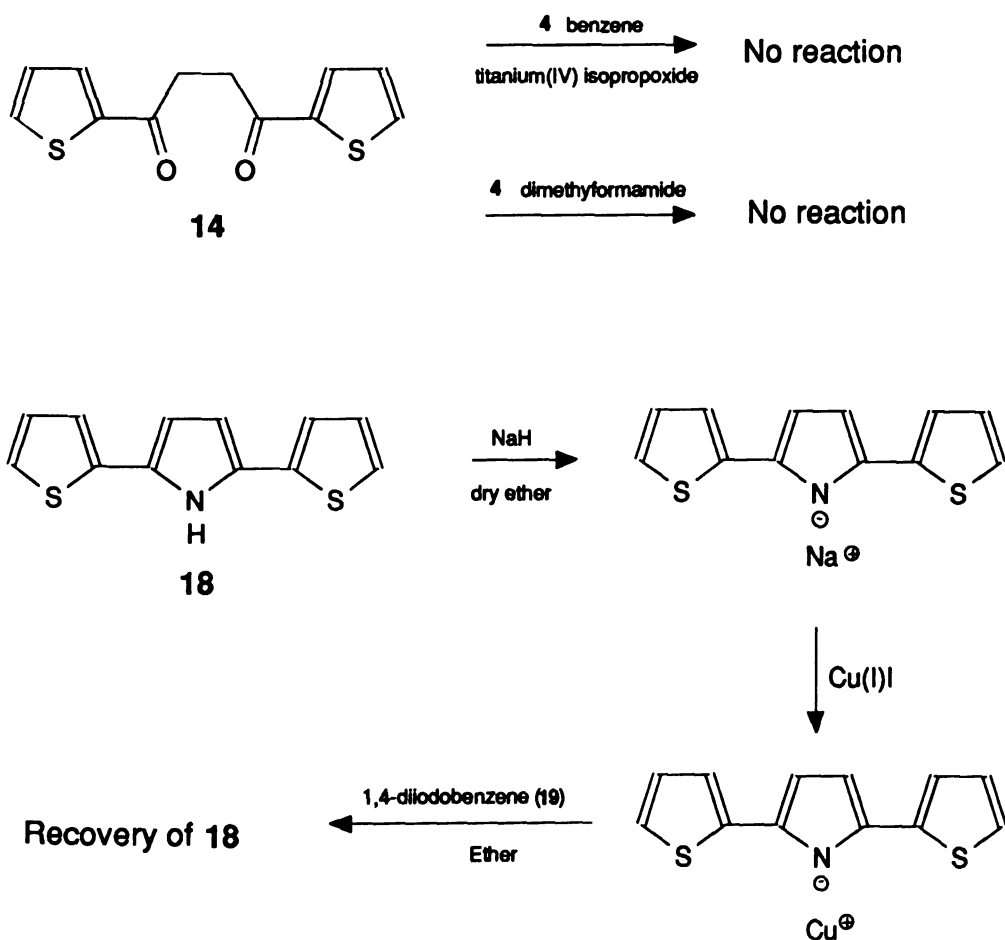
Scheme 14. Lewis acid catalyzed formation of pyrroles



A number of other reaction conditions were tried and are summarized in Scheme 15. Changing the conditions from acidic to basic by using dimethylformamide resulted in the recovery of starting materials. Since

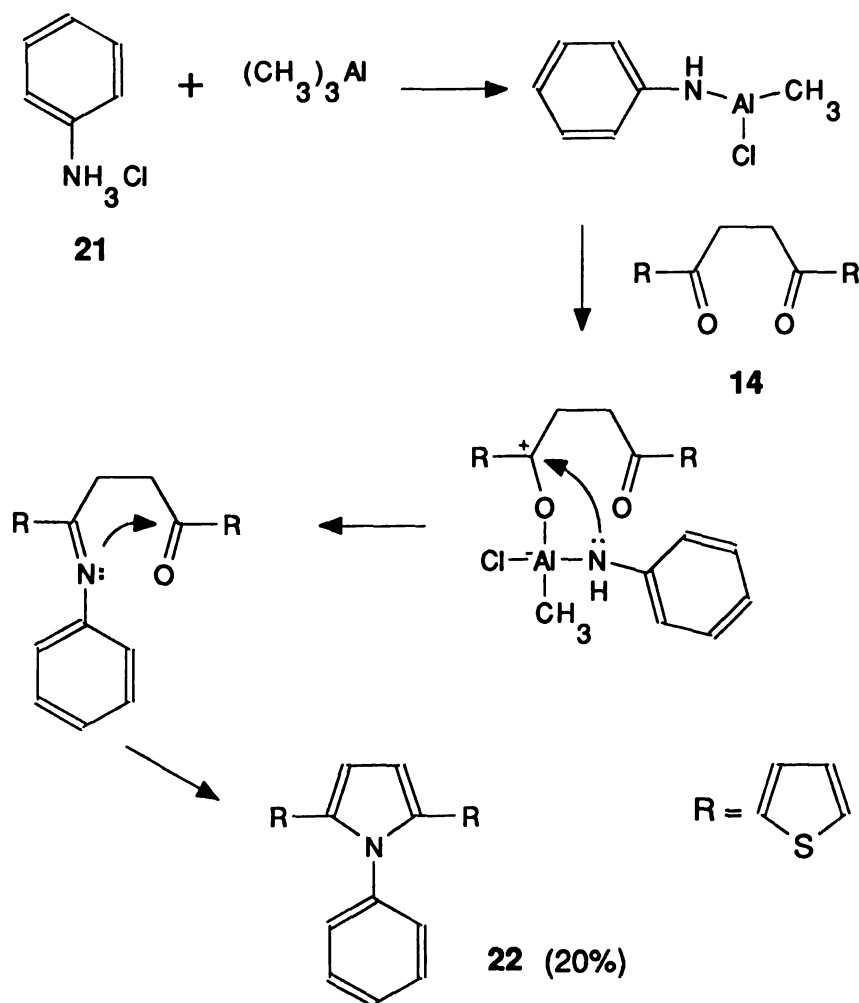
condensation of 1,4-diketone **14** with **4** gave very poor yields of desired product, it was suggested that a phenylation type reaction⁷¹ would provide a "back door" procedure to the desired compound. 2,5-Bis(2-thienyl)pyrrole (**18**), which has an acidic proton was reacted with sodium hydride to form the pyrrole anion. The pyrrole anion was then treated with copper(I) iodide to form the copper salt. To the copper salt was added 1,4-diiodobenzene (**19**), but only resulted in the recovery of the starting materials.

Scheme 15. Various attempts to make **6**



To be able to increase the yield of **6**, the amino groups of **4** have to be activated in such a way as to make them better nucleophiles. In our laboratory we are currently investigating a new method to make activated amines that can be reacted with 1,4-diketones to make pyrroles. Our method makes use of the reaction between trimethylaluminum with an amine to make a reactive alkyl or arylchloroaluminum amine. These aluminum reagents can be generated *in situ* and stored below 0° C for 1-2 days.

Scheme 16. Possible mechanism of alkylchloroaluminum amine reaction.



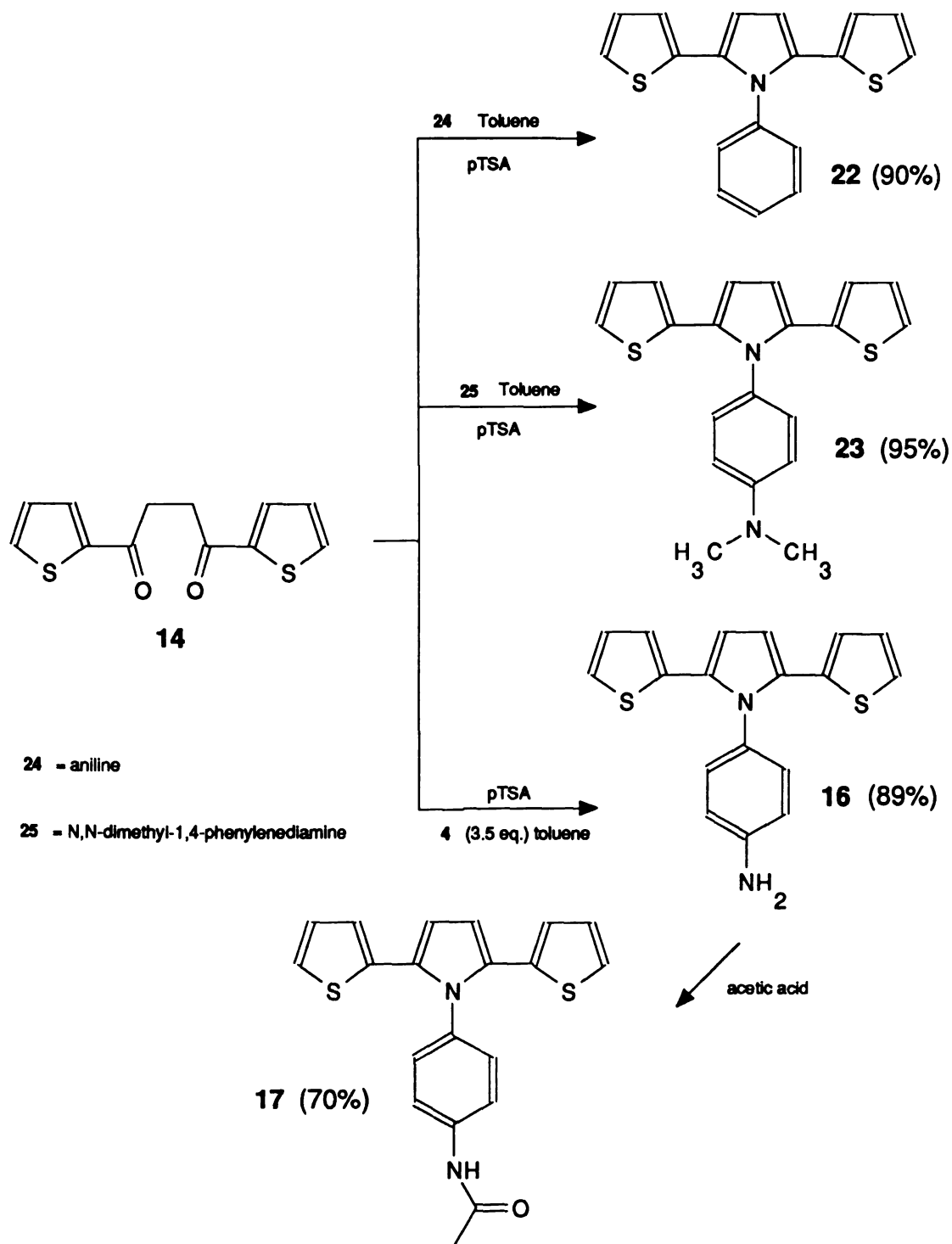
Weinreb and coworkers⁷² have used trimethylaluminum for the conversion of esters to the corresponding amides, and clearly demonstrated how reactive the alkylchloroaluminum amine reagents are.

As a preliminary trial, aniline hydrochloride was used as the amine salt (21). It was reacted with the trimethyl aluminum solution in toluene under nitrogen to give the corresponding benzochloroaluminum amine reagent which was then reacted with 1,4-diketone 14 to give the desired product 22 (20% yield) along with two unidentified products. A possible mechanism for the above reaction is outlined in Scheme 16.

Using p-phenylenediamine di-hydrochloride salt as the amine salt and reacting under the same conditions as aniline hydrochloride with trimethylaluminum resulted in the formation of 6 at 23% yield. Even though the yield is low it is higher than has been accomplished by any other method. This is the first time that an aluminum reagent has been used to activate an amino group to be condensed with a 1,4-diketone to make a pyrrole.

Other monomers based on the condensation of 1,4-diketone 14 with a variety of substituted anilines were carried out. These monomers all have the possibility of becoming conducting polymers. It is interesting to study the effect that the substituted phenyl groups have on the electrical and spectroscopic characteristics of the polymers. Scheme 17 outlines the synthesis of monomers 16, 17, 22, and 23.

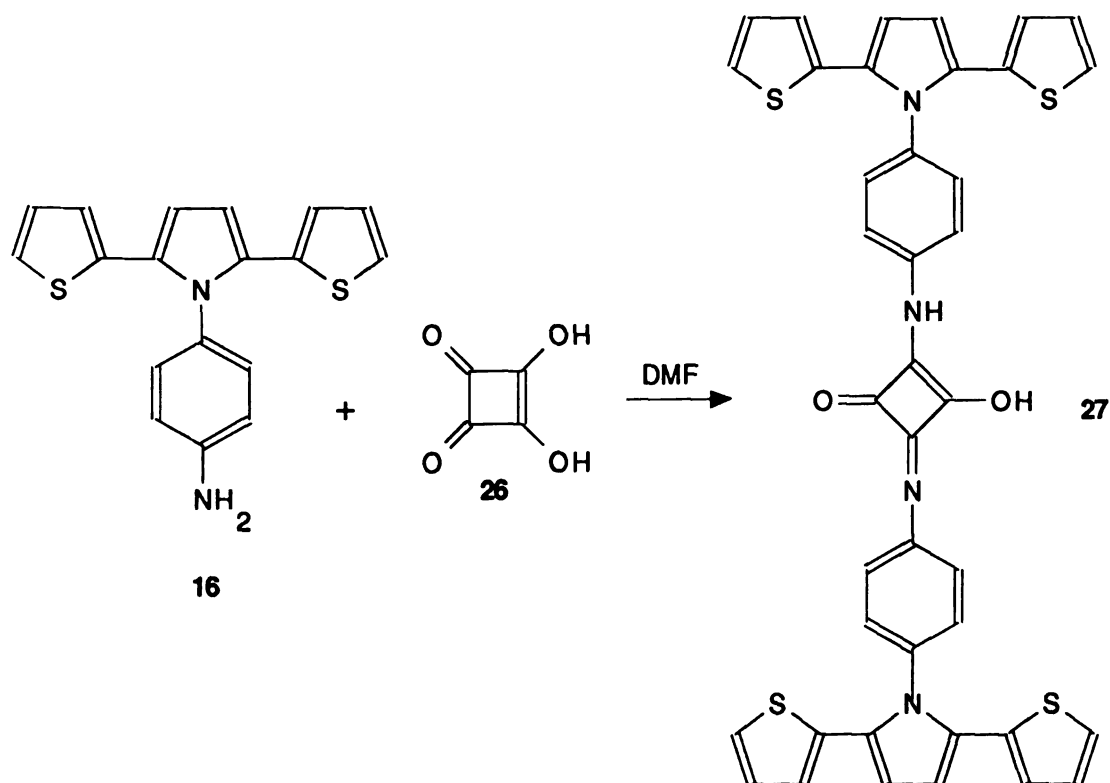
Another method to make a monomer having four distinct linking positions that could lead to a cross-linked conducting polymer is to use aniline 16 which has a free amino group and condense it with squaric acid as shown in Scheme 18. Gauger and coworkers⁷³ reacted a number of alkyl and aryl amines with squaric acid and were able to obtain the squaric acid-1,2-bisamides.

Scheme 17. Condensation of **14** with various substituted phenylamines.

Condensation of **16** with squaric acid in DMF, gave a yellow precipitate. FAB-MS revealed a fragmentation pattern consistent with a 2:1 condensation of the phenylamine and squaric acid. This is an interesting compound, because if it is polymerized, it may result in a self-doped conductive polymer (a conductive polymer with the counter ions covalently bound to the polymer backbone).^{74a, 74b,}

74c

Scheme 18. Condensation of **16** with squaric acid (**26**)



B. Electrochemistry and Conductivity

The polymerization of heteroaromatic monomers by irreversible electrooxidation is a process that depends very much upon the experimental conditions used.^{48, 75} It is very hard to duplicate the exact conditions of electropolymerization from monomer to monomer because making good films depend on the solvent, the counter ion and the concentration of the monomer in solution. From a practical standpoint a monomer concentration of about 1×10^{-3} M and a 10^{-1} M concentration of electrolyte is a good starting point. In addition, carrying out the electropolymerization at 0° C leads to better quality films than at room or higher temperature.^{47, 76, 77}

To be able to study the conductive materials as films, a suitable solvent has to be found (usually by trial and error) in which the monomer is soluble, but the polymer is insoluble, and at the same time the solvent has to have a sizeable working window free of electroactivity. Solvents with good working windows include acetonitrile, dichloromethane, tetrahydrofuran and propylene carbonate.⁷⁸

Conductive polymer films derived from heteroaromatic monomers usually are insoluble, which is very desirable if they are to be studied by electrochemical methods. If they are soluble then they have to be cast as films, which in itself is an advantage because they can be shaped.

Cyclic voltammograms of the corresponding monomers **1a**, **1b**, **6**, **16**, **17**, **18**, and **23**, (Figures 9 to 15), show that they form films by the expected E(CE)_n mechanism. This process is characterized by an initial irreversible oxidation peak that corresponds to the oxidation of monomer, followed by a reduction of the polymerized material. Subsequent scans indicate oxidation of the polymer, and again followed by oxidation of more monomer. An increase in current is

observed due to the fact that the electrode surface (area) is getting larger because the polymer is anchored on its surface.

Not all the synthesized heteroaromatic monomers led to the formation of films by electrochemical oxidation. A cyclic voltammogram of **22** (Figure 16) shows that there is no film growth, because as the monomer is electrooxidized to make polymer it dissolves in the solution. The polymers that dissolve as they are made are usually very short-length and not very conductive. The electropolymerization of **22** is very similar to that of **28** (Figure 17), where **28** has butyl substituents that make it soluble.⁷⁹

The electrochemical (as well as the electrical and optical) characteristics of the conductive polymers can be tuned by addition of substituents to the monomer from which they are derived. The polymer derived from **28** is completely soluble in most common organic solvents while a polymer made from **18** is not. This is obvious from the cyclic voltammograms of **28** and **18** shown in Figures 14 and 17.

The addition of small electron donating substituents such as methyl or butyl groups stabilize the radical cations formed by electrooxidation. The result is that the oxidation potential of the monomer is lower for the substituted monomer as long as there is no hindrance. This is illustrated by the oxidation potentials of **1a** and **1b**, at 0.52 V and 0.40 V vs. SSCE (Figures 9 and 10). This inductive effect is also evident from the oxidation potentials of **18** versus **28** at 1.15 V and 0.93 V vs. Ag/Ag⁺ respectively (Figures 14 and 17). When monomers are substituted with large functional groups, then steric effects override the electronic effects and the oxidation potential of the monomer is greater.³⁸ This is evident by comparing the oxidation potential of **17** and **18** (Figures 13 and 14) at 1.75 V and 1.80 V versus Ag/Ag⁺ respectively. The acetamide group did not lower the oxidation potential.

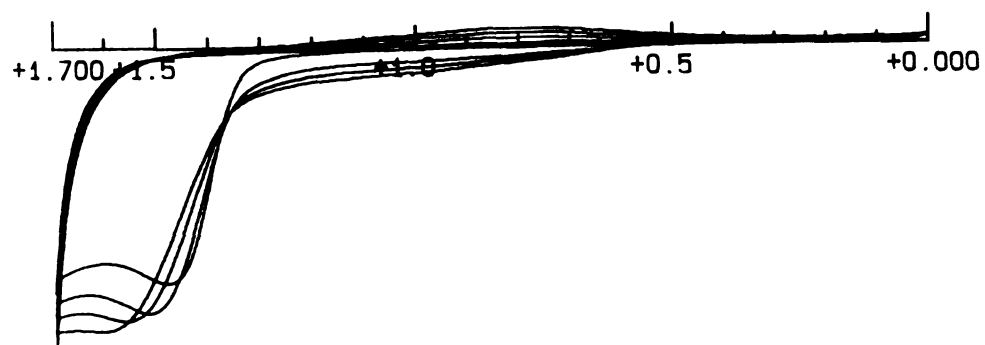
Figure 7. Electrochemical polymerization of 1,4-bis(1-pyrryl)benzene (**5**)
0.01 M monomer and 0.10 M TBABF₄ in acetonitrile. Potential vs.
Ag/Ag⁺.

CYCLIC VOLTAMMETRY

EXP. CONDITIONS:

INIT E (mV) = 0
HIGH E (mV) = 1700
LOW E (mV) = 0
V (mV/SEC) = 50
SWEEP SEGMENTS = 8
SMPL INT. (mV) = 2

↑
5μA
↓



E (VOLT)

Figure 7

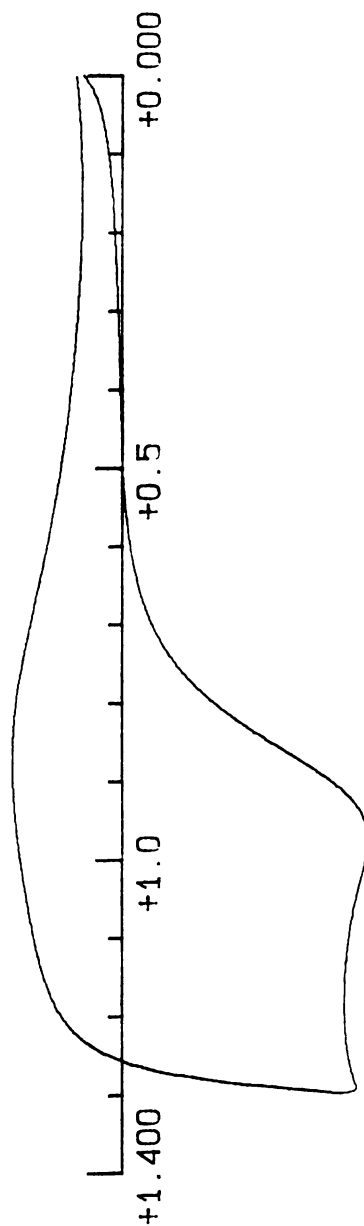
Figure 8. Cyclic voltammogram of polymerized **5** in acetonitrile with 0.10 M TBABF₄. Scan rate 50 mV/sec. Potential vs. Ag/Ag⁺.

CYCLIC VOLTAMMETRY

↑
2μA
↓

EXP. CONDITIONS.

INIT E (mV) = 0
HIGH E (mV) = 1400
LOW E (mV) = 0
V (mV/SEC) = 50
SWEEP SEGMENTS = 2
SMPL INT. (mV) = 2



E (VOLT) **Figure 8**

Figure 9. Electrochemical polymerization of 2,5-bis(2-pyrrolyl)thiophene (**1a**).
0.01 M monomer and 0.10 M TBABF₄ in acetonitrile. Potential vs.
SSCE.

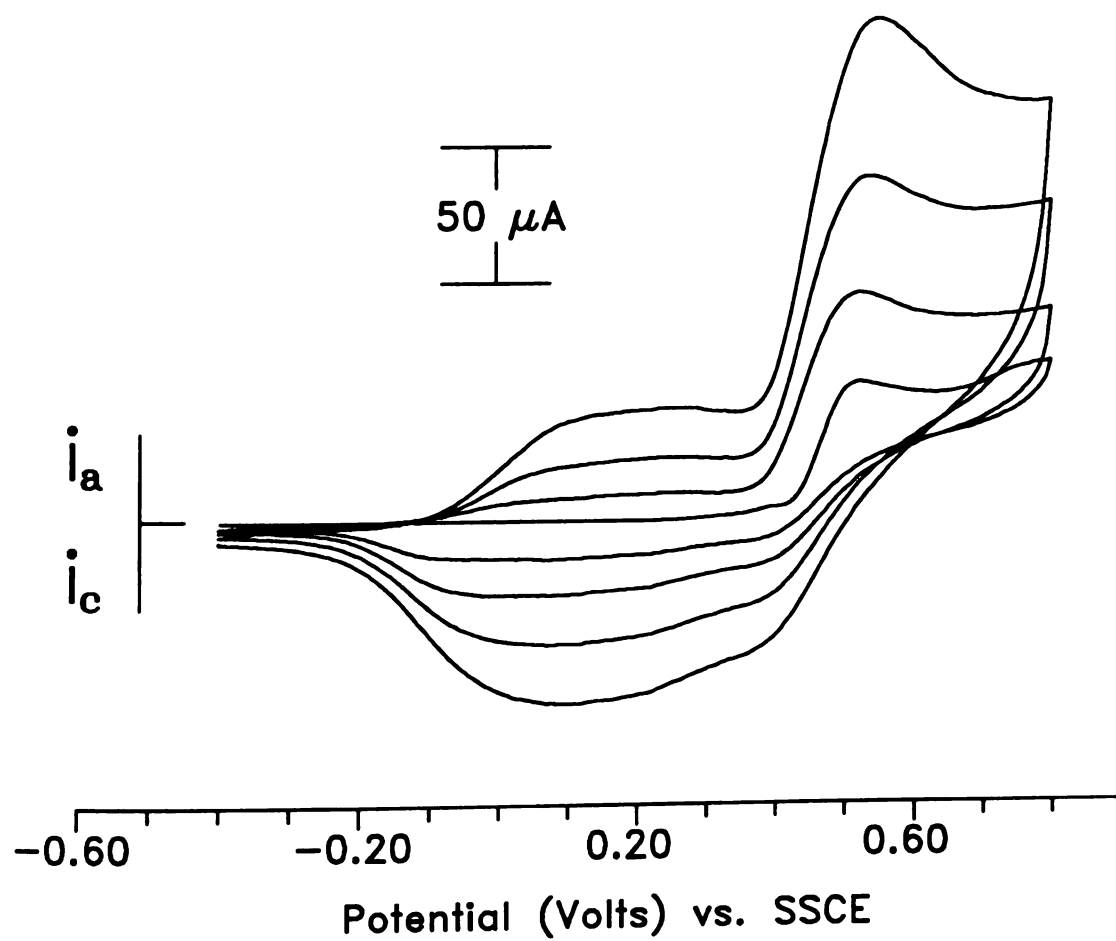


Figure 9

Figure 10. Electrochemical polymerization of 2,5-bis(4-methyl-2-pyrrolyl) thiophene (**1b**). 0.01 M monomer and 0.10 M TBABF₄, in acetonitrile. Potential vs. SSCE.

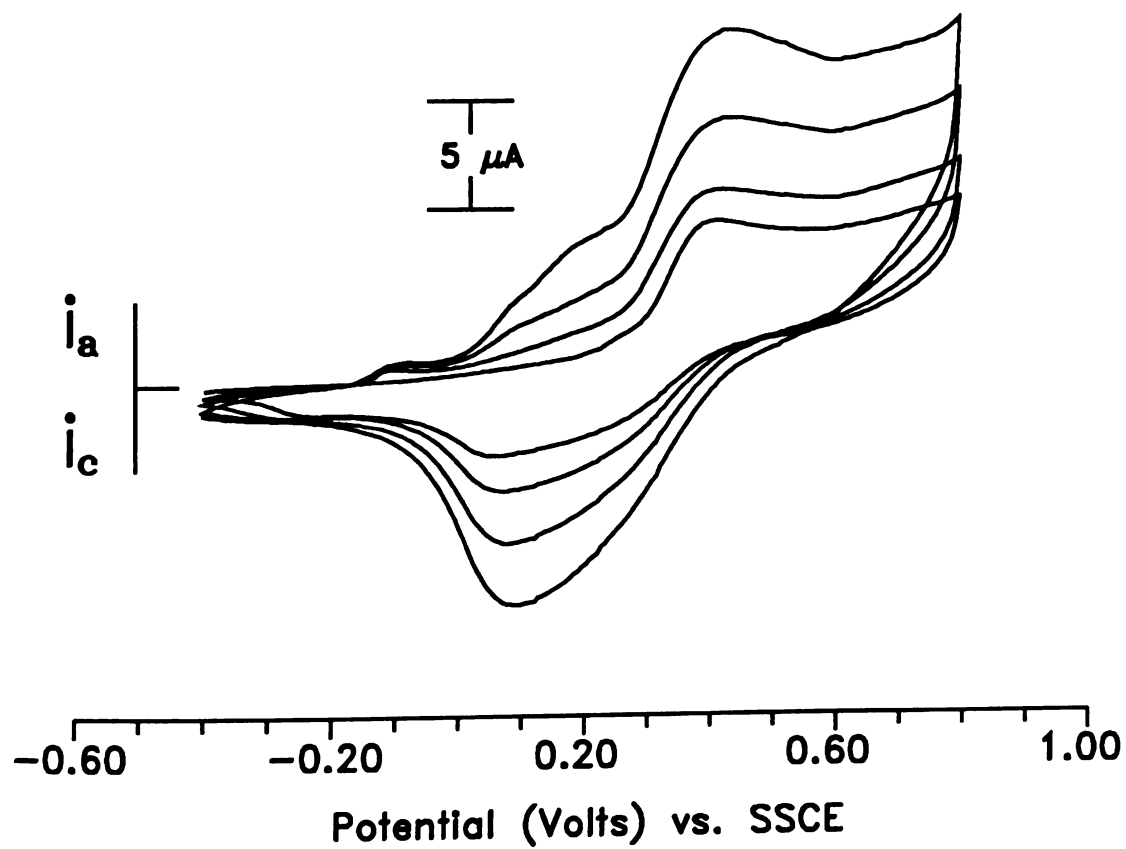


Figure 10

Figure 11. Electrochemical polymerization of 1,4-bis[2,5-bis(2-thienyl)-1-pyrrolyl]benzene (**6**). 1×10^{-3} M monomer and 0.10 M TBABF₄ in dichloromethane. Potential vs. Ag/Ag⁺.

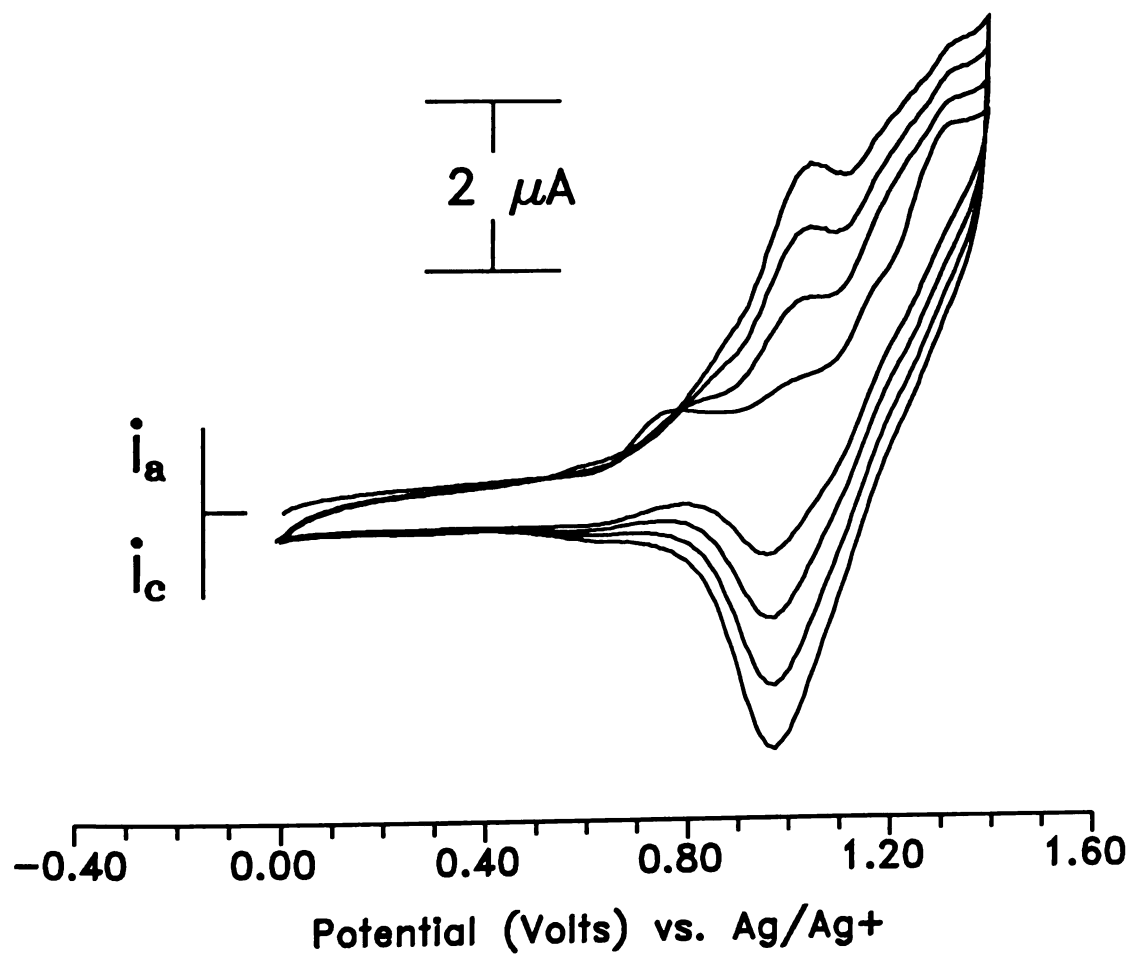


Figure 11

Figure 12. Electrochemical polymerization of 1-amino-4-[2,5-bis(2-thienyl)-1-pyrryl]benzene (**16**). 1×10^{-3} M monomer and 0.10 M TBABF₄ in dichloromethane. Potential vs. Ag/Ag⁺.

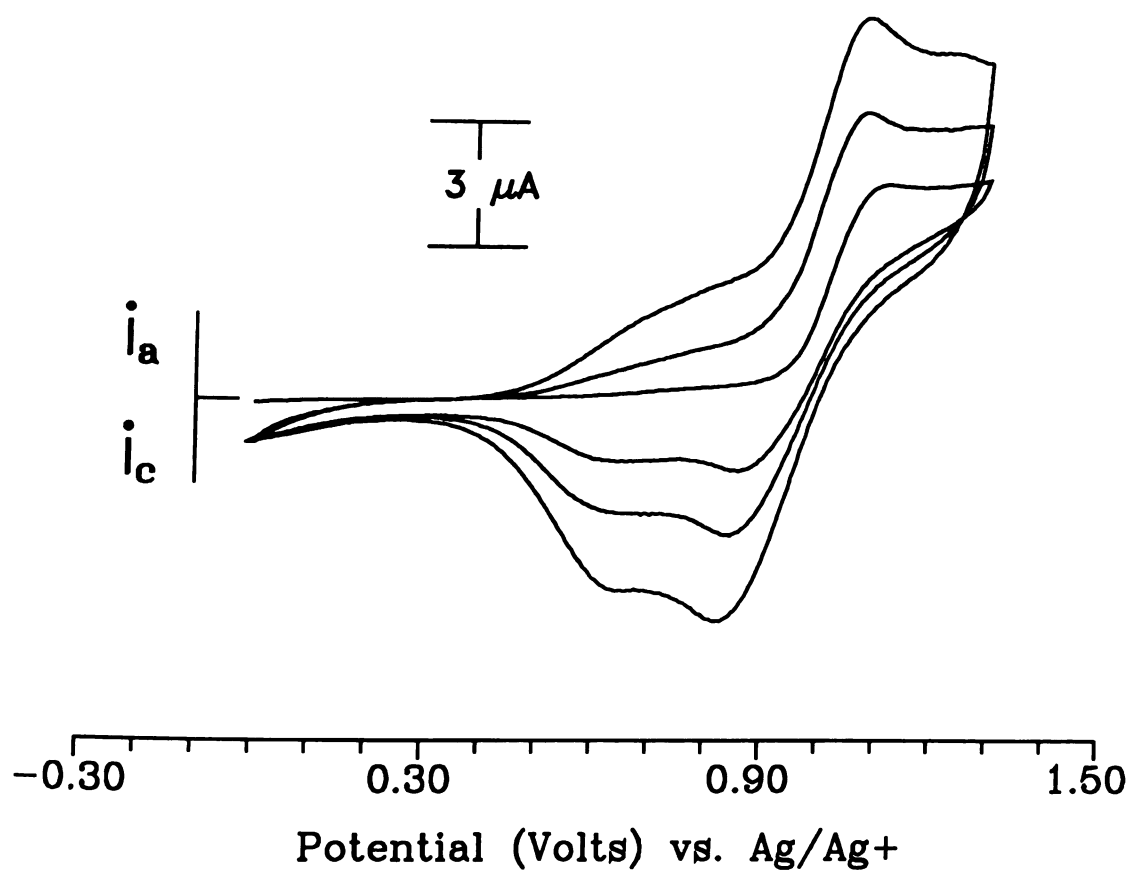
**Figure 12**

Figure 13. Electrochemical polymerization of N-[4-[2,5-bis(2-thienyl)-1-pyrryl]phenyl]acetamide (**17**). 1×10^{-3} M monomer and 0.10 M TBABF₄ in dichloromethane. Potential vs. Ag/Ag⁺.

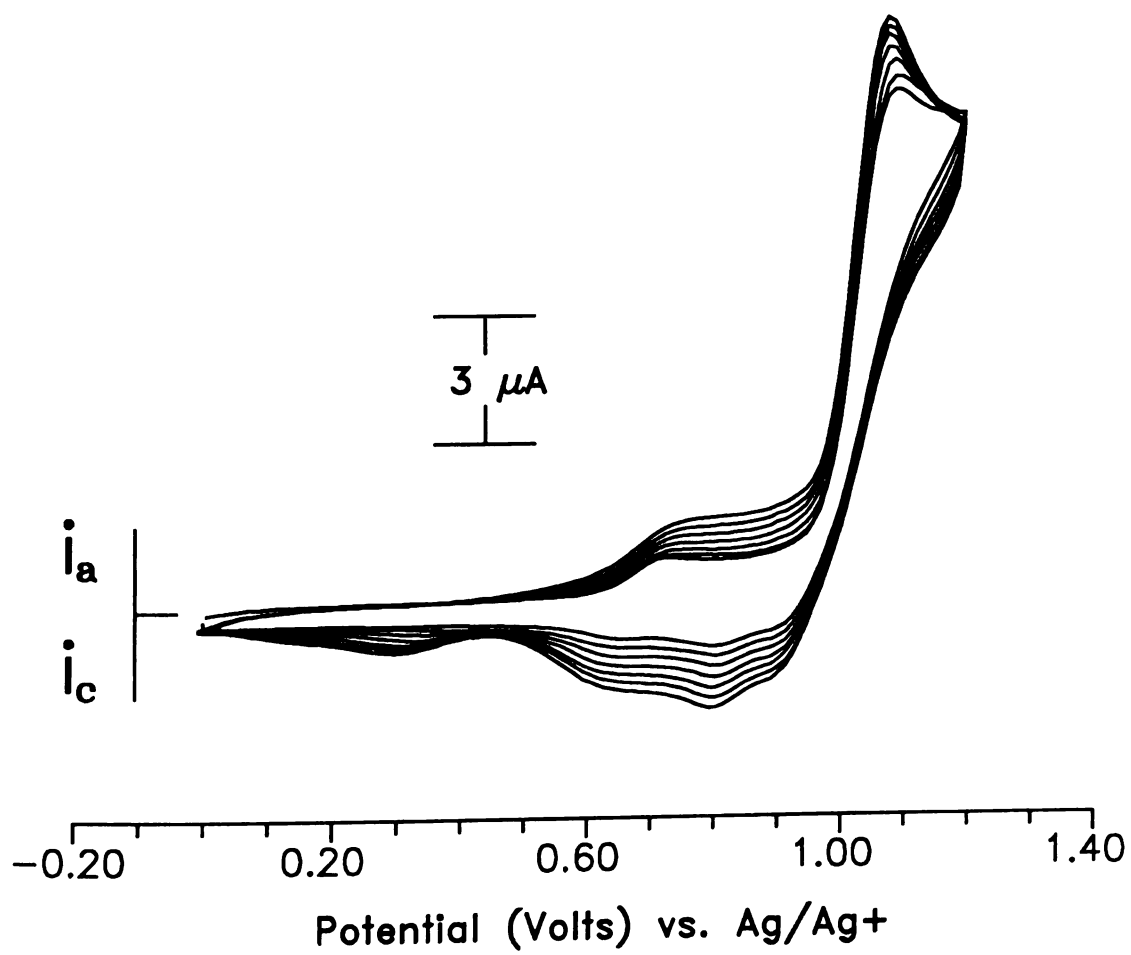
**Figure 13**

Figure 14. Electrochemical polymerization of 2,5-bis(2-thienyl)pyrrole (**18**).
1 X 10⁻³ M monomer and 0.10 M TBABF₄ in dichloromethane.
Potential vs. Ag/Ag⁺.

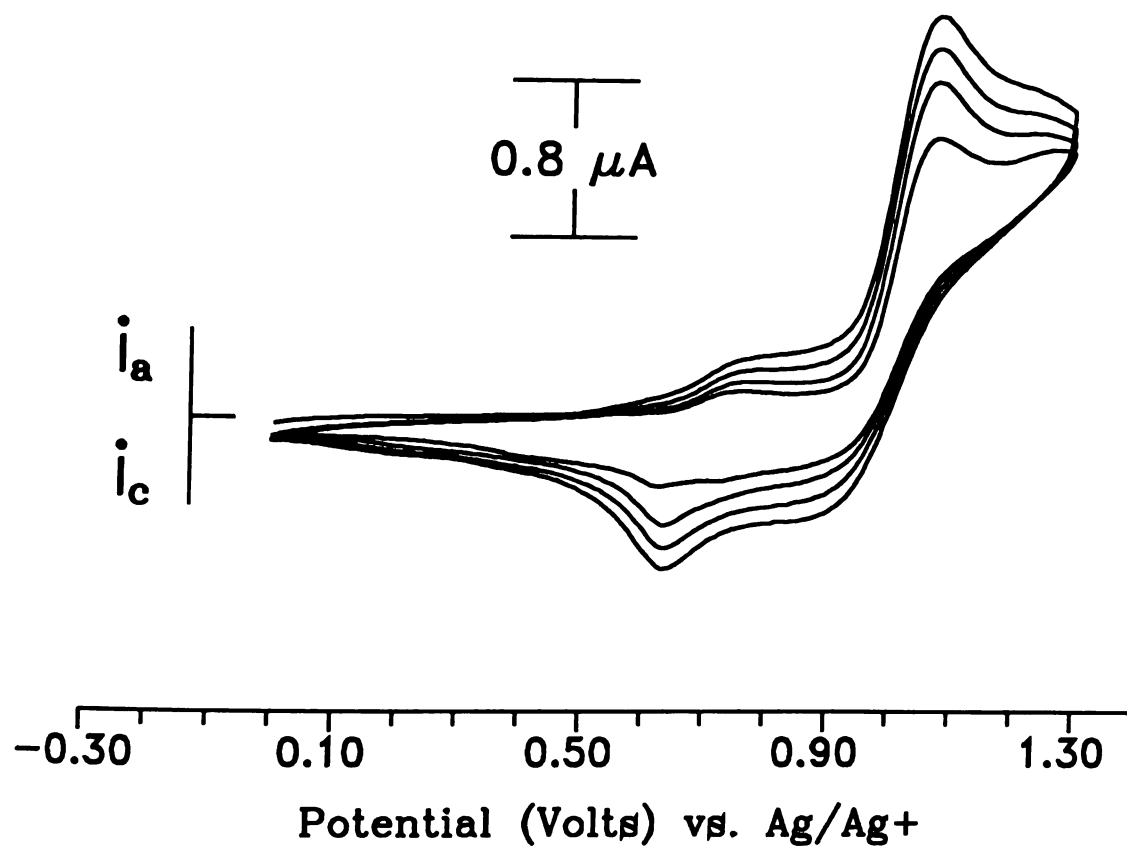


Figure 14

Figure 15. Electrochemical polymerization of 1-(dimethylamino)-4-[2,5-bis(2-thienyl)-1-pyrrolyl]benzene (**23**). 1×10^{-3} M monomer and 0.10 M TBABF₄ in tetrahydrofuran. Potential vs. Ag/Ag⁺.

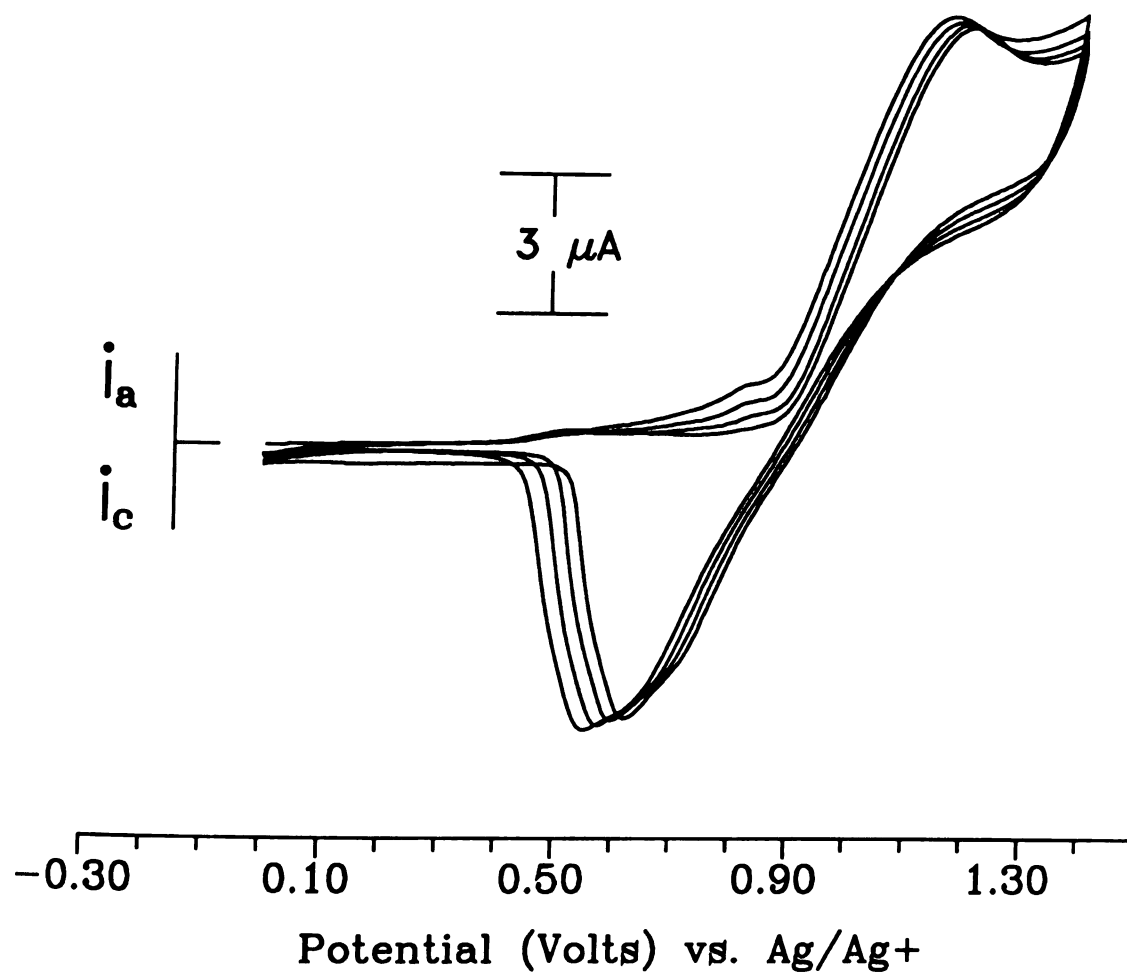


Figure 15

Figure 16. Electrochemical polymerization of N-[2,5-bis(2-thienyl)-1-pyrrolyl] benzene (**22**). 1×10^{-3} M monomer and 0.10 M TBABF₄ in dichloromethane. Potential vs. Ag/Ag⁺.

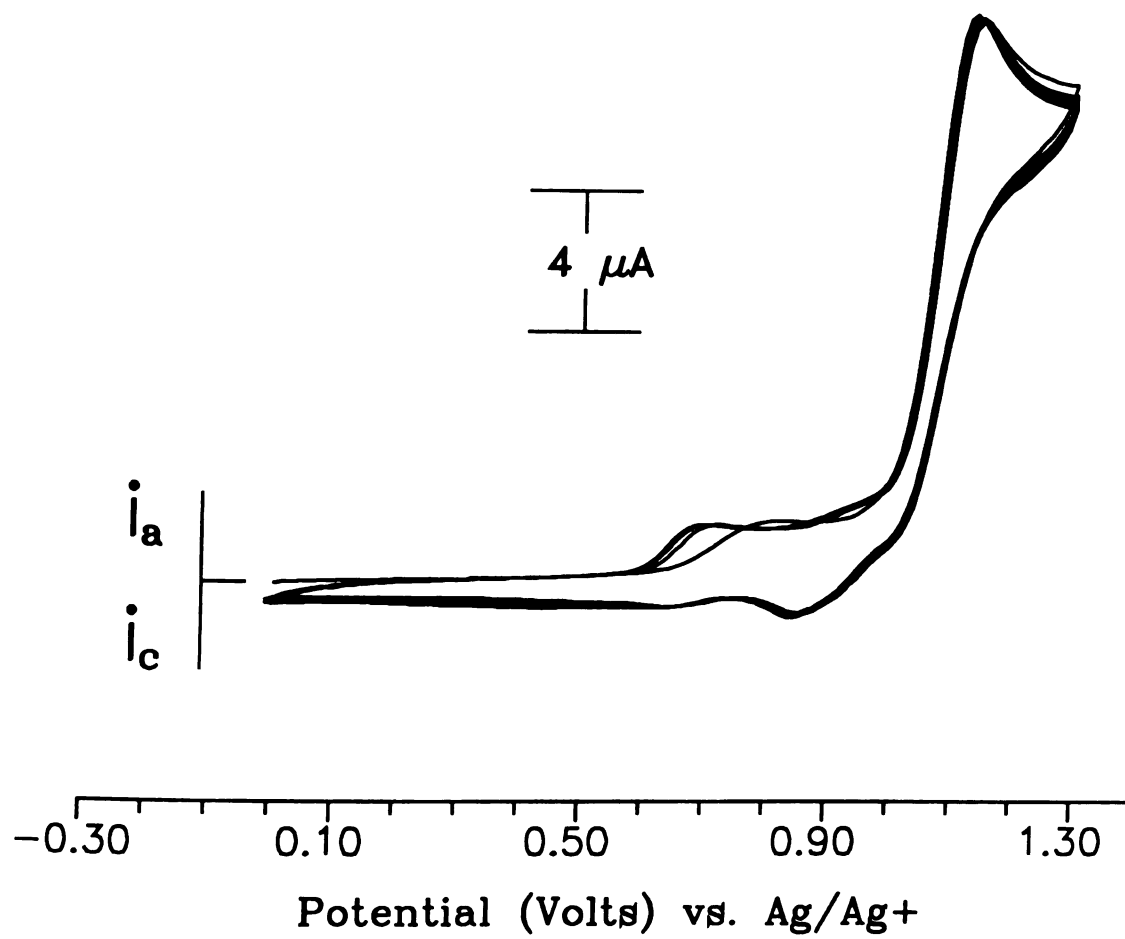
**Figure 16**

Figure 17. Electrochemical polymerization of 3,4-dibutyl-2,5-bis(2-thienyl) pyrrole (**28**). 1×10^{-3} M monomer and 0.10 M TBABF₄ in dichloromethane. Potential vs. Ag/Ag⁺.

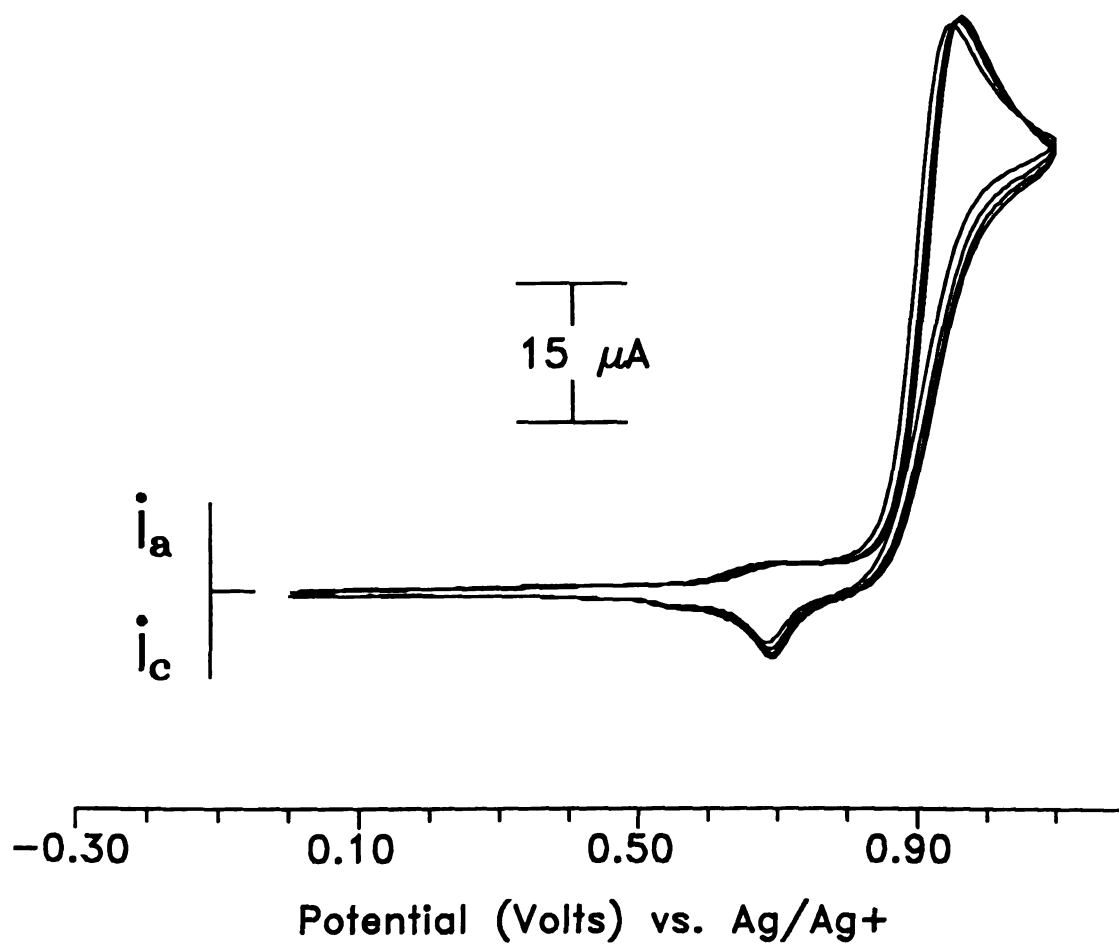


Figure 17

The electropolymerization of **23** by cyclic voltammetry is peculiar because subsequent scans appear at more cathodic potentials. These results suggest that the polymer is acting as a catalyst for the formation of more polymer (Figure 15). Electropolymerization of **5** shows the inverse of **23** (Figure 7). In this case the polymer film is not very conductive therefore subsequent scans have to appear at more anodic potentials needed to electrooxidize the monomer.

Once films have been deposited on the surface of the electrodes, it is desirable to determine their redox characteristics. Cyclic voltammetry is a technique well suited for this purpose. In this way the stability of the polymer as well as the degree of partial oxidation can be determined as a function of the applied potential.

Conductive polymer films anchored on the surface of electrodes do not show the same behavior as redox species in solution. For a reversible redox material in solution the peak currents (anodic and cathodic) are well defined and separated by $56 \text{ mV}/n$, where n is the number of electrons involved in the redox process, also the peak currents are proportional to the square root of the scan rate.⁸⁰ For anchored materials possessing non-interactive sites, the difference in potential between the anodic and cathodic peaks is zero, provided the electron transfer reaction is fast. Doubling the scan rate results in a doubling of the peak currents.⁷⁸ This scan rate dependence is similar to thin-layer electrochemistry where the volume of solution is less than the diffusion layer thickness. The same is true for a conductive polymer anchored on an electrode surface as illustrated by Figures 18 to 22, 24, 25. This happens due to the fact that there is no diffusion of material from the bulk solution. The only movement of charge is by electrons or holes hopping through the chains to or from the electrode-polymer interface. In a conductive polymer the difference between the anodic and cathodic peaks will not be zero or even $56 \text{ mV}/n$,

Figure 18. Cyclic voltammograms of polymerized 2,5-bis(2-pyrrolyl) thiophene (**1a**) in acetonitrile with 0.10 M TBABF₄, at 20, 10 and 5 mV/sec. Potential vs. SSCE.

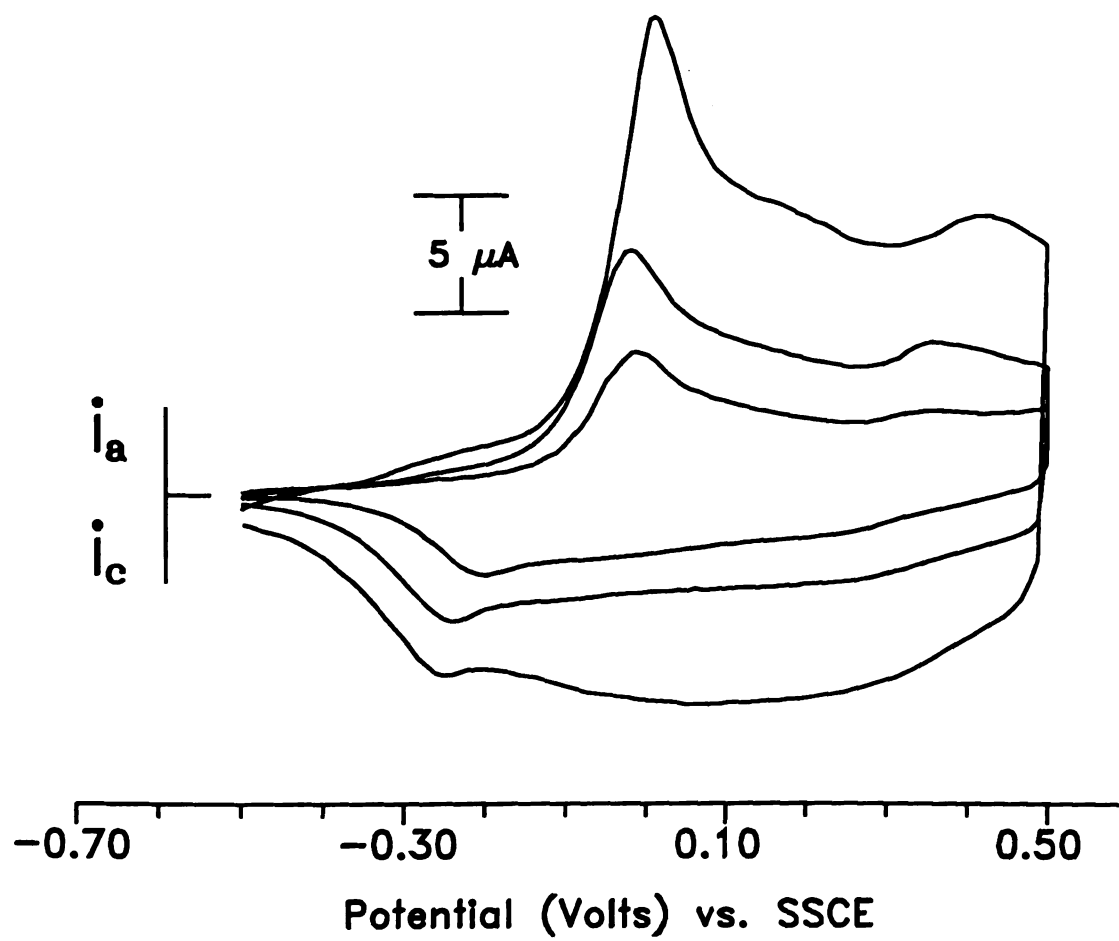


Figure 18

Figure 19. Cyclic voltammograms of polymerized 2,5-bis(4-methyl-2-pyrrolyl)thiophene (**1b**) in acetonitrile with 0.10 M TBABF₄ , at 50, 20, and 10 mV/sec. Potential vs. SSCE.

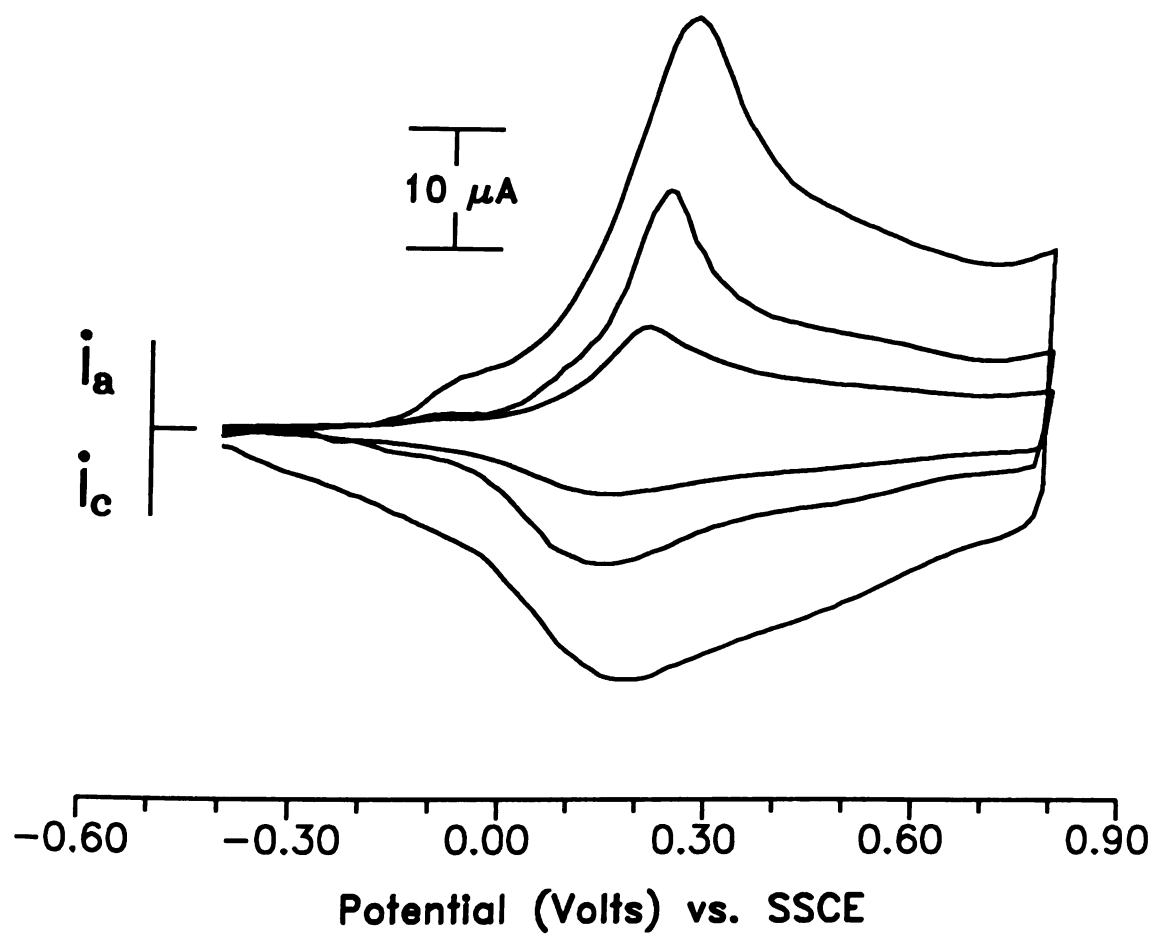


Figure 19

Figure 20 Cyclic voltammograms of polymerized 1,4-bis[2,5-bis(2-thienyl)-1-pyrrolyl]benzene (**6**) in dichloromethane with 0.10 M TBABF₄, at 50, 20, 10, and 5 mV/sec. Potential vs. Ag/Ag⁺.

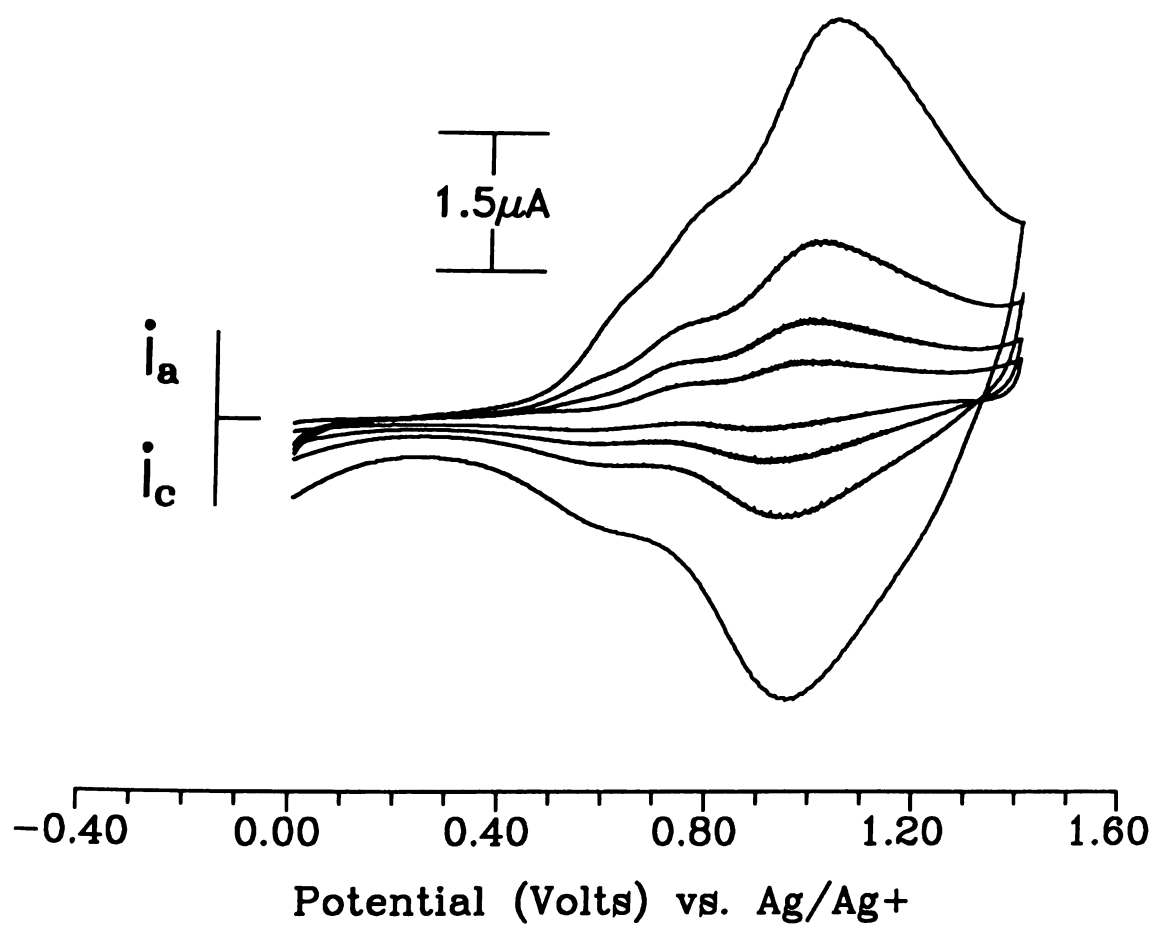


Figure 20

Figure 21. Cyclic voltammograms of polymerized 1-amino-4-[2,5-bis(2-thienyl)-1-pyrryl]benzene (**16**) in dichloromethane with 0.10 M TBABF₄, at 25, 10, and 5 mV/sec. Potential vs. Ag/Ag⁺.

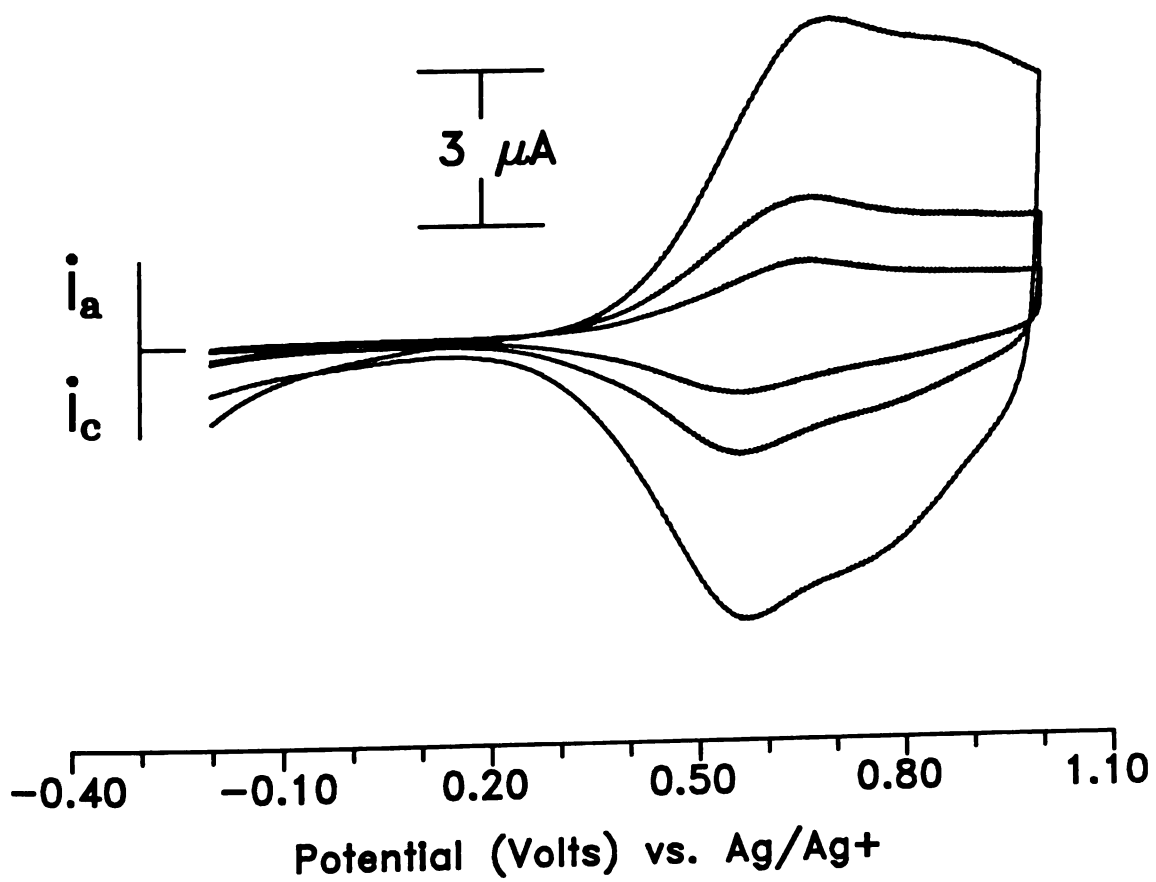


Figure 21

Figure 22. Cyclic voltammograms of polymerized N-[4-[2,5-bis(2-thienyl)-1-pyrrolyl]phenyl]acetamide (**17**) in dichloromethane, with 0.10 M TBABF₄, at 50, 25, and 10 mV/sec. Potential vs. Ag/Ag⁺.

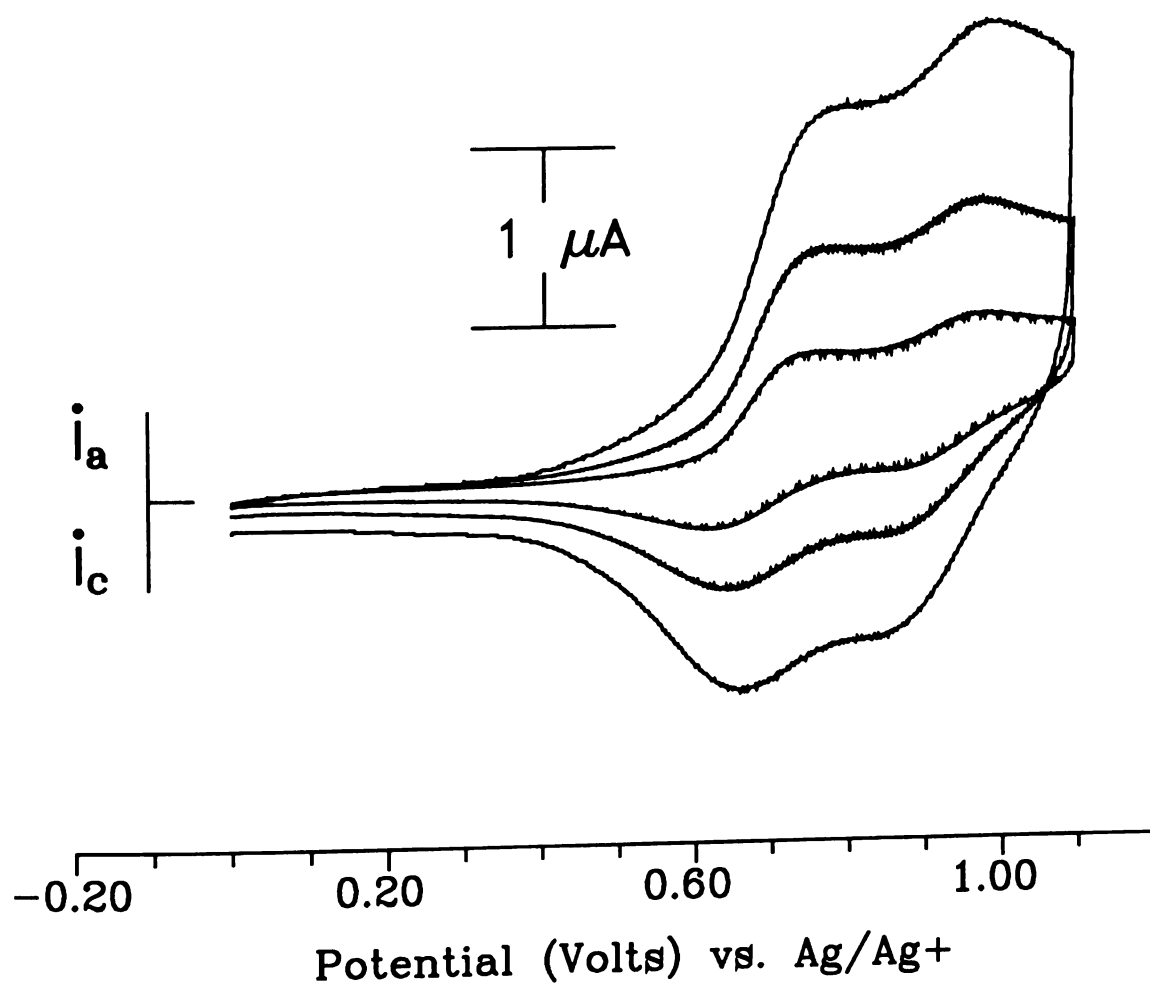


Figure 22

Figure 23. Cyclic voltammograms of polymerized 2,5-bis(2-thienyl)pyrrole (18) in dichloromethane, with 0.10 M TBABF₄, at 50, 25, and 10 mV/sec. Potential vs. Ag/Ag⁺. The polymer film slowly dissolves and hence is not well anchored to the electrode.

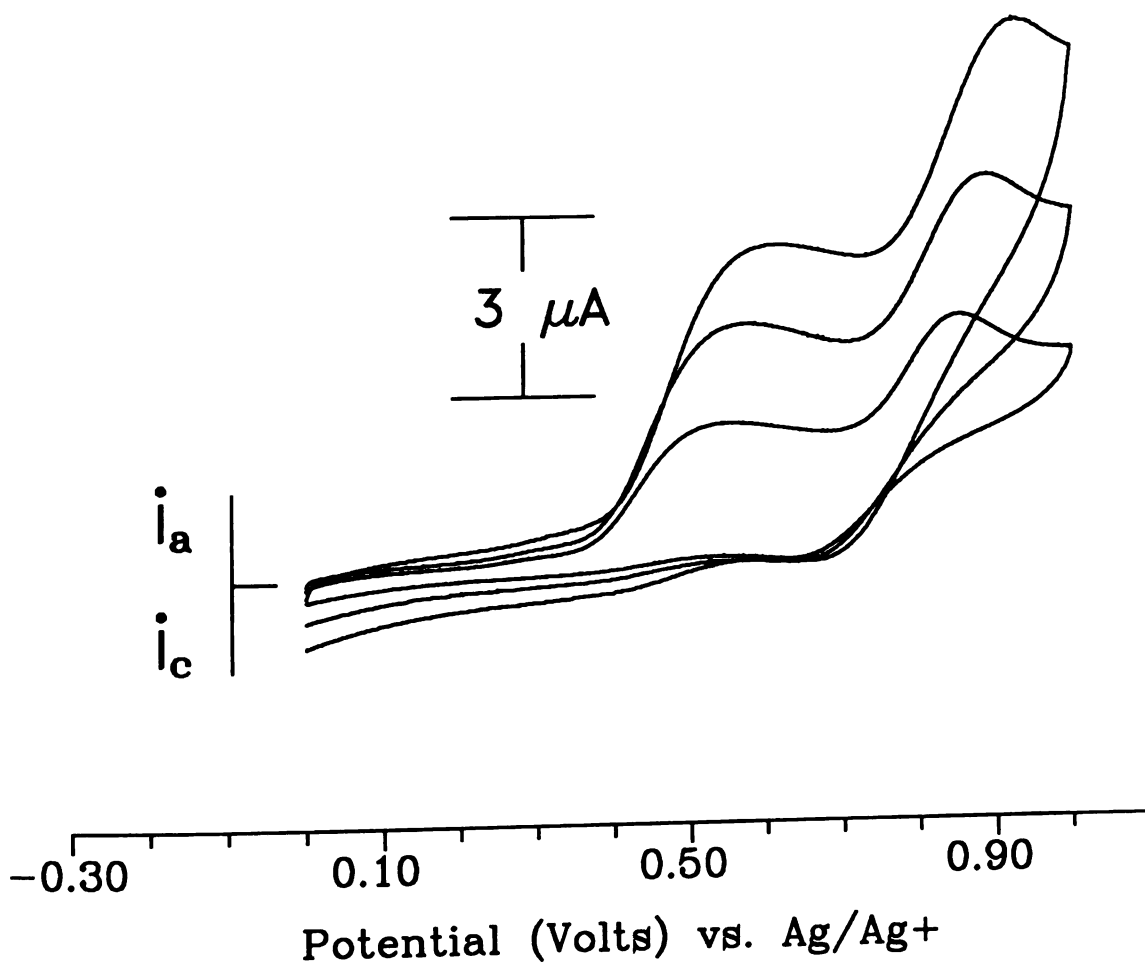


Figure 23

Figure 24. Cyclic voltammograms of polymerized 2,5-bis(2-thienyl)pyrrole (**18**) in dichloromethane, with 0.10 M TBABF₄, at 50, 25, and 10 mV/sec. Potential vs. Ag/Ag⁺. The film is well anchored and shows a linear relationship of peak current versus scan rate.

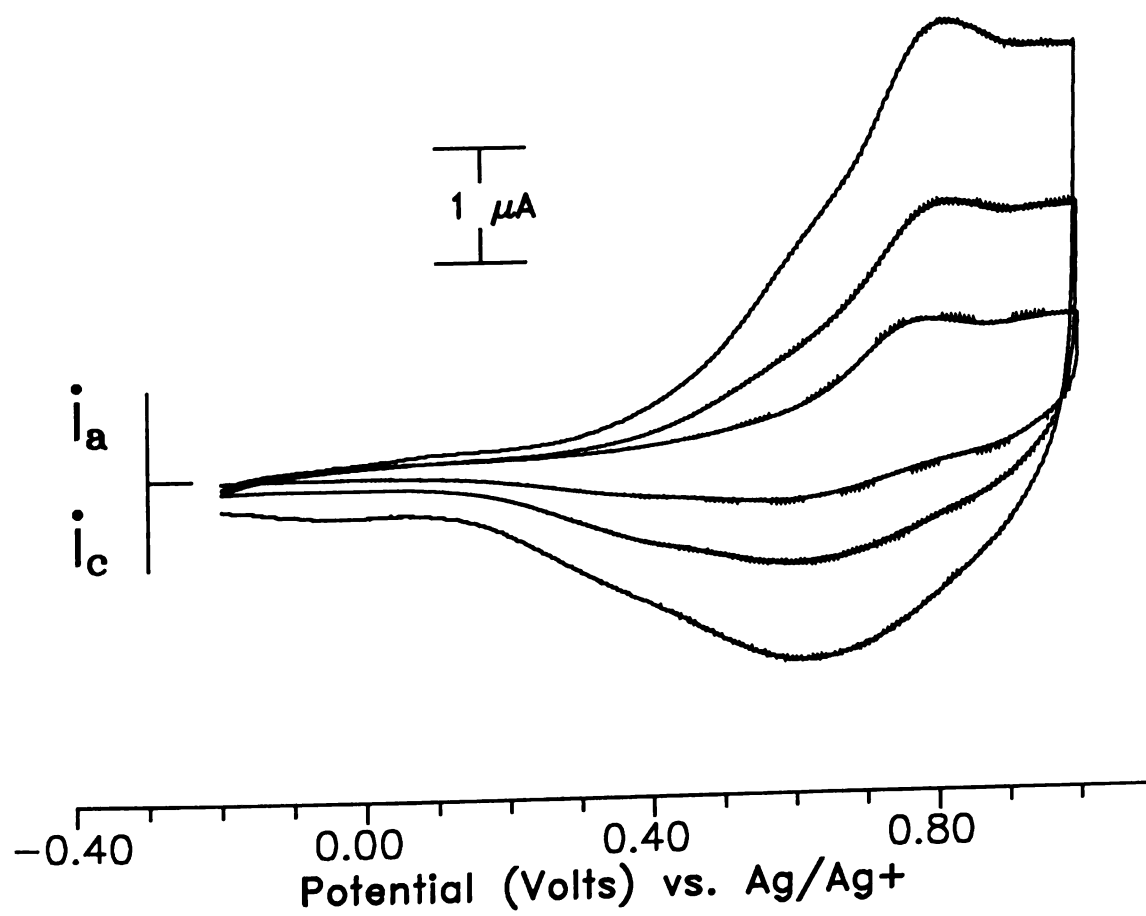


Figure 24

Figure 25. Cyclic voltammograms of polymerized 1-(dimethylamino)-4-[2,5-bis(2-thienyl)-1-pyrrolyl]benzene in tetrahydrofuran, with 0.10 M TBABF₄, at 50, 25, 10 , and 5 mV/sec. Potential vs. Ag/Ag⁺.

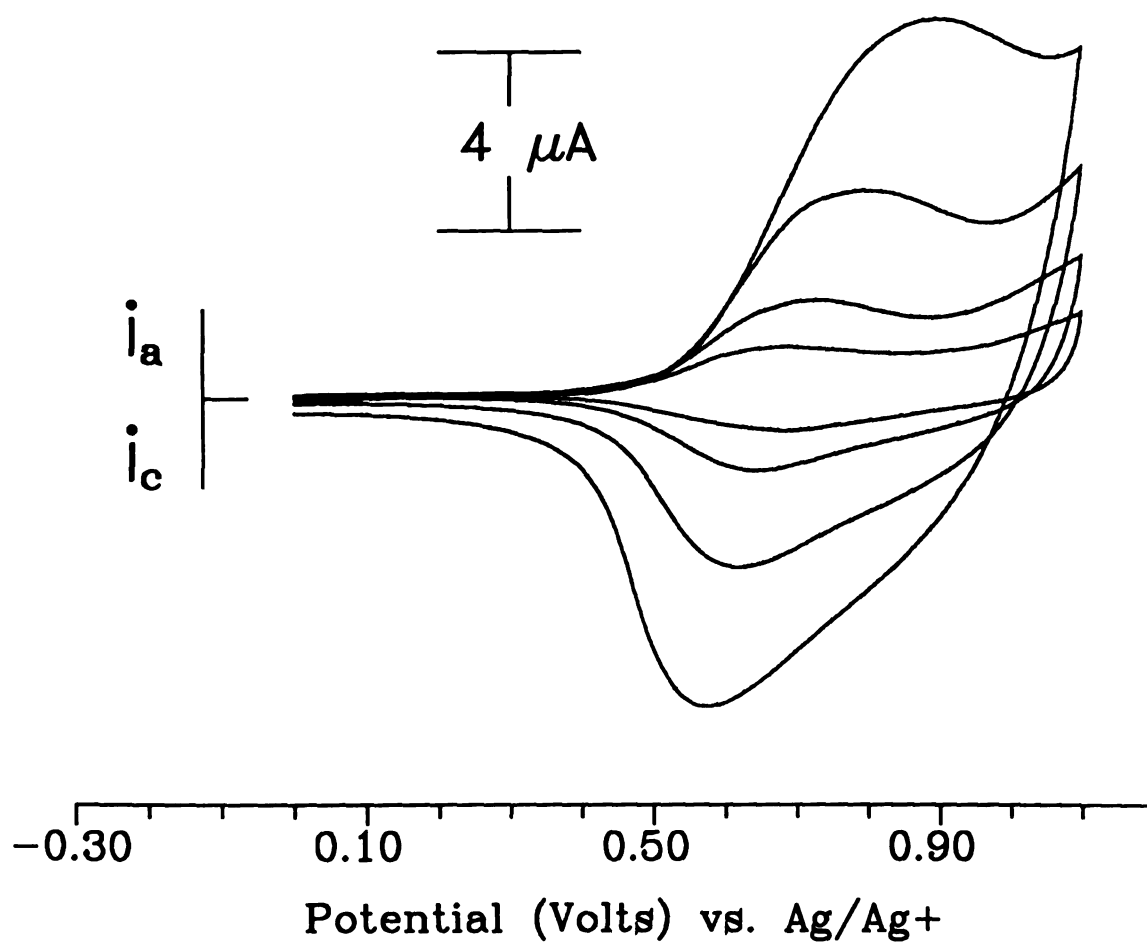


Figure 25

because conductive polymers do not have a single E^o value, but rather a distribution of E^o s.⁴⁸ This is illustrated by Figures 18 and 19. If the cyclic voltammogram of a conductive polymer film shows well-defined peak currents, it means that the distribution of polymer chain lengths is relatively narrow.

One interesting phenomenon associated with conductive polymer films is that upon scan reversal (in cyclic voltammetry) from the oxidized (conductive state) to the neutral (insulating state) there is a large jump in current (see Figures 18, 19, 20, 22, and 23). This behavior, known as the capacitive effect, arises from counter ions that have been intercalated into the polymer and cannot migrate out fast enough when the potential is changed (a typical capacitor).⁵⁴ This capacitive effect is a qualitative indication of how conductive the polymer film is. Polymers derived from **6** and **23** (Figures 20 and 25) are not expected to be very conductive since they do not show much of a capacitive effect. In contrast polymers derived from **1a** and **1b** (Figures 18 and 19) show large capacitive effects and are good conductors.

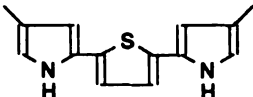

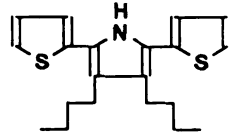
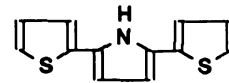
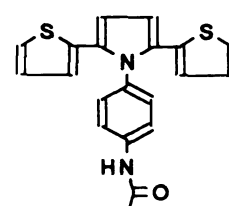
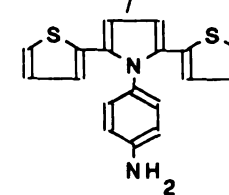
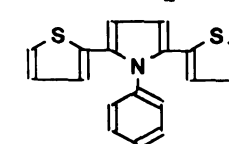
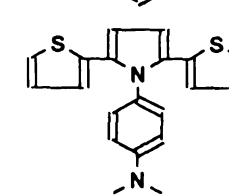
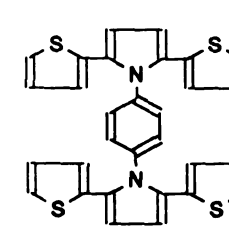
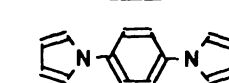
The conductivity values observed for heteroaromatic polymers can vary over several orders of magnitude (10^{-4} to 10^3 S/cm) depending upon the method of polymerization, doping, as well as the counter ion used.^{15, 16, 17} However, there are certain design factors that will determine to a very large extent the intrinsic conductivity of these systems. As a rule of thumb, placing small substituents at the β positions of the monomers will yield polymers with high conductivities, because it ensures α -linked polymers which can form very highly conjugated systems. This is illustrated by the polymer derived from **1a** and **1b**. Polymer from **1a** does not have substituents that direct the linkages to the α positions thus there are some α - β linkages. It had moderate conductivity in the oxidized form (25 S/cm). When the same compound was modified by placing methyl groups at the 3 position of the pyrroles, it ensured that the linkages would

be at the α (2) positions. A polymer derived from **1b** had a conductivity of 325 S/cm, more than a 10-fold increase.

Placing large functional groups (especially on the nitrogen of the pyrroles) instead lead to polymers with low conductivities, but with great electrochromic characteristics. Polymers derived from **6**, **16**, **17**, **23**, have low conductivities because the large functional groups disrupt the coplanarity conformation needed to increase the conjugation along the chains. If steric interference results in a deviation from coplanarity of greater than 40 % then a significant lowering of the conductivity is observed.⁴⁰ Polymers derived from **16** and **17** had conductivities of 1.79×10^{-2} and 7.4×10^{-5} S/cm respectively. The conductivity of polymers derived from **6** and **23** could not be measured because the polymer did not grow enough to make it across the gap to make contact.

Table 4 summarizes the electrochemical and electrical characteristics of a variety of heteroaromatic conductive polymers synthesized by Merrill, Benz, LeGoff and de Armas.

Table 4. Electrochemical data for synthesized monomers and polymers.

	Structure	Monomer Epa (V)	Polymer Epa (V)	Conductivity (s/cm)
1b		0.40(a)	0.21(a)	325
1a		0.52(a)	-0.02(a)	25
28		0.95(b)	-----	-----
18		1.06(b)	0.79(b)	280
17		1.10(b)	0.77(b)	7.4×10^{-2}
16		1.12(b)	0.67(b)	1.8×10^{-5}
22		1.15(b)	-----	-----
23		1.21(b)	0.69(b)	-----
6		1.32(b)	1.00(b)	-----
5		1.47(b)	0.97(b)	$< 10^{-5}$

(a) vs. SSCE (b) vs. Ag/Ag+

C. Spectroelectrochemistry

The electrochemical processes in conductive polymers are usually accompanied by spectral changes and spectroelectrochemistry is therefore a natural tool in the characterization of these materials. Spectroelectrochemistry is extremely important because these systems are so complex that electrochemical measurements without any spectral information may actually lead to erroneous conclusions.⁸¹ These spectral changes are important because they are the underlying reason for a variety of important technological applications. Although some conductive polymers possess low conductivity values, they in turn may show peculiar and useful non-linear optical responses, as is the case for the synthesized polymers included in this thesis.

The electrical conductivity and other physical properties of doped polyconjugated polymers is commonly explained on the basis of polaron/bipolaron theory (see Figure 2). The proposal that polarons and bipolarons plays a central role in determining the electronic properties of doped conductive polymers has recently led to considerable theoretical and experimental interest in these compounds.^{5, 82, 83}

Conductive polymers are usually made by the electrochemical oxidation of a heteroaromatic monomer. Polymers made this way are in the form of films, and can be doped or undoped reversibly by applying appropriate potentials.

A conductive polymer in the neutral form should exhibit only one absorption band that corresponds to the $\pi\text{--}\pi^*$ transition of the valence band to the conduction band (the band gap). This transition should be at lower energy values than the parent monomer $\pi\text{--}\pi^*$ transition. This results from the fact that in a conductive polymer there is more conjugation than the corresponding material

from which it was made. A decrease of the band gap results. The $\pi-\pi^*$ transition is an indication of the extent of conjugation.

When a conductive polymer is partially oxidized it leads to the formation of polarons (Figure 2). Further oxidation results in the formation of bipolarons. The relative stabilities of polarons and bipolarons is open to debate, as bipolarons are theoretically expected to be favoured over polarons,⁸⁵ while experimental evidence suggests that polarons may be a stable intermediate. Normally the maximum polaron concentration is quite low in polymers consisting mainly of thiophene.⁸⁶ In contrast, high concentrations are found in polymers consisting mainly of pyrrole units.^{87, 88}

The spectra of polymerized **1a** is shown in Figure 26 at different oxidation levels. Curve **a** shows one main peak at 460 nm (2.69 eV) which corresponds to the band gap ($\pi-\pi^*$ transition) of the neutral polymer, and a smaller peak at 365 nm (3.39 eV) corresponding to the band gap of the oxidized polymer. This is a result from the fact that initially the polymer is in the oxidized form and it is very hard to completely reduce it to the neutral form. As the level of oxidation is increased (trace **b**) two new transitions appear, one at 586 nm (2.11 eV) and another broad one above 900 nm (>1.4 eV). These two transitions are from the bipolaron bands. The peak at 586 nm corresponds to excitation from the valence band to the high energy bipolaron band. The broad peak in the near-IR corresponds to the transition from the valence band to the low energy bipolaron band. As the extent of oxidation is increased the intensity of the neutral polymer band gap decreases (at 460 nm) and the intensity of the oxidized polymer band gap increases (365 nm). Trace **c** shows the spectrum of polymerized **1a** when it is oxidized to about 30%. It indicates that the band gap has increased at the expense of the formation of bipolaron bands. The polymer derived from **1a** is a

Figure 26. *In situ* spectroelectrochemistry of polymerized **1a** film on an ITO electrode, with 0.10 M TBABF₄ in acetonitrile. Trace **a** at 0.00 V, trace **b** at 0.20 V, and trace **c** at 0.80 V. Potentials versus SSCE.

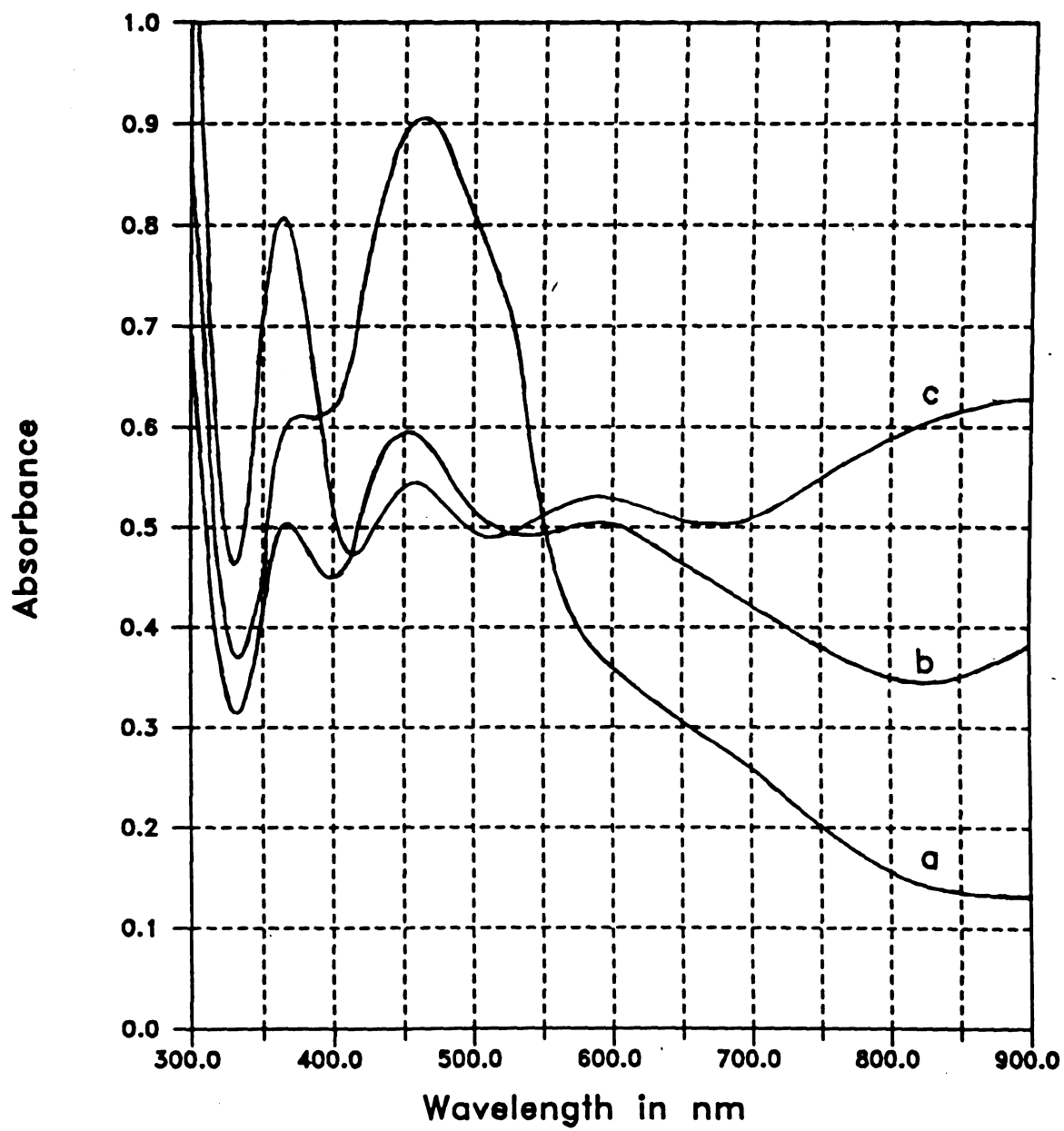


Figure 26

Figure 27. *In situ* spectroelectrochemistry of polymerized **1b** film on an ITO electrode, with 0.10 M TBABF₄ in acetonitrile. Trace **a** at -0.10 V, and trace **b** at 0.20 V. Potentials versus SSCE.

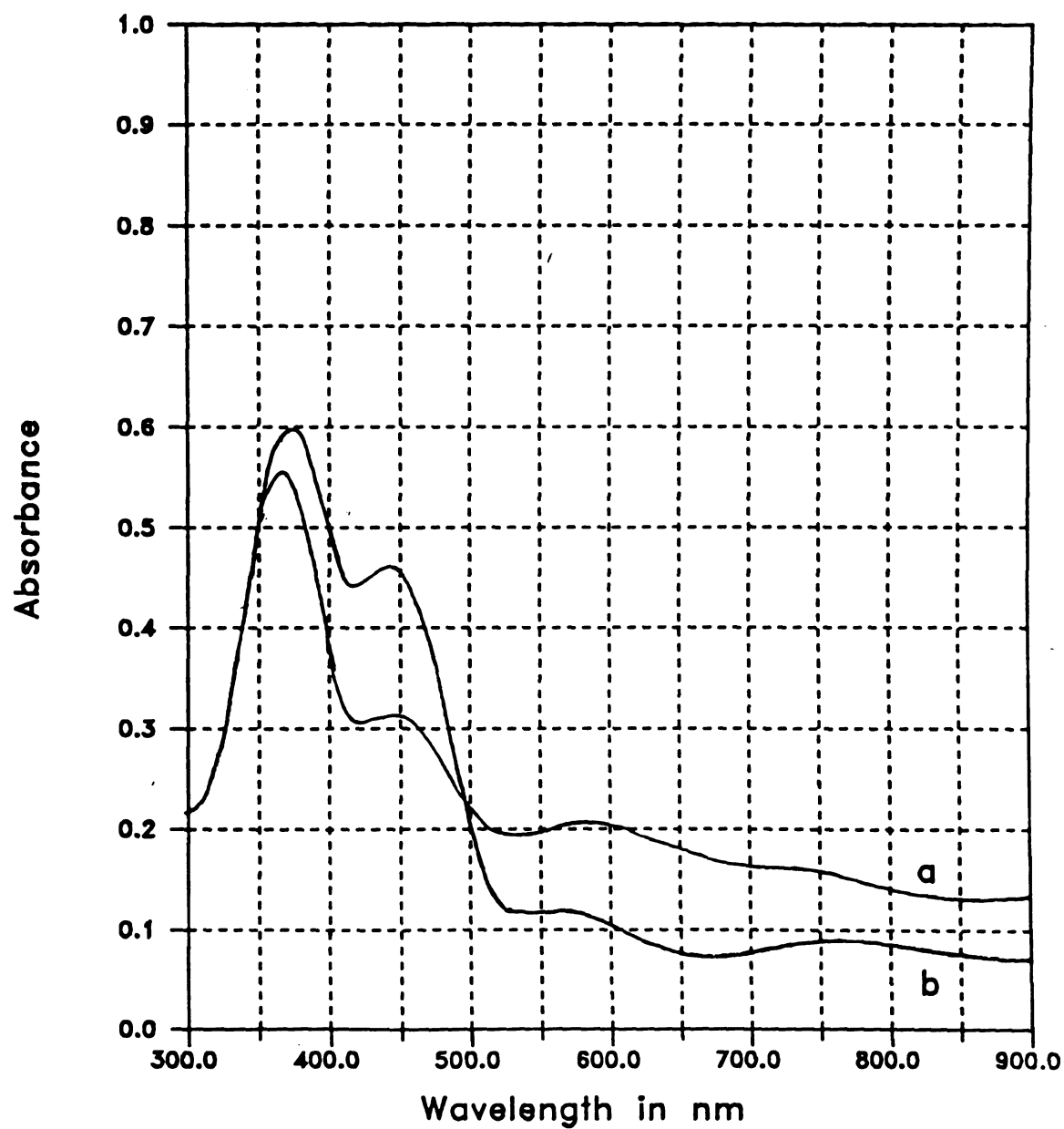


Figure 27

shiny, dark blue film in the oxidized form, and clear, light green in the neutral state.

Figure 27 shows the spectra of polymerized **1b** at two different partially oxidized levels. Trace **a** depicts the band gap of the neutral polymer at 446 nm (2.78 eV) and the oxidized polymer band gap at 365 nm (3.39 eV). For the less oxidized (5 % oxidation) polymer there is a broad transition at 764 nm (1.62 eV) which is evidence for the formation of polaron states. This is consistent with a polymer consisting mainly of pyrrole units. The bipolaron bands are situated at 568 nm (2.18 eV) and below 900 nm (1.4 eV). Polymerized **1b** is a shiny, dark blue film in the oxidized form and clear, light green in the neutral form. One striking observation of the oxidized forms of **1a** and **1b** is that the band gap of both polymers fall at the same wavelength, although **1b** has methyl substituents at the 3 positions. This finding suggests that it is possible to tune the conductivity without affecting the electronic characteristics of the polymer.

The spectra of polymerized **6** is shown in Figure 28. For this polymer no polarons are observed, in accord with a polymer consisting mainly of thiophene units. The band gap of the oxidized form of the polymer lies at 364 nm (3.41 eV), while the neutral form band gap is at 472 nm (2.63 eV). The bipolaron bands are located at 609 nm (2.04 eV) and 844 nm (1.47 eV) respectively. In the oxidized form, this polymer is dark-blue while in the neutral form it is a clear yellowish-brown. The fact that the band gap of the neutral polymer is relatively large suggests that there is not much conjugation, if any, through the phenylene bridges. This is expected since the most stable configuration of the phenyl group places it orthogonal to the pyrrole rings.

The spectra of a conductive polymer derived from **16** is shown in Figure 29. This polymer has a well defined color change upon doping. In the neutral

Figure 28. *In situ* spectroelectrochemistry of polymerized **6** film on an ITO electrode, with 0.10 M TBABF₄ in dichloromethane. Trace **a** at 0.00 V, trace **b** at 0.70 V, and trace **c** at 1.40 V. Potentials versus Ag/ Ag⁺.

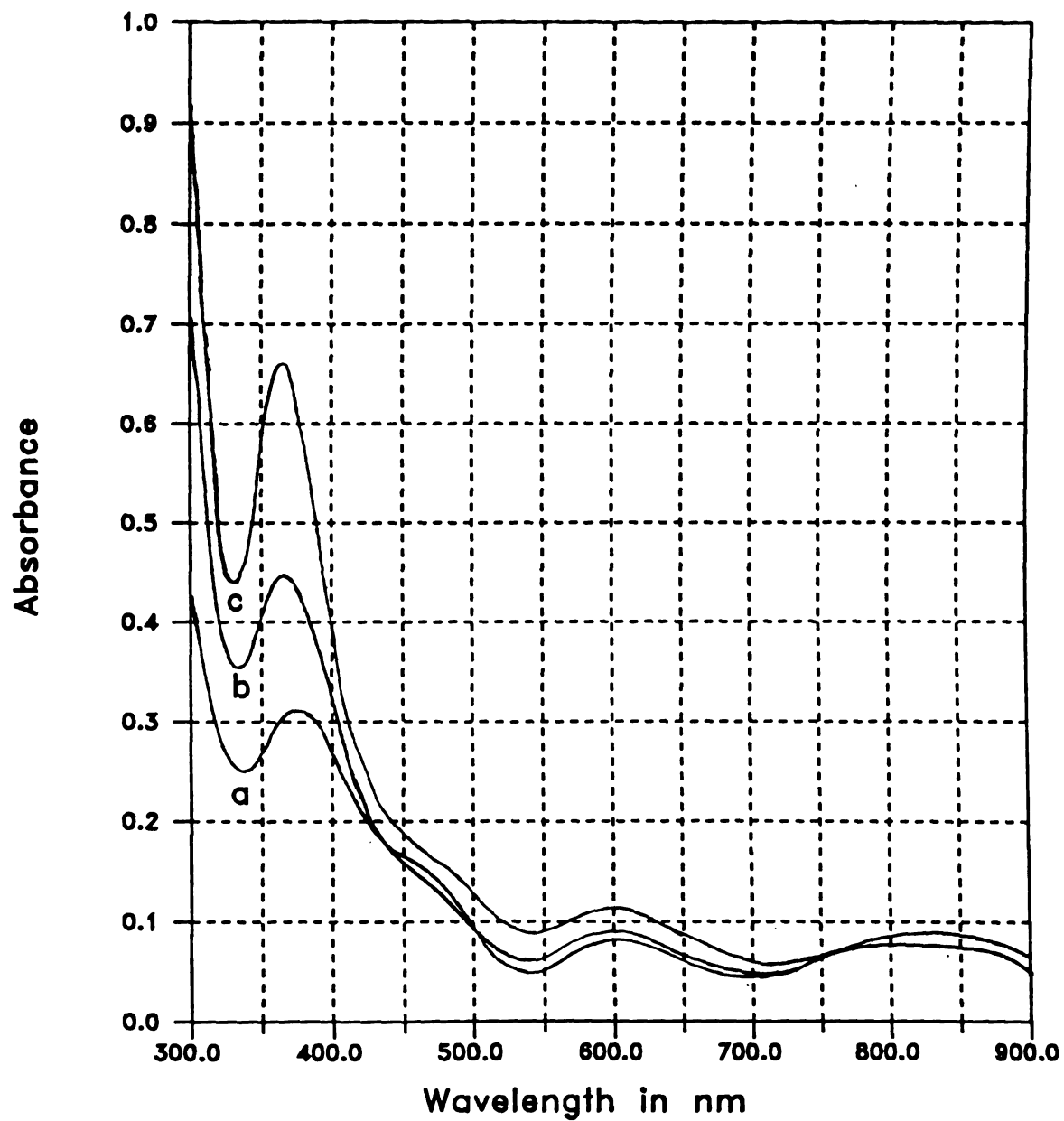


Figure 28

Figure 29. *In situ* spectroelectrochemistry of polymerized **16** film on an ITO electrode, with 0.10 M TBABF₄ in dichloromethane. Trace **a** at 0.00 V, trace **b** at 0.60 V, and trace **c** at 0.80 V. Potentials versus Ag/ Ag⁺.

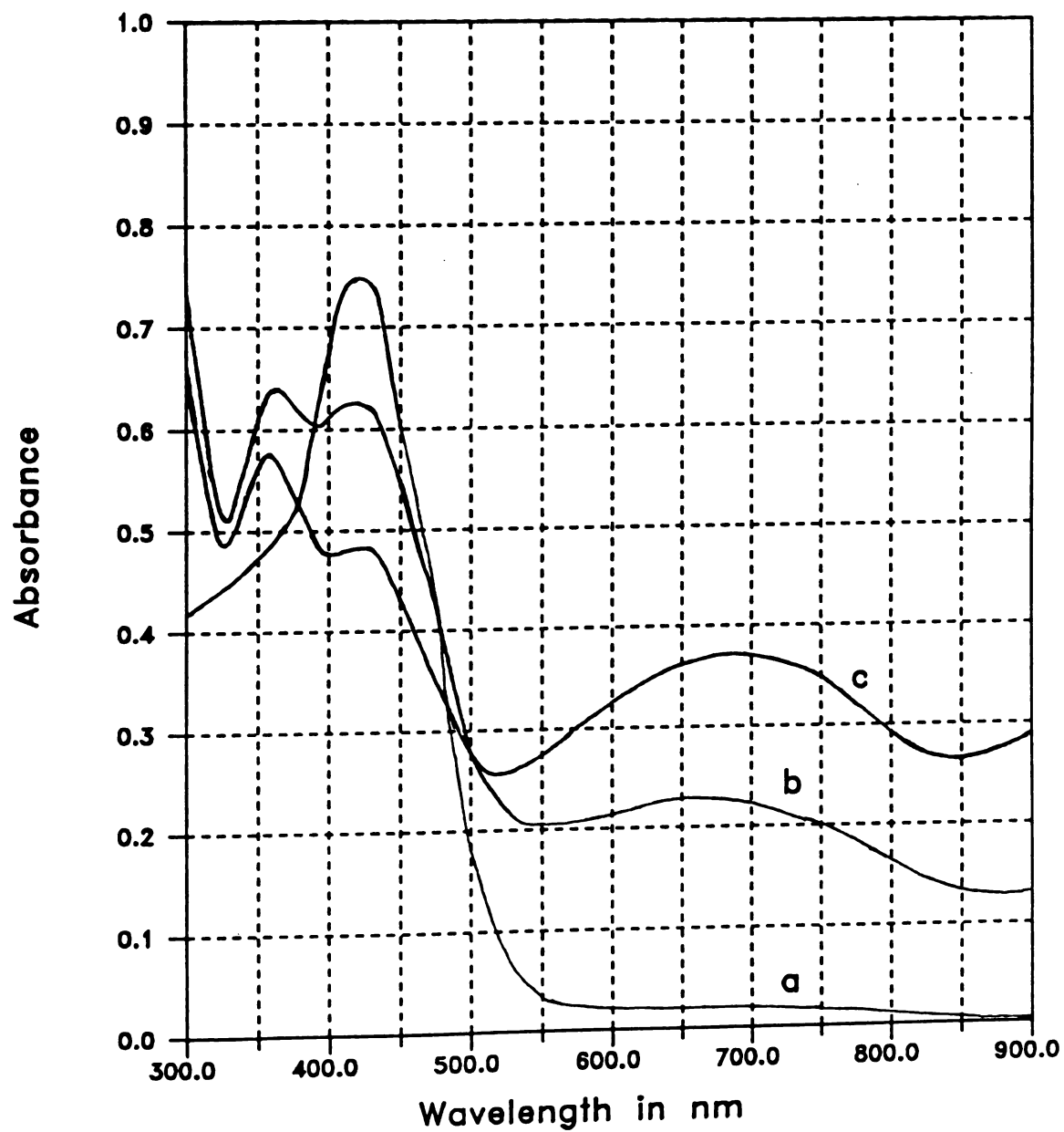


Figure 29

Figure 30. *In situ* spectroelectrochemistry of polymerized **17** film on an ITO electrode, with 0.10 M TBABF₄ in dichloromethane. Trace **a** at 0.00 V, trace **b** at 0.50 V, and trace **c** at 0.75 V. Potentials versus Ag/Ag⁺.

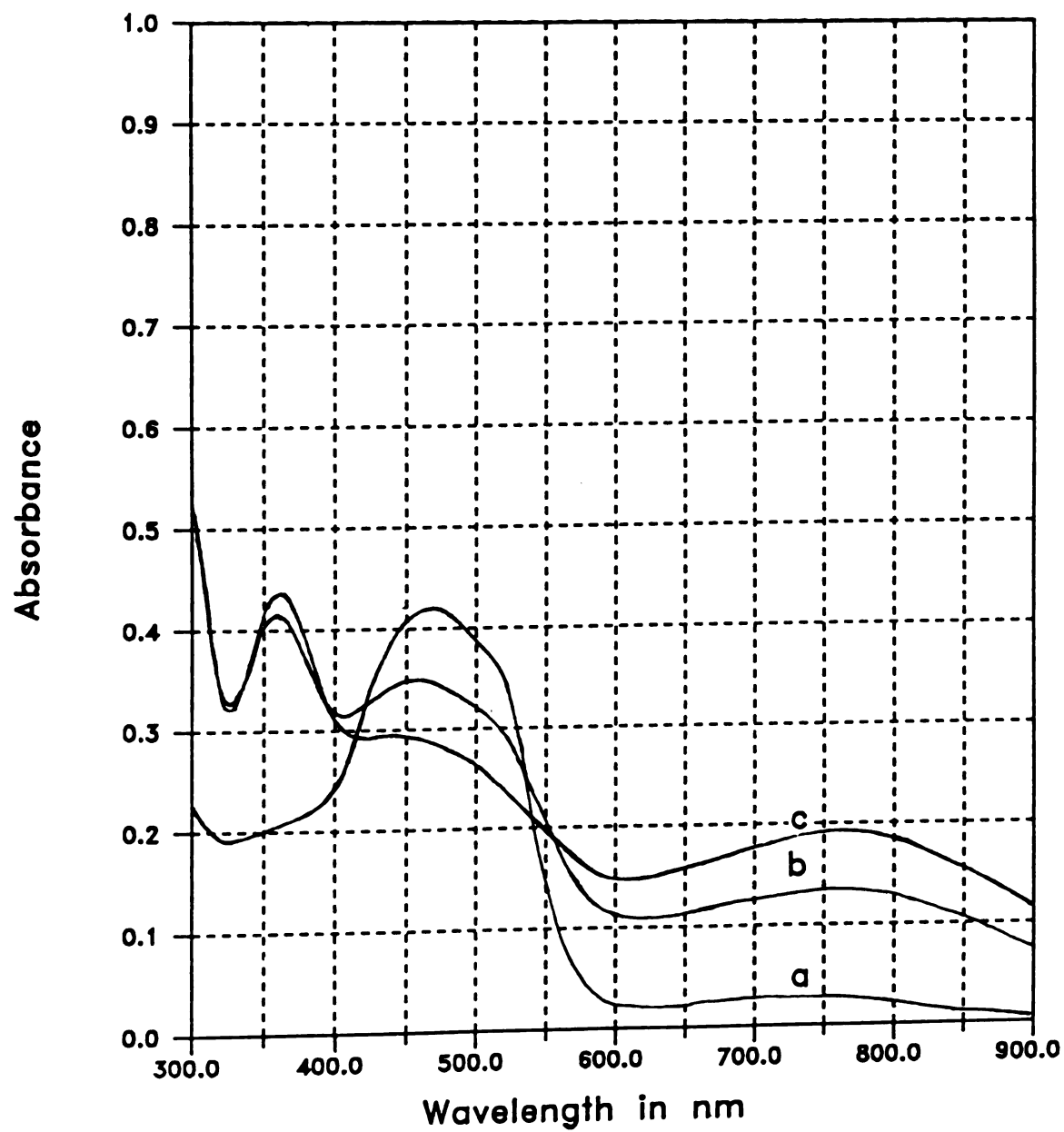


Figure 30

Figure 31. *In situ* spectroelectrochemistry of polymerized **23** film on an ITO electrode with 0.10 M TBABF₄ in tetrahydrofuran. Trace **a** at 0.00 V, and trace **b** at 1.00 V. Potentials versus Ag/Ag⁺.

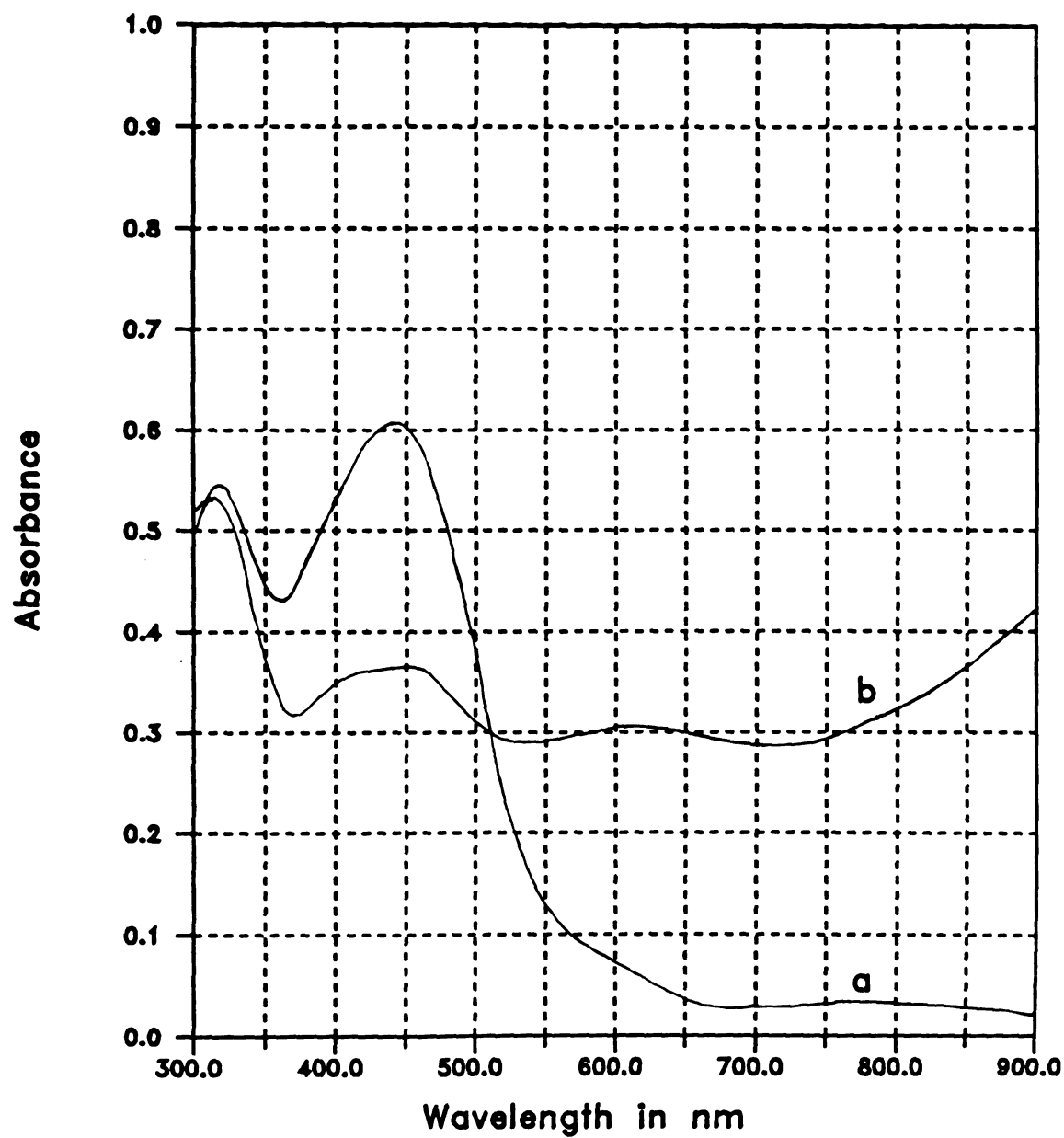


Figure 31

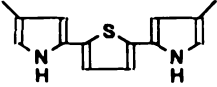
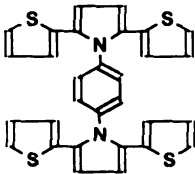
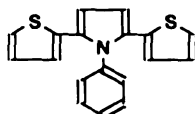
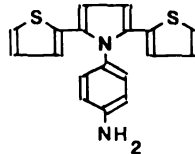
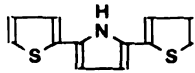
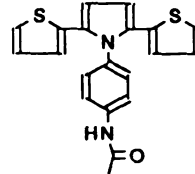
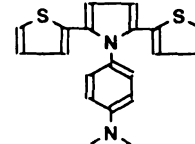
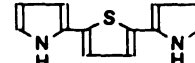
form it is a clear, light yellow, but switches to a dark-blue-green color upon oxidation. The band gap of the neutral polymer (trace **a**) is at 426 nm (2.91 eV), while in the oxidized form the band gap (trace **c**) is at 360 nm (3.44 eV). It is peculiar that the band gap of the oxidized form of **16** is very similar to the band gap of oxidized polymer **6**. Apparently the aminobenzene group does not alter this property. The bipolaron bands lie at 697 nm (1.78 eV) and >900 nm (1.4 eV). This conductive polymer is interesting, because if the phenyl group is functionalized in a certain way, there may be non-linear optical effects, that are useful in frequency multiplication.

Oxidized polymer of **17** (trace **c** of Figure 30), also has a band gap transition at 360 nm (3.44 eV), similar to **6** and **16**. The phenyl acetamide functionality does not alter the band gap of the oxidized polymer, however the neutral polymer band gap at 480 nm (2.58 eV, trace **a**) is quite different from both **6** and **16**. The high energy bipolaron band is located at 772 nm (1.61 eV). The lower energy bipolaron band is probably in the near-IR. Polymer **17** was dark-blue-green in the oxidized form and clear-red-brown in the neutral form.

Polymerized **23** (Figure 29) is peculiar, because the oxidized form shows a band gap at 316 nm (3.92 eV, trace **b**), much higher in energy than those of **6**, **16**, and **17**. The band gap of the neutral polymer (trace **a**) is at 449 nm (2.76 eV) with the bipolarons at 622 nm (1.99 eV) and >900 nm (1.4 eV). The polymer films were dark blue in the oxidized form and clear-green in the neutral form. The methyl groups make this polymer slightly soluble.

The spectrochemical data for polymers derived from **1a**, **1b**, **6**, **16**, **17**, and **23** suggests that the conduction mechanism in these systems is consistent with polaron/bipolaron formation. Table 5 summarizes the spectrochemical data for these systems.

Table 5. Summary of spectroscopic data of synthesized polymers.

	Structure	Monomer $\pi\text{-}\pi^*$ (nm)	Neutral polymer $\pi\text{-}\pi^*$ (nm)	Oxidized polymer $\pi\text{-}\pi^*$ (nm)
1b		325	446	365
6		325	472	364
22		336	-----	-----
16		340	426	360
1a		340	448	365
17		341	480	360
23		342	449	316
18		377	460	365

CONCLUSION

Using 2,5-bis(2-pyrrolyl)thiophene (**1a**) and 2,5-bis(4-methyl-2-pyrrolyl)thiophene (**1b**) as monomers, yields copolymers that have a known stoichiometry and sequence distribution of heterocyclic units. These copolymers exhibit excellent stability both in the neutral and oxidized state, and show relatively high conductivity values. As predicted, the electronic properties of the copolymers are intermediate between those of the corresponding homopolymers, polypyrrole and polythiophene. Placing the methyl substituents in the 4 positions of the pyrroles, block the formation of undesired α,β' and β,β' coupling reactions, and at the same time, the methyl groups lower the oxidation potential of the monomer, diminishing the probability of undesirable side reactions. As a result, a more ordered and hence more conductive α,α' -linked copolymer is obtained. This is reflected in a ten-fold increase in the conductivity of **1b** (325 S/cm) over **1a** (25 S/cm).

Copolymers of **1a** and **1b** respectively, show excellent spectroelectrochemical response. Both copolymers are shiny, dark blue color in the oxidized form and clear, light green in the neutral form. Spectroelectrochemical results are consistent with a polaron/bipolaron model, and demonstrate that the addition of small substituents (methyls) has hardly any effect in the band gap of the copolymers. Thus, it is possible to "tune" the conductivity without affecting the band-gap.

The synthesis of monomer **6**, capable of polymerizing to form a multidimensional conductive polymer, proved more difficult than anticipated

because the condensation of a 1,4-diketone **14** with phenylenediamine is very slow. A new method, using trimethylaluminum to activate the amine functionality, is being developed that allows the condensation with 1,4-diketones to be carried out at room temperature. Using this new method, monomer **6** was synthesized with a 23% yield.

Electrochemical polymerization of **6** resulted in a polymer that is not very conductive, because the bulky phenylene groups cause the pyrrole to twist out of the plane lowering the conjugation with the thiophenes needed to attain high conductivity. Cyclic voltammograms of **6** resemble those of a polymer that possesses non-interactive sites.

Monomers **16**, **17**, **22**, and **23** were synthesized with good yield, and when electrooxidized resulted in the formation of polymers with low conductivities because of steric interference of the bulky phenylene group. However, *in situ* spectroelectrochemistry results suggest that these systems also form bipolarons. The substitution of the derivatized phenylene group at the pyrrole nitrogen gives each of these polymers peculiar electrochromic characteristics. Neutral polymers of **16**, **17**, and **23**, are light yellowish brown, light red brown, and light green respectively. In the oxidized form they are all dark blue color. Polymers derived from **18**, and **22** could not be studied by *in situ* spectroelectrochemistry because they are completely soluble in the polymerizing media.

Monomer **16** can be used as a starting material for the formation of other monomers that can be used to make "self doped" conductive polymers. Monomer **28** was our attempt to make such a system, but **28** is insoluble in any of the media used for electropolymerization. There are other possible substituents that can be condensed with **16** to make self doped systems and will be the theme in future projects.

APPENDIX



Figure A1. 300 MHz ^1H -NMR spectrum of 1,4-bis[2,5-bis(2-thienyl)-1-pyrryl]benzene (**6**).

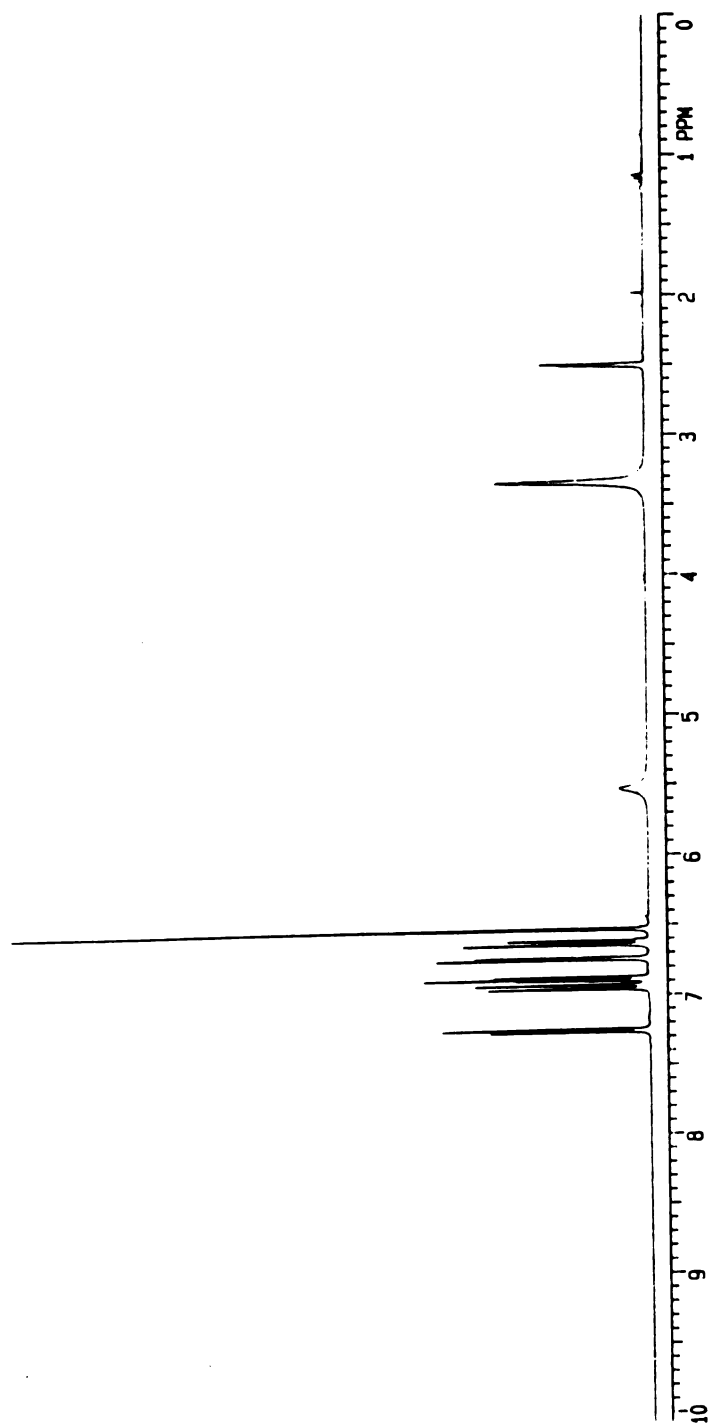


Figure A2. 300 MHz ^1H -NMR spectrum of 1-amino-4-[2,5-bis(2-thienyl)-1-pyrryl]benzene (16).

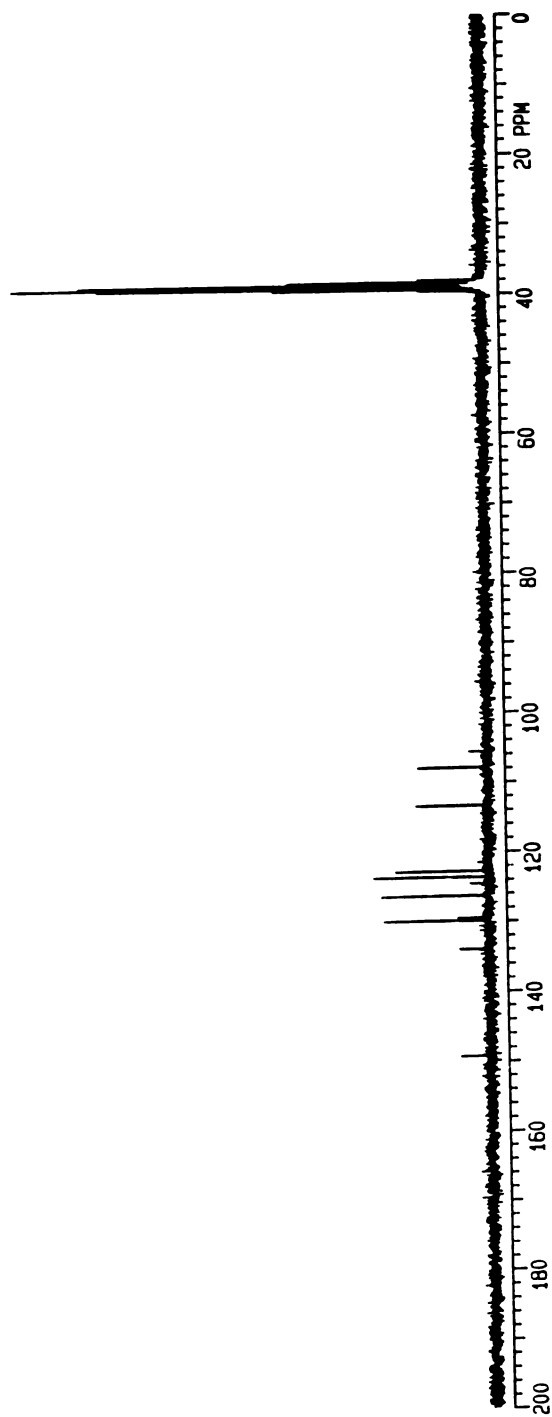


Figure A3. 75.4 MHz ^{13}C -NMR spectrum of 1-amino-4-[2,5-bis(2-thienyl)-1-pyrryl]benzene (**16**).

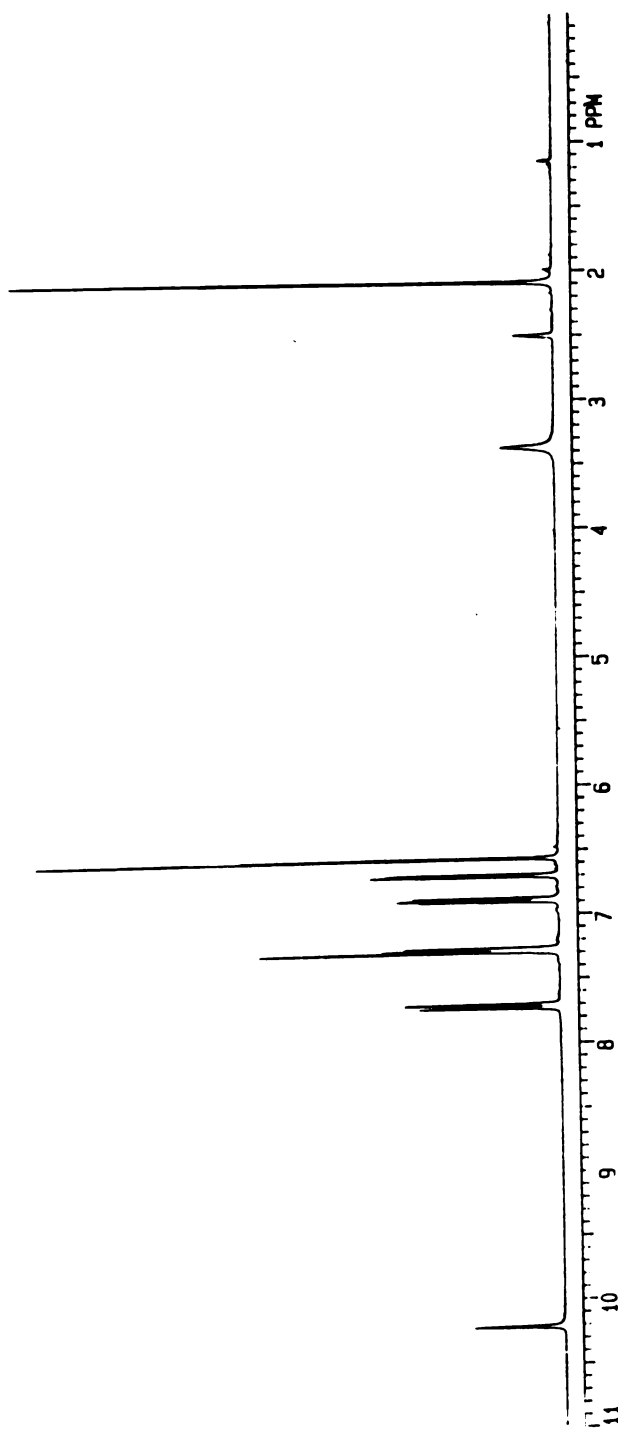


Figure A4. 300 MHz ¹H-NMR spectrum of N[4-[2,5-bis(2-thienyl)-1-pyrryl]phenyl]acetamide (17).

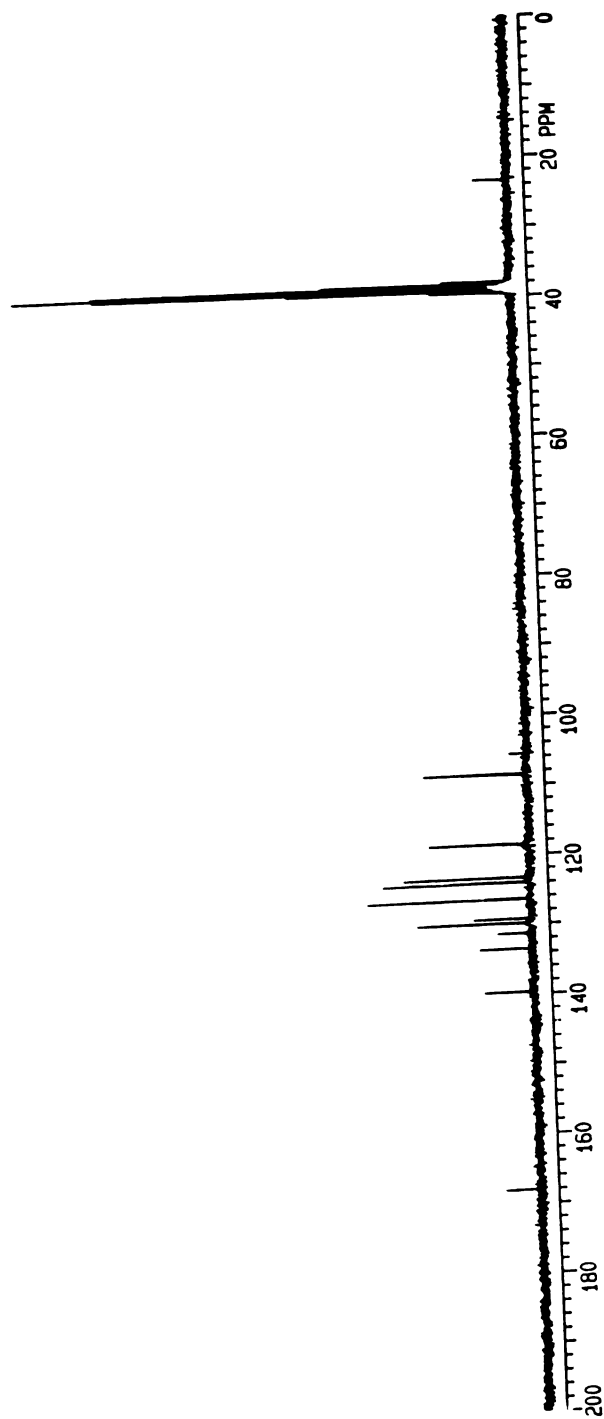


Figure A5. 75.4 MHz ^{13}C -NMR spectrum of N[4-[2,5-bis(2-thienyl)-1-pyrryl]phenyl]acetamide (17).

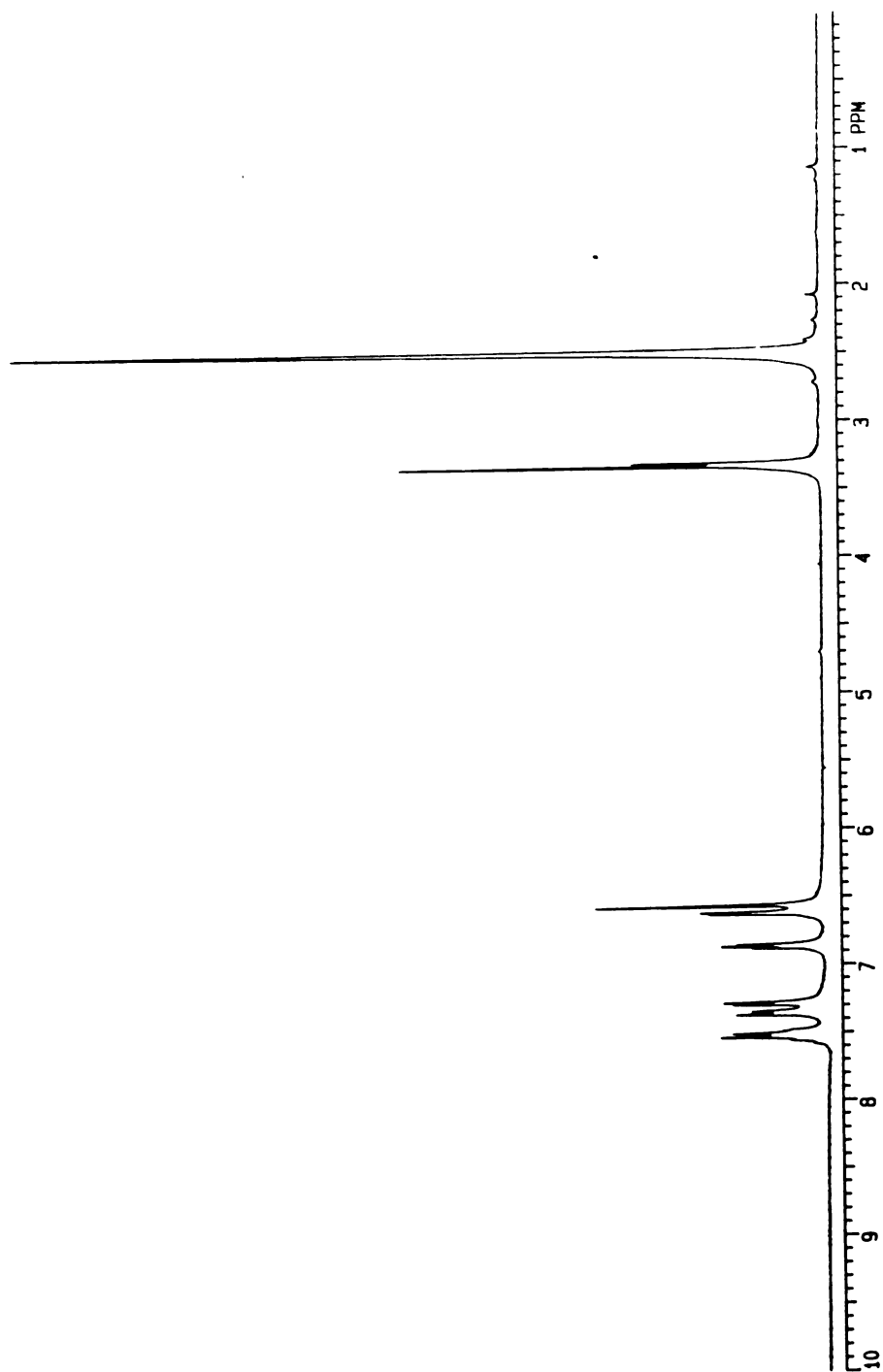


Figure A6. 300 MHz ^1H -NMR spectrum of N-[2,5-bis(2-thienyl)-1-pyrrolyl]benzene (22).

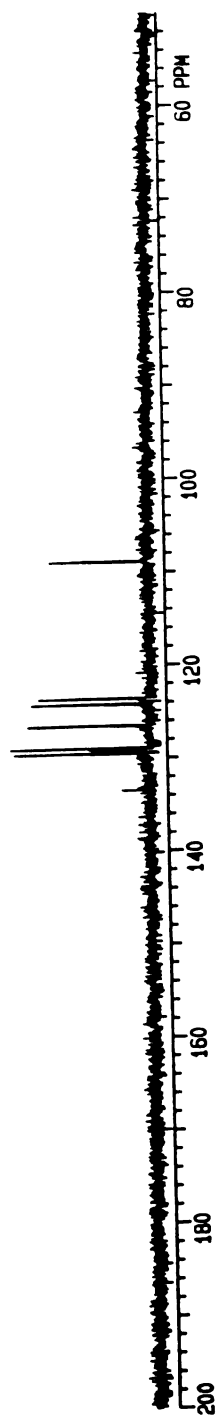


Figure A7. 75.4 MHz ^{13}C -NMR spectrum of N-[2,5-bis(2-thienyl)]-1-pyrryl]benzene (22).

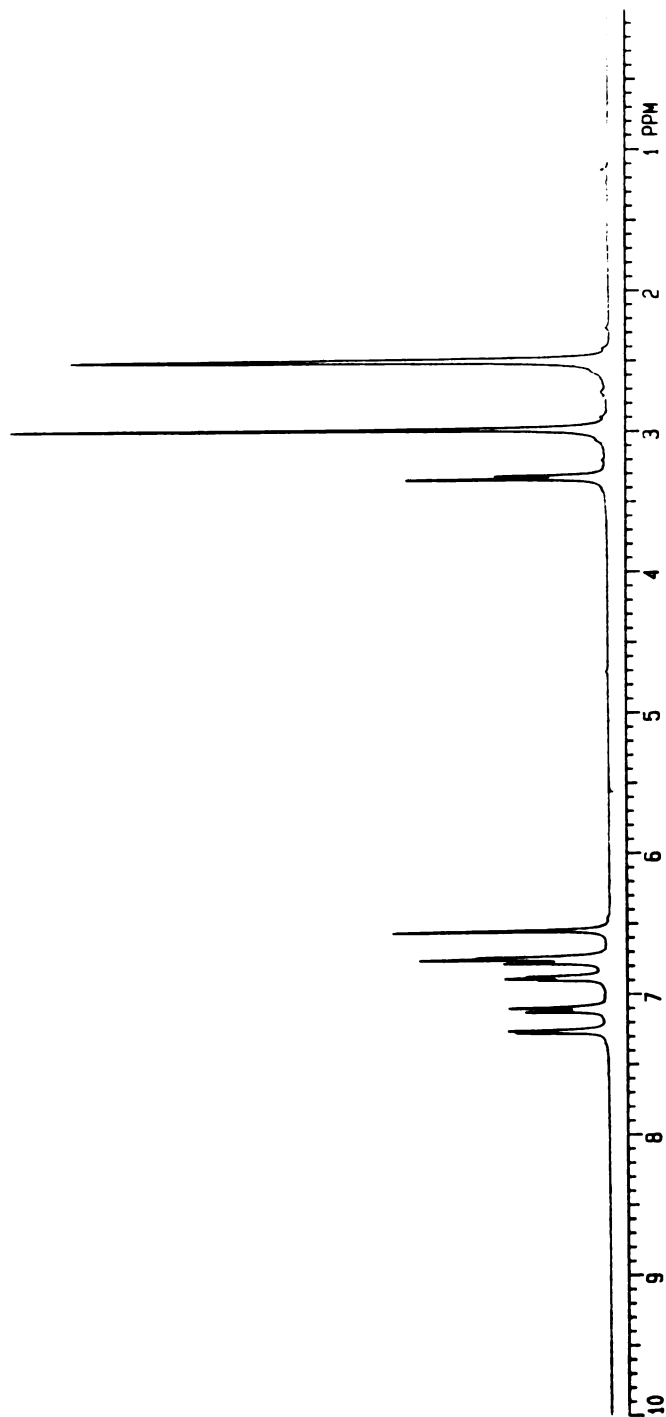


Figure A8. 300 MHz ¹H-NMR spectrum of 1-(dimethylamino)-4-[2,5-bis(2-thienyl)-1-pyrryl]benzene (**23**).

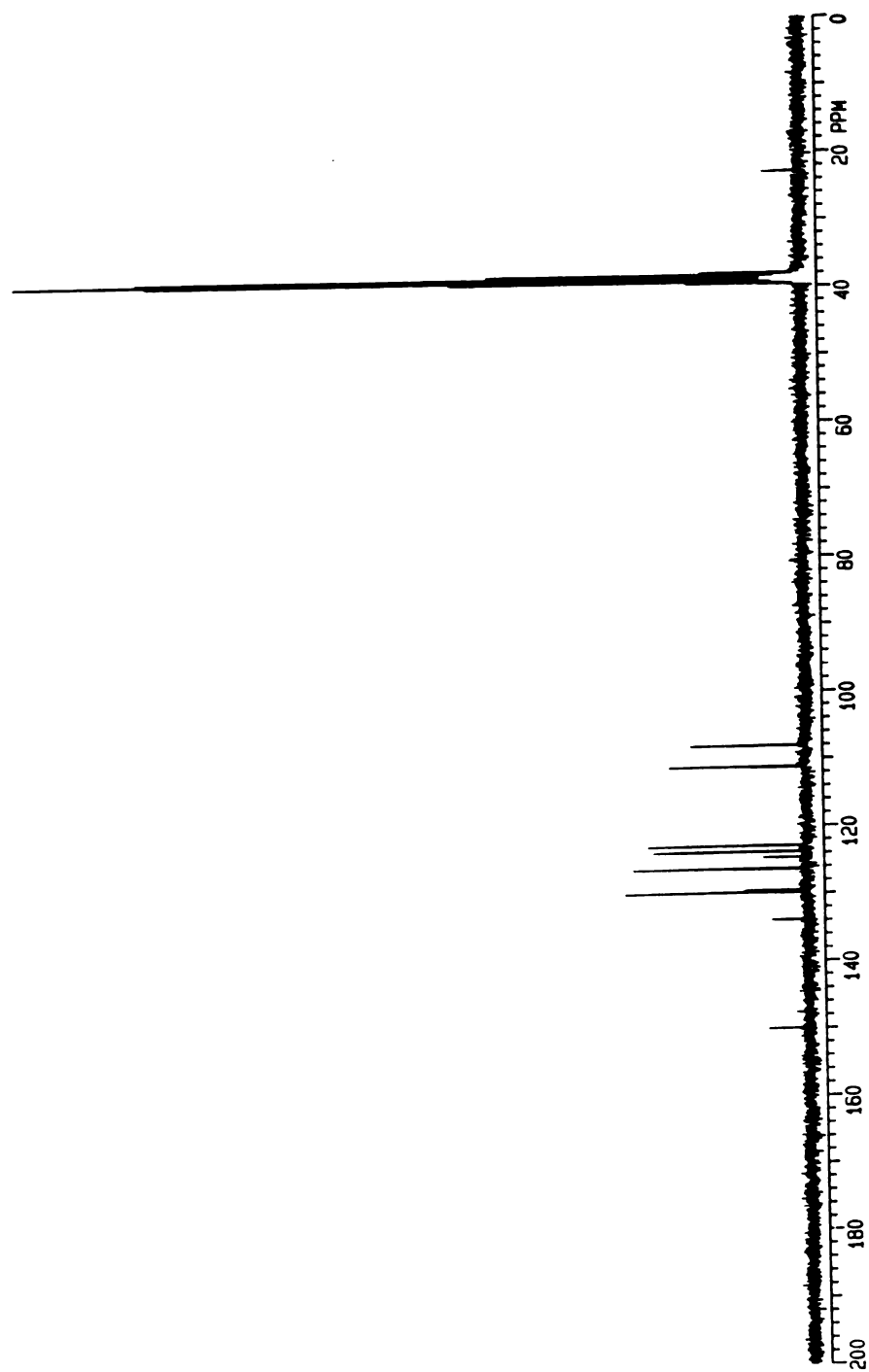


Figure A9. 75.4 MHz ^{13}C -NMR spectrum of 1-(dimethylamino)-4-[2,5-bis(2-thienyl)-1-pyrryl]benzene (23).

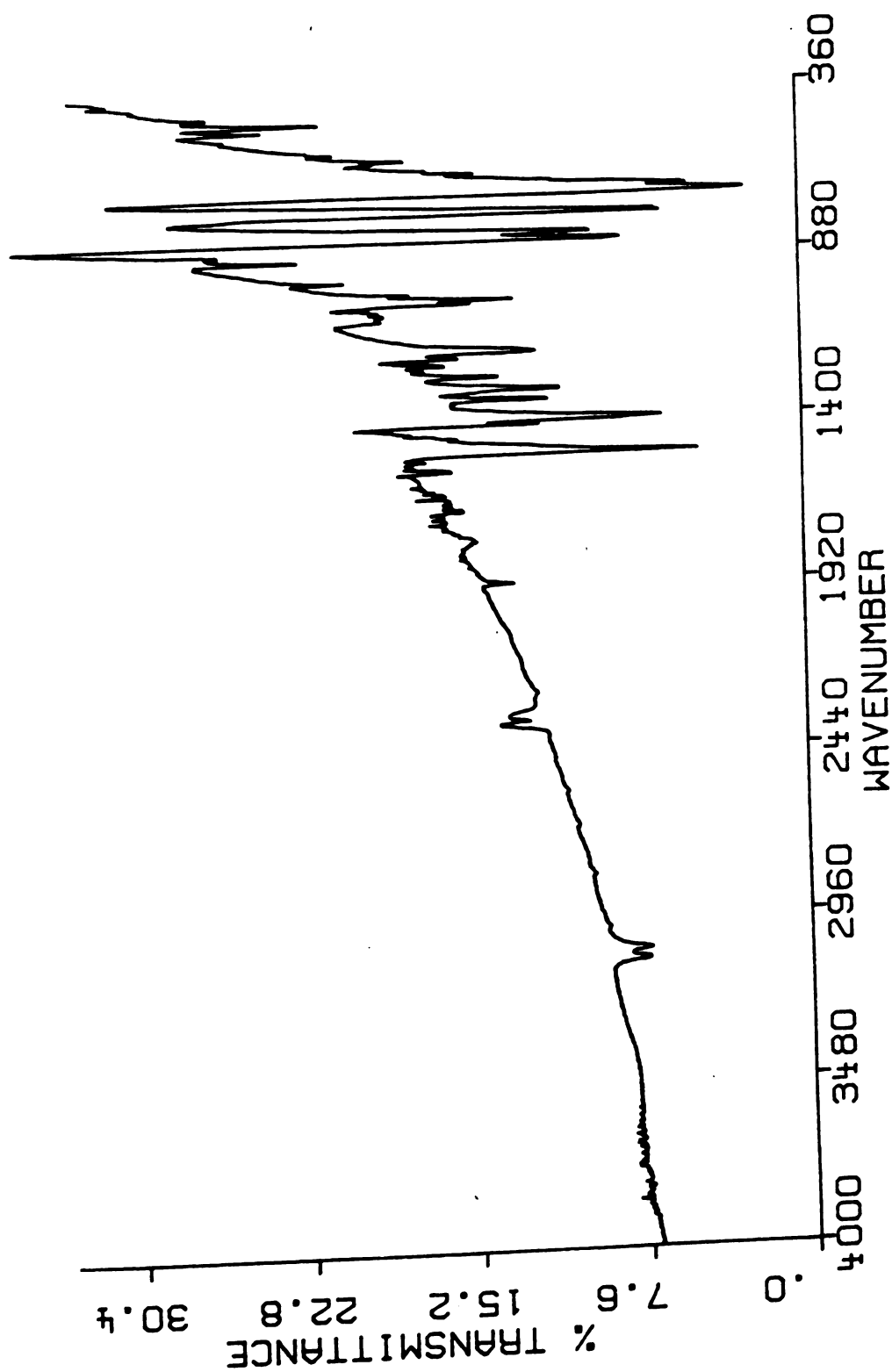


Figure A10. Fourier-transform IR spectrum of 1,4-bis[2,5-bis(2-thienyl)-1-pyrryl]benzene (**6**) in KBr.

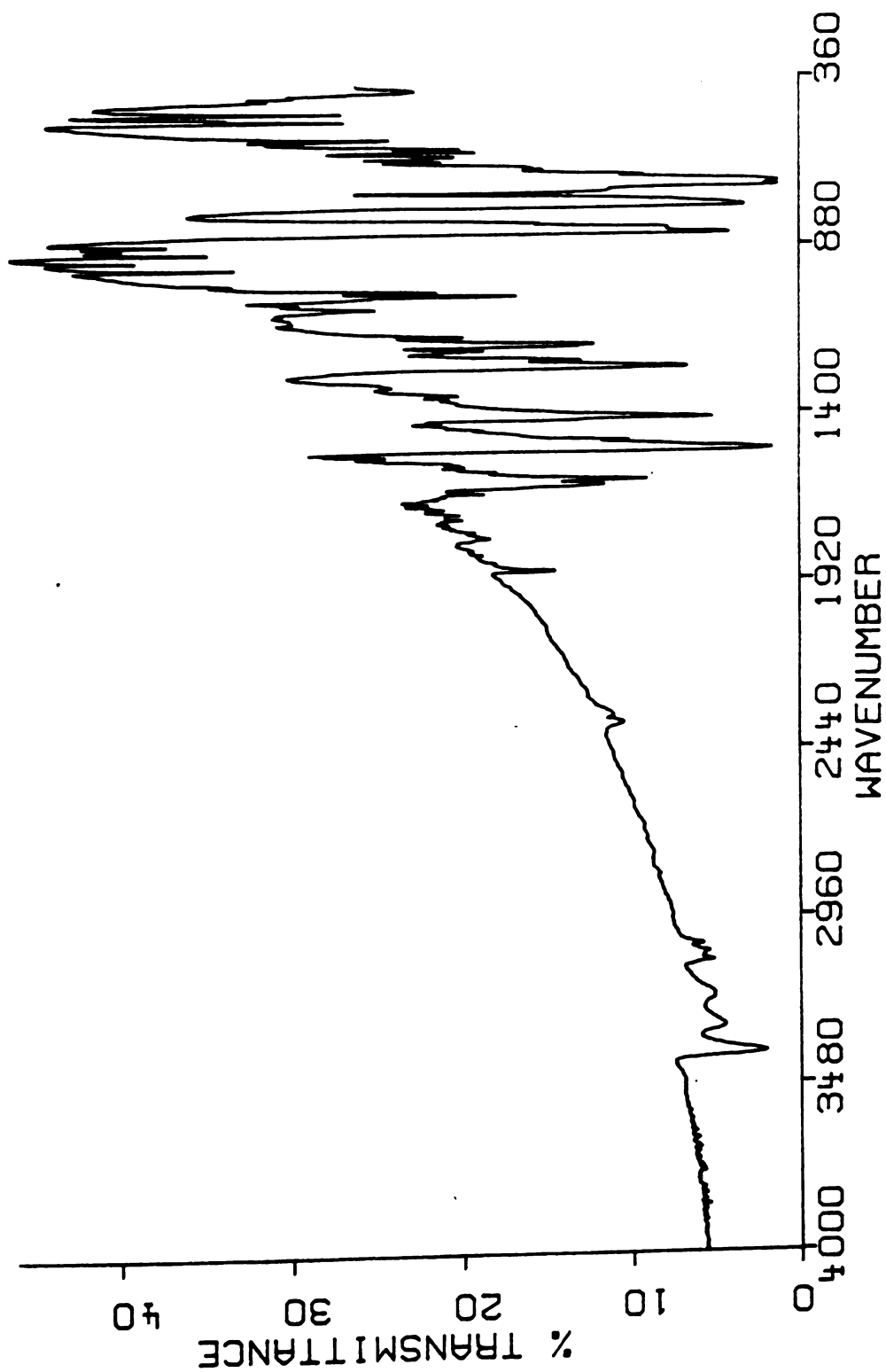


Figure A11. Fourier-transform IR spectrum of 1-amino-4-[2,5-bis(2-thienyl)]-1-pyrrolylbenzene (**16**) in KBr.

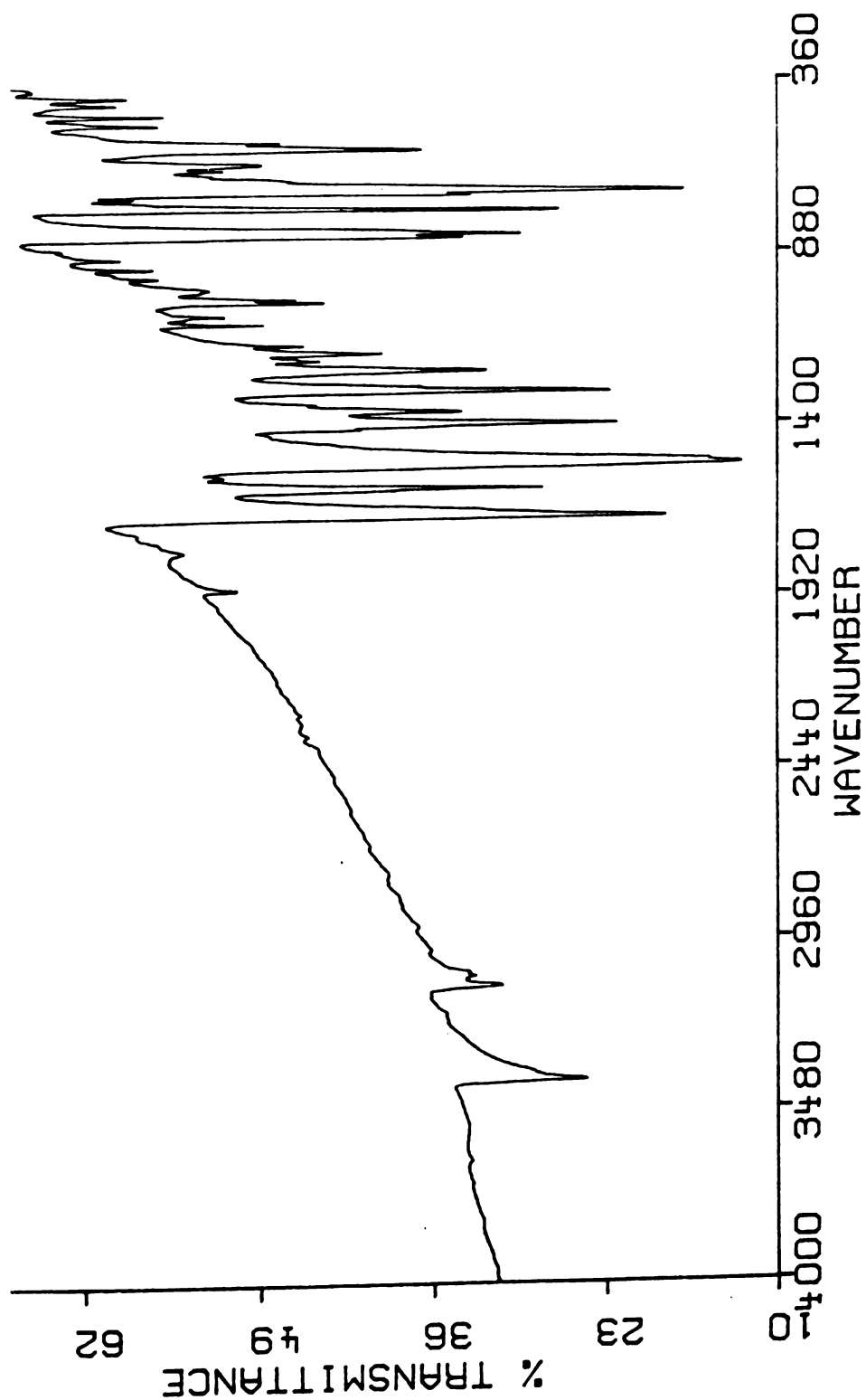


Figure A12. Fourier-transform IR spectrum of N[4-[2,5-bis(2-thienyl)-1-pyrryl]phenyl]acetamide (**17**) in KBr.

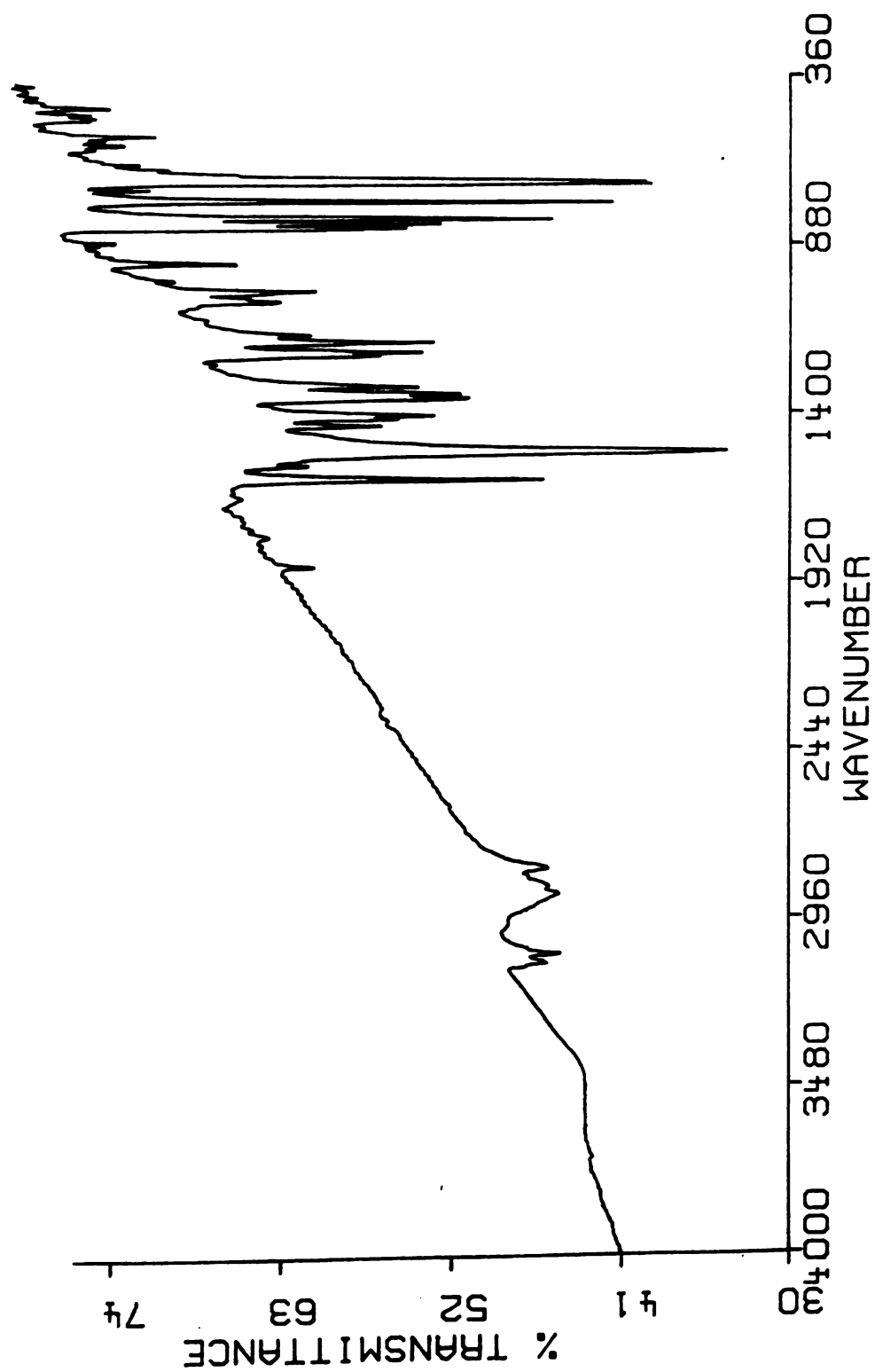


Figure A13. Fourier-transform IR spectrum of N-[2,5-bis(2-thienyl)-1-pyrryl]benzene (**22**) in KBr.

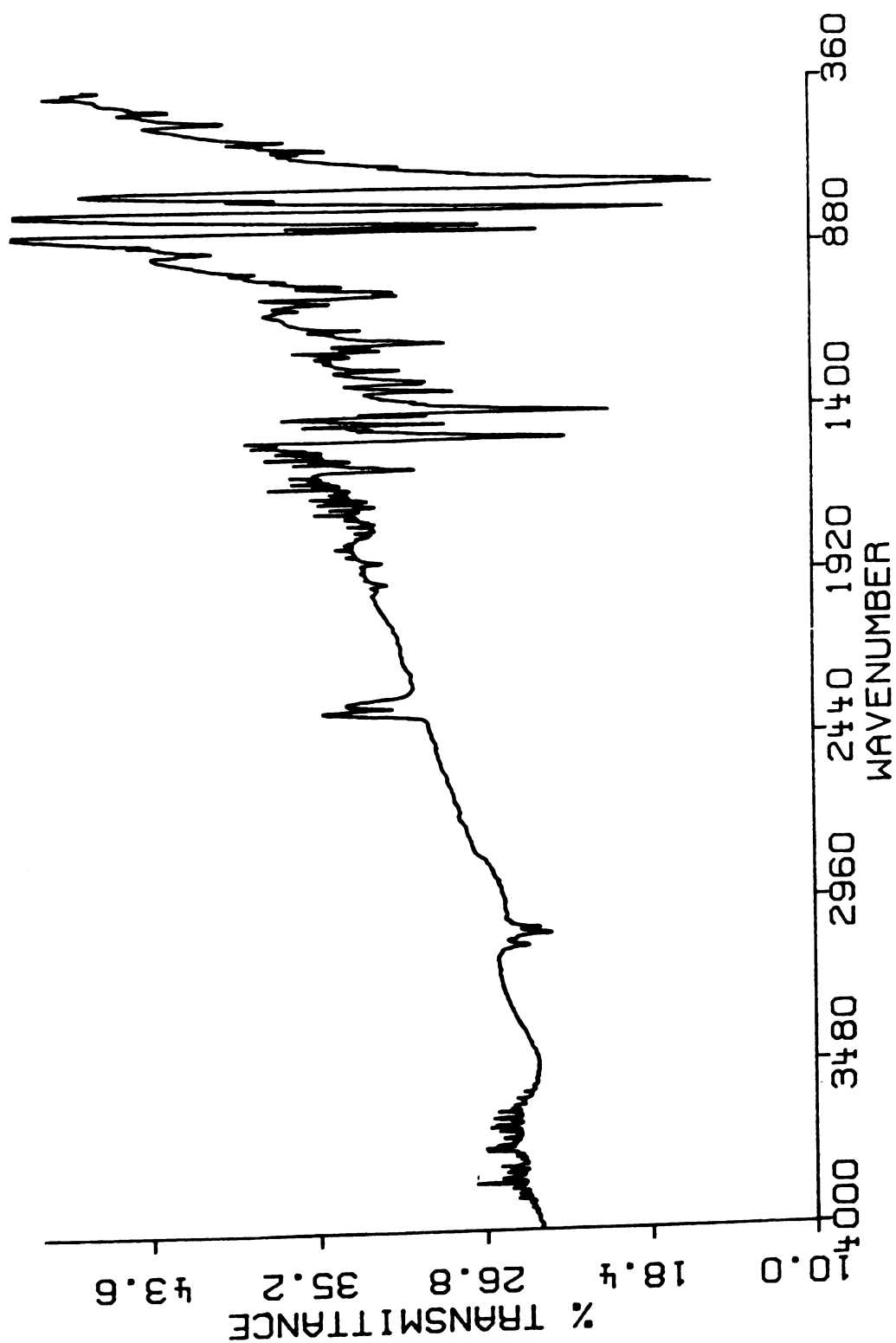


Figure A14. Fourier-transform IR spectrum of 1-(dimethylamino)-4-[2,5-bis(2-thienyl)-1-pyrryl]benzene (**23**) in KBr.

LIST OF REFERENCES

1. Cowan, D.O.; Wiygul, F.M. *Chem. Eng. News* **1986**, *64*, 28.
2. Kanatzidis, M.G. *Chem. Eng. News* **1990**, *68*, 36.
3. Chiang, C.K.; Fincher, C.R.; Park, Y.W.; Heeger, A.J.; Shirakawa, H.; Louis, E.J.; Gau, S.C.; McDiarmid, A.G. *Phys. Rev. Lett.* **1977**, *39*, 1098.
4. Krieger, J. *Chem. Eng. News* **1987**, *65*, 20.
5. Bredas, J.L.; Street, G.B. *Acc. Chem. Res* **1985**, *18*, 309.
6. Reynolds, J.R. *Chemtech* **1988**, *18*, 440.
7. Chiang, C.K.; Drury, M.A.; Gau, S.C.; Heeger, A.J.; Louis, E.J.; McDiarmid, A.G.; Park, Y.W.; Shirakawa, H. *J. Am. Chem. Soc.* **1978**, *100*, 1013.
- 8a. Diaz, F.A.; Castillo, T.I.; Logan, J.A.; Lee, W.Y.; *J. Electroanal. Chem.* **1981**, *129*, 115.
- 8b. Waltman, R.J.; Bargon, J.; Diaz, A.F. *J. Phys. Chem.* **1983**, *87*, 1459.
9. Diaz, A.F.; Castillo, J.I. *J. Chem. Soc. Chem. Commun.* **1980**, 397.
10. Munsteadt, H.; Kohler, G.; Mowald, H.; Negle, D.; Bitthim, R.; Ely, G., Meissner, E. *Synth. Met.* **1987**, *18*, 256.
11. Ofer, D.; Cooks, R.M.; Wrighton, M.S. *J. Am. Chem. Soc.* **1990**, *112*, 7869.
12. Thackeray, J.W.; White, H.S.; Wrighton, M.S. *J. Phys. Chem.* **1985**, *89*, 5133.
13. Alper, J. *Science* **1989**, *246*, 208.

14. Boyle, A.; Geneis, E.M.; Lapkowski, M. *Synth. Met.* **1989**, *28*, C-769.
15. Ferraris, J.P.; Hanlon, T.R. *Polymer* **1989**, *30*, 1319.
16. Waltman, R.J.; Bargon, J. *Can. J. Chem.* **1986**, *64*, 76.
17. Olmedo, L.; Chanteloube, I.; Germain, A.; Petit, M. *Synth. Met.* **1989**, *30*, 159.
18. Merrill, B.A.; Ph.D. Thesis, Michigan State University, 1990.
19. Kobayashi, M.; Chen, J.; Chung, T.C.; Moraes, F.; Heeger, A.J. Wuld, F. *Synth. Met.* **1984**, *9*, 77.
20. Waltman, R.J.; Diaz, A.F.; Bargon, J. *J. Phys. Chem.* **1984**, *88*, 4343.
21. Adams, R.N. Electrochemistry at Solid Electrodes; Marcel Dekker Inc.: New York, 1969.
22. Adams, R. N. *Acc. Chem. Res* **1969**, 175.
23. Bargon, J.; Mohmad, S.; Waltman, R.J. *IBM J. Res. Dev.* **1983**, *27*, 330.
24. Skotheim, T.A., Ed. Handbook of Conducting Polymers; Marcel Dekker:New York, 1986.
25. Diaz, A.F. *Chem. Script.*, **1981**, *17*, 145.
26. Nicholson, R.S.; Shain, I. *Anal. Chem.* **1964**, *36*, 706.
27. Nazzari, A.; Street, G.B. *J. Chem. Soc. Chem. Commun.* **1984**, 83.
28. Gardini, G.P. *Adv. Heterocycl. Chem.* **1973**, *15*, 67.
29. Street, G.B.; Clarke, T.C.; Geiss, R.H.; Lee, V.Y.; Pflugar, P.; Scott, J.C. *J. Phys. Colloq.* **1983**, *C3(6)*, 599.
30. Tanaka, K.; Schichiri, T.; Yamabe, T. *Synth. Met.* **1986**, *14*, 271.
31. Ruhe, J.; Ezquerro, T.A.; Wegner, G. *Synth. Met.* **1989**, *28*, 177.
32. Elsenbaumer, R.L.; Jen, K.Y.; Oboudi, R. *Synth. Met.* **1986**, *15*, 169.

33. Zotti, G.; Schiavon, G. *Synth. Met.* **1989**, *28*, C183.
34. Diaz, A.F.; Castillo, J.; Kanazawa, K.K.; Logan, J.A.; Salmon, M.; Fajardo, O. *J. Electroanal. Chem.* **1982**, *133*, 233.
35. Bredas, J.L.; Street, G.B.; Themans, B.; Andre, J.M. *J. Chem. Phys.* **1985**, *83*, 1323.
36. Kanazawa, K.K.; Diaz, A.F.; Krounbi, M.T.; Street, G.B. *Synth. Met.* **1981**, *4*, 119.
37. Salmon, M.; Diaz, A.; Giotia, J. *Chem. Mat.* **1982**, *5*, 66.
38. Geneis, E.M.; Syed, A.A.; Salmon, M. *Synth. Met.*, **1985**, *11*, 353.
39. Bakhshi, A.K.; Ladik, J.; Seel, M. *Phys. Rev. B.* **1987**, *35*, 704.
40. Bredas, J.L. *J. Chem. Phys.* **1985**, *82*, 3808.
41. Ferraris, J.P.; Skiles, G.D. *Polymer* **1987**, *28*, 179.
42. Inganas, O.; Liedberg, B.; Ru-Chang, W.; Winberg, H. *Synth. Met.* **1985**, *11*, 239.
43. Naitoh, S. *Synth. Met.* **1987**, *18*, 237.
44. Winberg, H.; Metselaar, J. *Synth. Met.* **1984**, *14*, 1.
45. Ferraris, J.P.; Hanlon, G.D.; *Polymer* **1989**, *30*, 1319.
46. Yumoto, Y.; Yoshimura, S. *Synth. Met.* **1986**, *13*, 185.
47. Roncali, J.; Lemaire, R.; Garrew, R.; Garnier, F. *Synth. Met.* **1987**, *21*, 209.
48. Heinze, J.; Mortensen, J.; Hinkelmann, K. *Synth. Met.* **1987**, *21*, 209.
49. Merrill, B.A.; LeGoff, E. *J. Org. Chem.* **1990**, *55*, 2904.
50. Goldenberg, L.M.; Lyobouskaya, R.N.; Nazarova, I.B.; Roschupkina, O.S. *Synth. Met.* **1991**, *40*, 393.
51. Aviram, A. *J. Am. Chem. Soc.* **1988**, *110*, 5687.
52. Elming, N.; Clauson-Kaas, N. *Acta Chem. Scand.* **1952**, *6*, 867.

53. Tanguy, J.; Mermilliod, N. *Synth. Met.* **1987**, *21*, 129.
54. Tanguy, J.; Mermilliod, N.; Hoclet, M. *Synth. Met.* **1987**, *18*, 7.
55. Tanguy, J.; Slama, M.; Hoclet, M.; Baudouin, J.L. *Synth. Met.* **1989** *28*, C145.
56. Still, W.C.; Kahn, M.; Mitra, A.; *J. Org. Chem.* **1979**, *43*, 2923.
57. Patil, A.O.; Heeger, A.J.; Wuld, F. *Chem. Rev.* **1988**, *88*, 183.
58. Bredas, J.L.; Scott, J.C.; Yakushi, K.; Street, G.B. *Phys. Rev. B.* **1984**, *30*, 1023.
59. Lippe, J.; Holze, R. *Synth. Met.* **1991**, *41-43*, 2927.
60. Smits, F.M. *Bell Systems Tech. J.* **1958**, 711.
61. Paul, E.W.; Ricco, A.J.;Wrighton, M.S. *J. Phys. Chem.* **1985**, *89*, 1441.
62. Genies, E.M.; Hany, P.; Lapkowsky, M.; Santier, C.H.; Olmedo, L.; *Synth. Met.* **1988**, *25*, 29.
63. Ofer, D.; Crooks, R.M.; Wrighton, M.S. *J. Am. Chem. Soc.* **1990**, *112*, 7869.
64. Kittlesen, G.P.; White, H.S.; Wrighton, M.S. *J. Am. Chem. Soc.* **1984**, *106*, 7389.
65. Olmedo, L.; Chanteloube, I.; Germain, A.; Petit, M. *Synth. Met.* **1989**, *28*, 165.
66. Schiavon, G.; Sitran, S.; Zotti, G. *Synth. Met.* **1989**, *32*, 209.
67. Holze, R.; Lippe, J. *Synth. Met.* **1990**, *38*, 99.
68. Nagarajan, K.; Shenoy, S. *Ind. J. Chem.* **1989**, *28B*, 587.
69. Nozaki, H.; Koyama, T.; Mori, T. *Tetrahedron* **1969**, *25*, 5359.
70. Broadbent, H.S.; Burnham, W.S.; Olsen, R.K.; Sheeley, R.M. *J. Heterocy. Chem.* **1968**, *5*, 757.
71. Bacon, R.; Karim, A. *Chem Comm.* **1969**, 486, 578.

- 72. Weinreb, S.M.; Levin, J.I.; Turos, E. *Synth. Comm.* **1982**, *12*, 989.
- 73. Gauger, J.; Manecke, G.; *Chem. Ber.* **1970**, *103*, 2696.
- 74a. Treibs, A.; Jakob, K. *Liebigs Am. Chem.* **1966**, *699*, 153.
- 74b. Patil, A.; Ikenoue, Y.; Basescu, N.; Colaneri, N.; Chen, J.; Wuld, F.; Heeger, A. *Synth. Met.* **1987**, *20*, 151.
- 74c. Ikenoue, Y.; Uotani, N.; Patil, A.; Wudl, F.; Heeger, A.J. *Synth. Met.* **1989**, *30*, 305.
- 75. Peres, R.; Pernaut, J.M. *Synth. Met.* **1989**, *28*, C59.
- 76. Slama, M.; Tanguy, J. *Synth. Met.* **1989**, *28*, C139.
- 77. Kuwabata, S.; Okamoto, K.; Ikeda, O.; Yoneyama, H. *Synth. Met.* **1987**, *18*, 101.
- 78. Bard, A.J.; Faulkner, L.R. Electrochemical Methods; Wiley & Sons: New York, 1980.
- 79. LeBlevenec, L.F.; Ph.D. Thesis, Michigan State University, 1990.
- 80. Fry, A.J. Synthetic Organic Electrochemistry; Wiley & Sons: New York, 1989.
- 81. Kankare, J.; Lukkari, J. *Synth. Met.* **1991**, *41-43*, 2839.
- 82. Doblhofer, K.; Zhong, C. *Synth. Met.* **1991**, *41-43*, 2865.
- 83. Bredas, J.; Themans, B.; Fripiat, J.; Andre, J.; Chance, R. *Phys. Rev.* **1984**, *29*, 6761.

MICHIGAN STATE UNIV. LIBRARIES



31293009026414